BOKU
Institute of Hydrology
and Water Management

International Institute for
Applied Systems Analysis
IIASA www.iiasa.ac.at

THE REPUBLIC OF UGANDA
MINISTRY OF WATER AND ENVIRONMENT

ASSESSMENT OF NATIONAL WATER QUALITY DEGRADATION IN UGANDA

MAPPING OF DRIVERS, PRESSURES, AND THE CURRENT STATUS

AUSTRIAN
DEVELOPMENT
COOPERATION

Mathew Herrnegger[1], Jennifer Raskin[1], Oliver Konold[1], Florian Sorger-Domenigg[2], Ting Tang[2], Gabriel Stecher[1]

[1]Institute Institute of Hydrology and Water Management, Department of Water, Atmosphere and Environment, BOKU University, Vienna

[2]International Institute for Applied Systems Analysis (IIASA)

This document was prepared within the project "Sustainable water quality management supporting Uganda's development ambitions | SWAQ-Uganda" and is part of Deliverables 1.1 and 2.6.

The project aims to contribute to the sustainable management of water resources in Uganda, with the expected outcomes of "improved knowledge and enhanced capacity in water quality management" in support of policy making and effective water resources management. The project is led by the International Institute for Applied Systems Analysis (IIASA), with the Directorate of Water Resources Management (DWRM) of the Ministry of Water and Environment (MWE) of Uganda and the University of Natural Resources and Life Sciences, Vienna (BOKU) as partners. The project (No.2507-01/2020) is funded by the Austrian Development Agency (ADA) and own contributions of the three partner organizations.

Cite as: Herrnegger, M., Raskin, J., Konold, O., Sorger-Domenigg, F., Tang, T., Stecher, G. (2024). Assessment of National Water Quality Degradation: Mapping of Drivers, Pressures, and Current Status. Report prepared in the frame of the project "Sustainable water quality management supporting Uganda's development ambitions | SWAQ-Uganda". Institute of Hydrology and Water Management, University of Natural Resources and Life Sciences, Vienna (BOKU); International Institute for Applied Systems Analysis (IIASA). Available under https://uganda.boku.ac.at

Last updated: June 24, 2024.

Foreword
Page 2

CONTENTS

INTRODUCTION

The primary goal of effective water resource management is to appropriately allocate sufficient quantity and quality of water for various uses. In recent years, this goal has been hindered by socioeconomic and climatic developments which have resulted in significant pressures on water quality and quantity. In Uganda, water quality challenges are major threats to human health, biodiversity, overall ecosystem health, and economic development. Small scale studies have discovered contamination of water sources with fecal coliforms, bacteria, nutrients, heavy metals, and other contaminants.

Uganda is a part of the Nile River Basin, which runs from South to North and flows into the Mediterranean Sea. Upstream regions of the basin include the countries of Burundi, Democratic Republic of Congo (DRC), Kenya, Tanzania, and Rwanda, while downstream regions include South Sudan, Sudan and Egypt. Lake Victoria, Africa's largest lake and the source of the Nile, is shared with bordering countries Tanzania and Kenya. Thus, due to its geographical position, Uganda's water resource management also impacts other countries.

Although Uganda – on average - has plentiful water resources within its borders, these resources are often unusable due to degradation of water resources, contamination during floods and landslides, limited funding for water management, insufficient collaboration across sectors responsible for water management, and non-compliance with national wastewater standards (MWE, 2022a). In Uganda, limited capacity and scarcity of data inhibit effective management of water quality.

To manage water quality on a national scale, Uganda has established a legal mandate for clean water for all. This mandate is embodied in the Uganda Vision 2040 and National Development Plans. In accordance with Sustainable Development Goal 6 (SDG 6): Clean Water and Sanitation, Uganda's government has increased focus on improving access to clean water by expanding accessibility to water for underserved areas, activating water points that have been non-operational, and creating new water facilities that can be accessed at more affordable rates (VNR, 2020). In an effort to improve water quality, the government of Uganda is engaged in monitoring and the enforcement of laws regarding dumping, release of hazardous chemicals, and pollution (VNR, 2020). Uganda continuously monitors industrial facilities that discharge wastewater such as dairies, factories, food processing plants and pharmaceutical factories (VNR, 2020). However, compliance of industrial effluent to standards is generally low, with approximately half of all industrial facilities emitting effluents that do not comply with standards set forth for biochemical oxygen demand (BOD) and total suspended solids (TSS) (VNR, 2020). Improvement in water quality continues to be a crucial focus of the Ministry of Water and Environment in Uganda.

Effective planning for water quality management requires a comprehensive understanding of the drivers and pressures that contribute to water quality degradation. To fill gaps in existing knowledge, a national mapping initiative focused on identifying these crucial factors was established under the project "Sustainable water quality management supporting Uganda's development ambitions (SWAQ-Uganda)." This national mapping effort is documented in this report and also includes a geodatabase detailing data pertinent to water management, and a WebGIS at https://uganda.boku.ac.at/.

The main objective of the present document is to enhance the comprehension of drivers and pressures affecting water quality across Uganda. This document, respective geodatabase and WebGIS allow for a better understanding of the factors responsible for water quality degradation in Uganda. This project provides valuable information regarding the physical, chemical, and ecological status, dominant pollution sources, critical source areas, and potential agricultural management options. Among others, included here are datasets on socioeconomics, climate, water sources, land use land cover, agriculture, livestock, mining, and wastewater treatment. Most data were collected from sources available in the public domain, including global datasets. Some data were obtained from the Ministry of Water and Environment in Uganda or other personal communications with experts. Where possible, this data collection effort focused on obtaining the most up-to-date data to present the current status of water quality degradation. Data sources used include methodologies such as on-site collection, surveys, machine learning and other modeling methods. To streamline and interpret the diverse data layers, this information was also synthesized into a Water Quality Pressure Index (WQPI). The WQPI is a composite indicator that combines data on water quality pressures and drivers into one value. This index provides a consolidated and insightful measure, aiding in the effective assessment and management of water quality issues in Uganda.

GEODATABASE AND MAPS

The geodatabase is structured in 6 general groups of datasets. These groups are i) General data, ii) Water, iii) Environment, iv) Agriculture, v) Socioeconomic and vi) Climate. Several datasets are stored in each of these groups. These categories allow users to access data based upon potential pollution sources and the implications for water quality. An overview of the geodatabase is presented in Table 1.

Table 1: Structure of the Geodatabase developed for the National Mapping of Water Quality Drivers and Pressures

Geodatabase Structure – Datasets on National Water Quality Drivers and Pressures

General Data	Water	Environment	Socioeconomic	Climate	Agriculture
General Mapping	**Water Monitoring**	**Land Cover**	**Main Drivers**	**Precipitation**	**Livestock**
Uganda State Border	Water Management Zones	Land cover (NFA & FAO)	Population Density	Long term monthly/annual	Tropical Livestock Units
International Borders	Gauging Stations	Wetland distribution	Gross Domestic Product	Precipitation Extremes	Production Systems
Districts	WQ Monitoring Sites	NDVI monthly/annual	**Industries**	Trends	N and P production
Subregions	**Infrastructure & Access**	Protected Areas	Mineral Concessions		Manure
Towns	Wastewater treatment plants	Canopy Height			**Annual Agricultural Survey**
Road Network	Hydropower	**Soil**			Fertilizer use
Lakes		USDA Typology			Irrigation use
River Network		Total N topsoil/subsoil			Pesticide use
National Parks		Total P			
Map Background		Extractable P			
DEM (Merit 90x90m)		Soil Erosion Risk			
Hillshade (Eduard)		**Ecology**			
Canopy Height		Ecoregions			
		ZARDIS			

The maps in this report are grouped into four categories. Each dataset is plotted in a consistent map layout on individual pages. Below each map, a short description of the data is provided. This includes sources and further descriptions such as spatial features, characteristics, and resolution for raster files.

The first section of the report summarizes general data, such as landcover, topography, vegetation, administrative borders, and water management efforts in Uganda. The second section presents water quality drivers, followed by a section, which reviews water quality pressures. The final section presents the Water Quality Pressure Index (WQPI) developed within the scope of the SWAQ Uganda project. An outline of figures listed under each section is provided in Table 2.

Table 2. Structure of National Mapping Report including subcategories and respective figures titles

OVERVIEW OF MAPS

General Data	Water quality drivers	Water quality pressures	Water Quality Pressure Index
Figure 1: **Overview of Uganda**	Figure 12: **Uganda population density**	Figure 33: **Tropical Livestock Units (TLUs)**	Figure 49: **Water Quality Pressure Index**
Figure 2: **Topography of Uganda**	Figure 13: **Gridded gross domestic product (GDP)**	Figure 34: **Chickens in extensive production systems**	Figure 50: **Stream Network Water Quality Pressure Index: WQPI considering the stream network and hierarchy**
Figure 3: **Regions and Districts of Uganda**	Figure 14: **Long-term mean annual precipitation (1991-2020)**	Figure 35: **Chickens in intensive production systems**	
Figure 4: **Subregions of Uganda**	Figure 15: **Decadal precipitation conditions**	Figure 36: **Pigs in extensive production systems**	
Figure 5: **Water Management Zones (WMZ) of Uganda**	Figure 16: **Precipitation trends (1991-2020)**	Figure 37: **Pigs in semi-intensive production systems**	
Figure 6: **Protected areas in Uganda**	Figure 17: **Long-term mean monthly precipitation (1991-2020)**	Figure 38: **Pigs in intensive production systems**	
Figure 7: **Ecoregions in Uganda**	Figure 18: **Daily precipitation extremes**	Figure 39: **Nitrogen production from manure**	
Figure 8: **ZARDIS Agro-Ecological Zones of Uganda**	Figure 19: **Uganda Landcover**	Figure 40: **Phosphorus production from manure**	
Figure 9: **Discharge gauging stations in Uganda**	Figure 20: **Historical wetlands in Uganda**	Figure 41: **Annual Agricultural Survey 2018: Households using any fertilizer**	
Figure 10: **Existing water quality monitoring sites in Uganda**	Figure 21: **Wetlands in Uganda in 2008**	Figure 42: **Annual Agricultural Survey 2018: Households using inorganic fertilizer**	
Figure 11: **Hydropower in Uganda**	Figure 22: **Wetlands in Uganda in 1994**	Figure 43: **Annual Agricultural Survey 2018: Households using organic fertilizer**	
	Figure 23: **Long-term mean Normalized Difference Vegetation Index (NDVI; 2001-2020)**	Figure 44: **Annual Agricultural Survey 2018: Households using irrigation**	
	Figure 24: **Vegetation Dynamics – NDVI**	Figure 45: **Annual Agricultural Survey 2018: Households using pesticides**	
	Figure 25: **Long-term mean monthly NDVI (2001-2020)**	Figure 46: **Wastewater treatment plants (WWTPs) in Uganda**	
	Figure 26: **Forest canopy height (2019)**	Figure 47: **Mineral concessions in Uganda**	
	Figure 27: **Soil types in Uganda**	Figure 48: **Active Mining Leases and Licenses in Uganda**	
	Figure 28: **Total Nitrogen content at soil depth of 0-20cm**		
	Figure 29: **Total Nitrogen content at soil depth of 20-50cm**		
	Figure 30: **Total Phosphorus content at soil depth 0-30cm**		
	Figure 31: **Extractable Phosphorus content at soil depth 0-30cm**		
	Figure 32: **Soil erosion risk**		

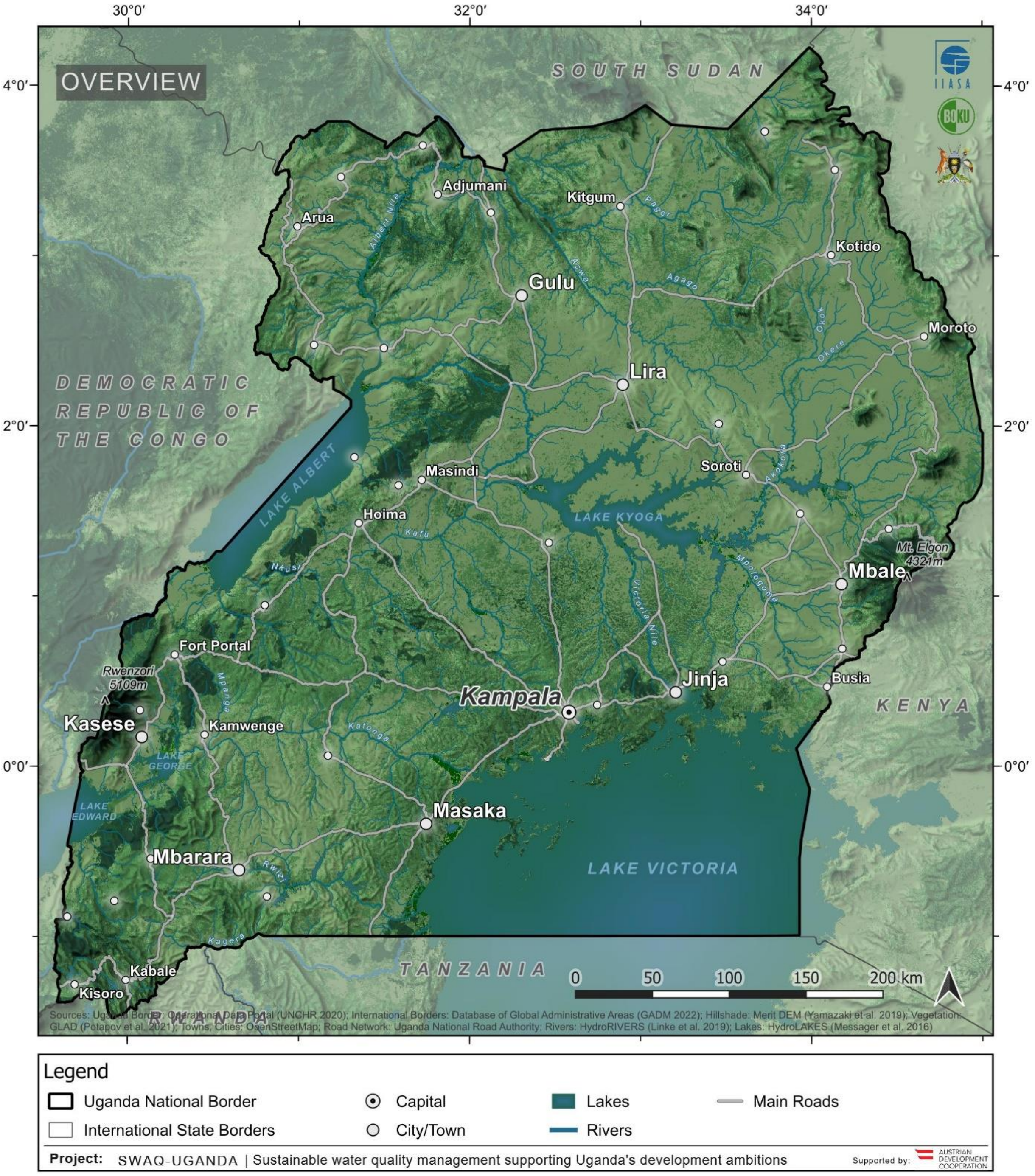

Figure 1: Overview of Uganda

Figure 1 presents an **overview of Uganda**. This base map includes major towns, main roads, river courses, large lakes, and international borders. The national border of Uganda was derived from a shapefile for district boundaries published 17th November 2020 (UNHCR, 2020). International borders were acquired from the Database of Global Administrative Areas (GADM, 2022). Data representing major towns were obtained from the Uganda Bureau of Statistics (UBOS, 2012). Rivers were derived from HydroRIVERS (Lehner & Grill, 2013) and lakes are based on HydroLAKES (Messager et al., 2016). The road network data was based on the Uganda Roads dataset provided by the World Bank, combined with complementary data derived from OpenStreetMap (World Bank Group, 2007). Vegetation data was obtained online from the Global Land Analysis and Discovery (GLAD) laboratory at the University of Maryland (Potapov et al., 2021). The topography layer is based on the MERIT DEM (Yamazaki et al., 2019).

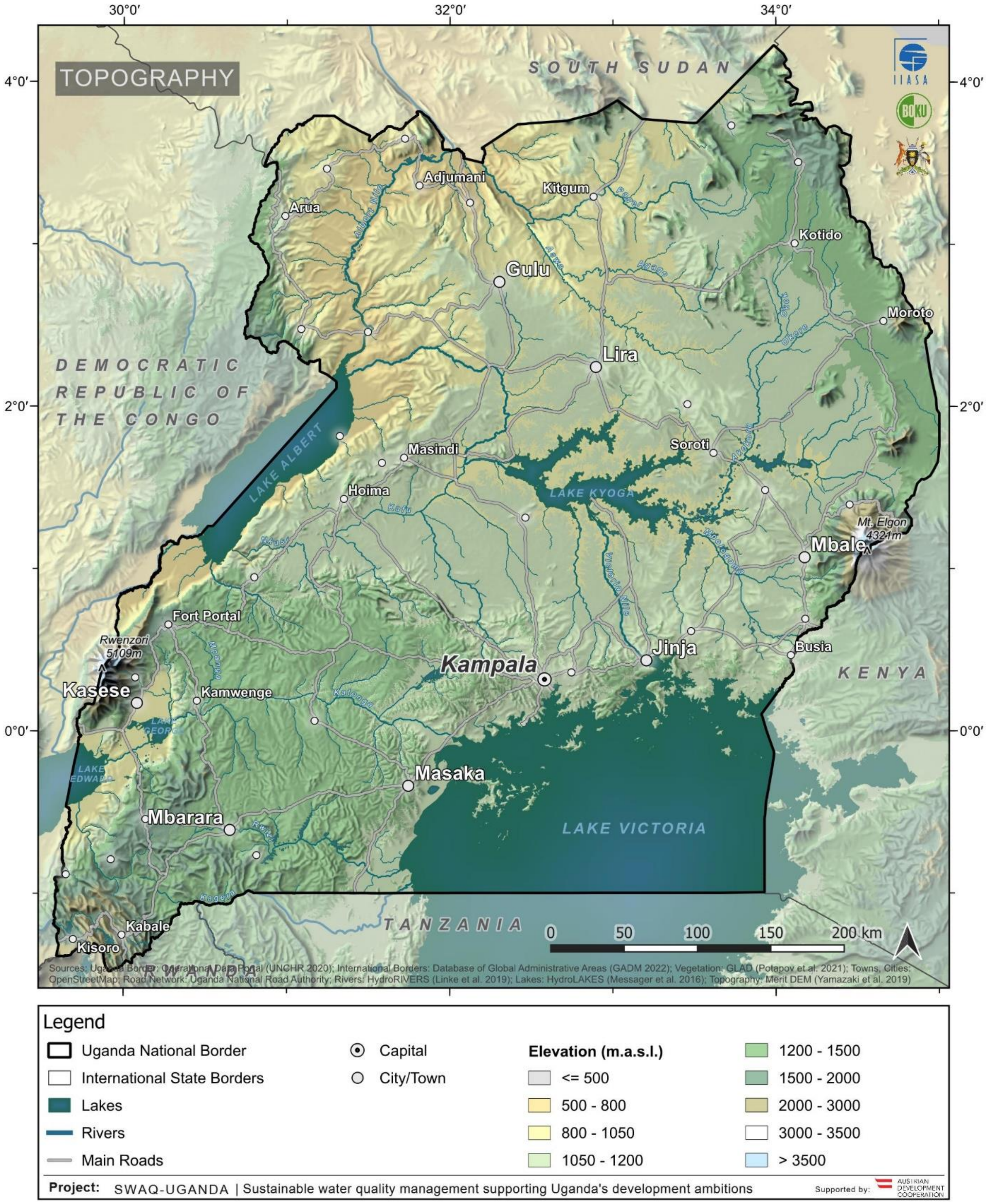

Figure 2: Topography of Uganda

Figure 2 represents a **topographic map** of Uganda showing altitudinal range. The MERIT Digital Elevation Model (Yamazaki et al., 2019) was employed. Large areas of Uganda lie within an altitude range between 1050 to 1500 meters above sea level (m.a.s.l). Major topographic features rising higher than 3500 m.a.s.l. are located in the east (Mt. Elgon) and in the west of Uganda (Rwenzori Mountains). Towards the southwest the altitude rises higher than 2000 m.a.s.l. Lower elevations are observed in the northwest.

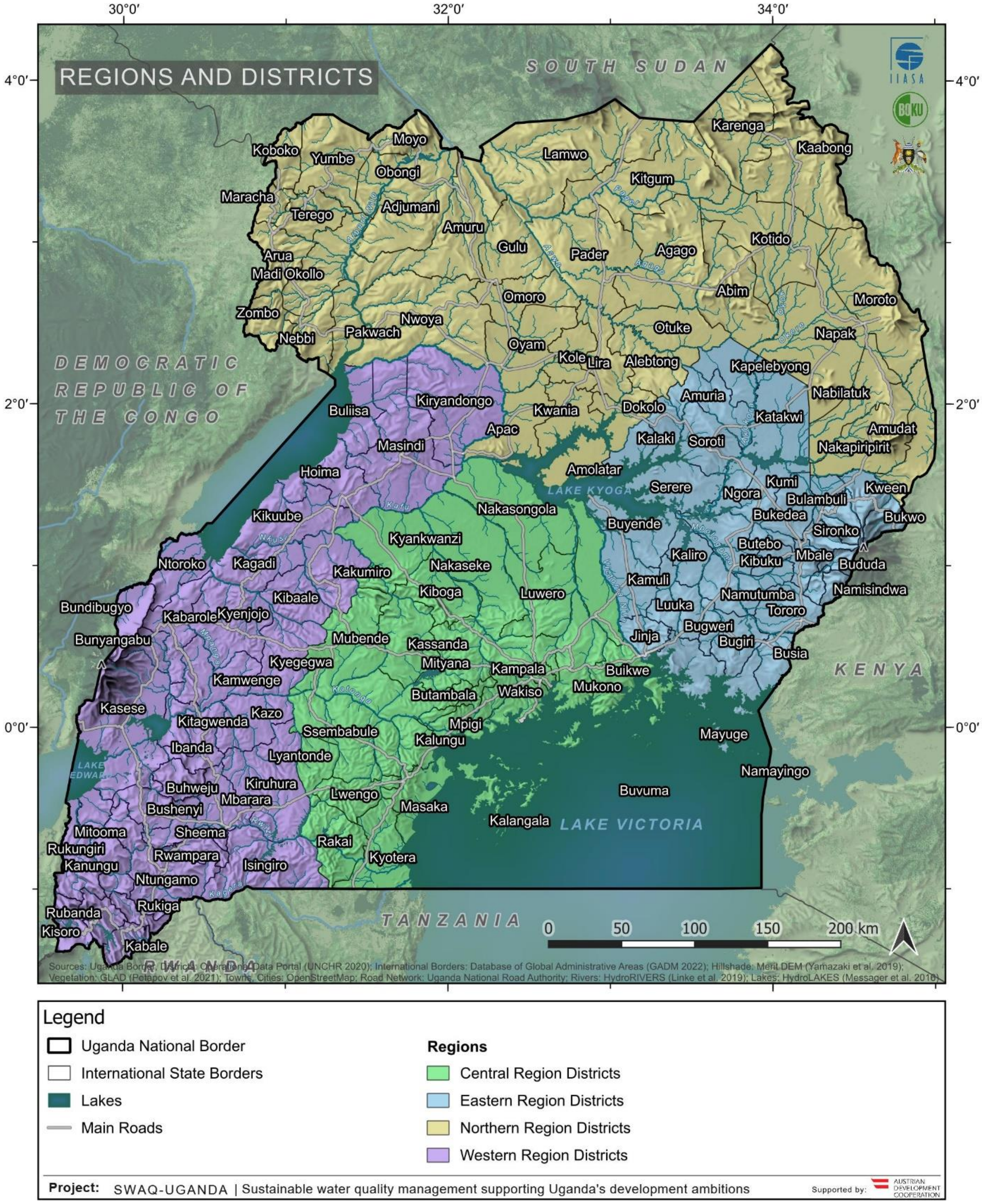

Figure 3: Regions and Districts of Uganda

Figure 3 exhibits the **administrative regions and districts** in Uganda as of 2020. Uganda districts are the most basic unit for management. There are a total of 136 districts grouped into 4 administrative regions: central, eastern, western and northern regions. This shapefile was downloaded from UNCHR's Operational Data Portal (UNHCR, 2020).

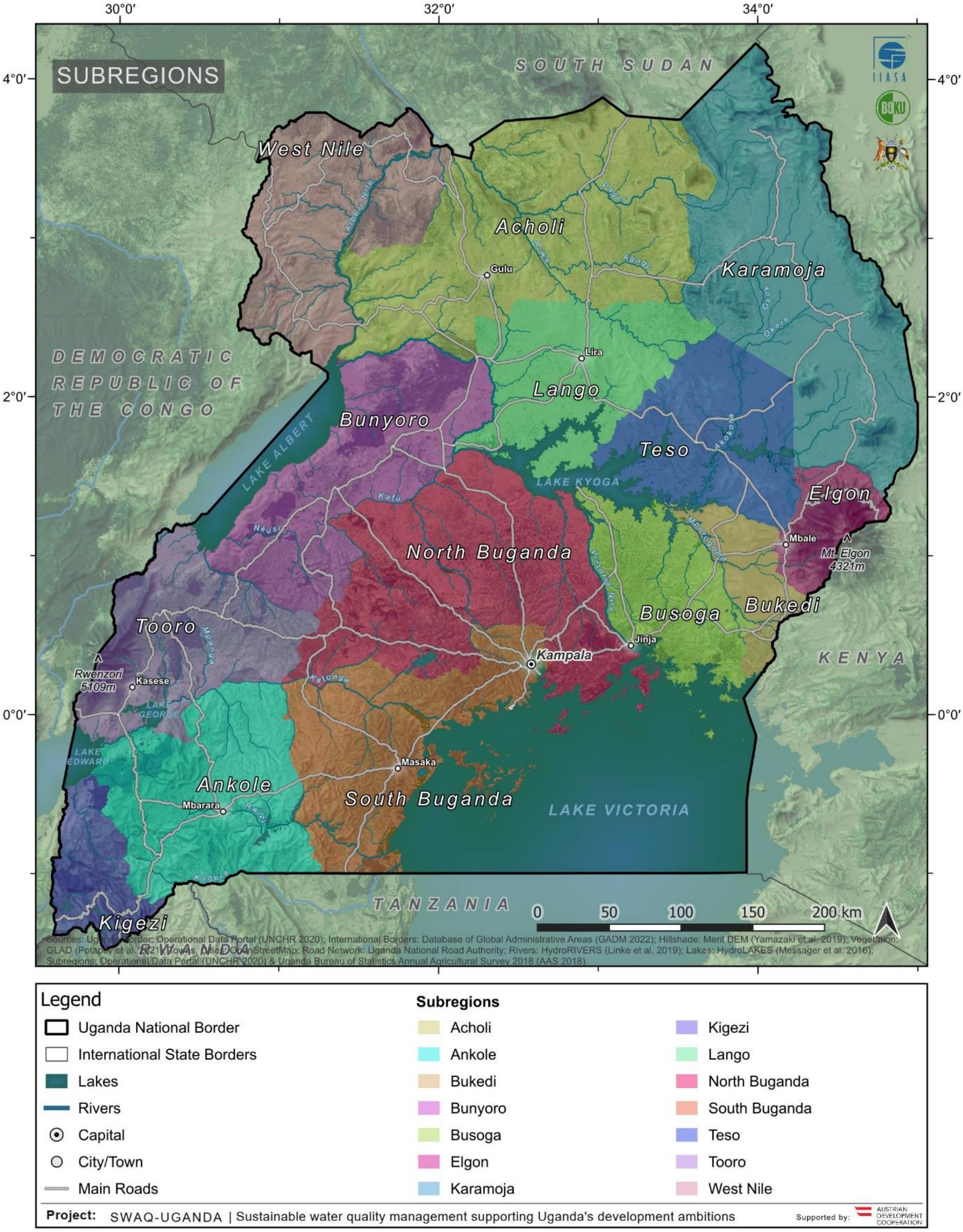

Figure 4: Subregions of Uganda

Figure 4 presents the 14 **subregions** of Uganda. These subregions were derived from the Uganda district shapefile obtained from UNCHR's Operational Data Portal and from information provided by *Figure 1.2: Map of the sub-regions in Uganda* in the Uganda Bureau of Statistics (UBOS) 2018 Annual Agricultural Survey (UBOS AAS, 2020; UNHCR, 2020).

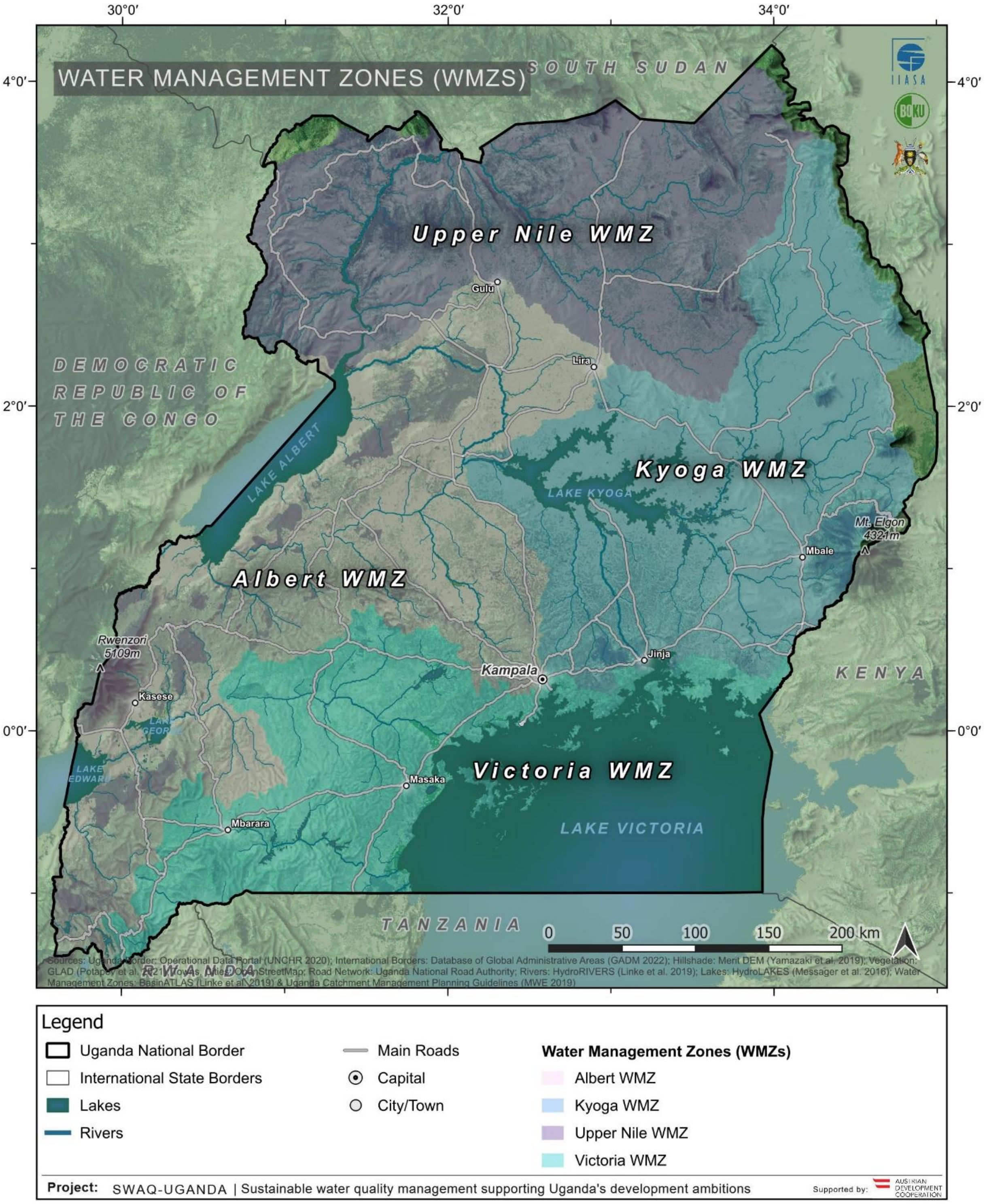

Figure 5: Water Management Zones (WMZ) of Uganda

Figure 5 displays the four **water management zones (WMZ)** in Uganda. WMZs constitute the primary administrative and reporting units for water resources management. They represent the four major hydrological basins and are roughly in line with the four administrative regions shown in Figure 3. However, the WMZs are delineated independently based on the hydrological drainage areas. The four WMZs include the Upper Nile, Kyoga, Victoria and Albert. This shapefile was derived from BasinATLAS HydroSHEDS level 5,6,7 (Linke et al., 2019) and from the Ministry of Water and Environment Uganda Catchment Management Planning Guidelines (Directorate of Water Resources Management, 2019).

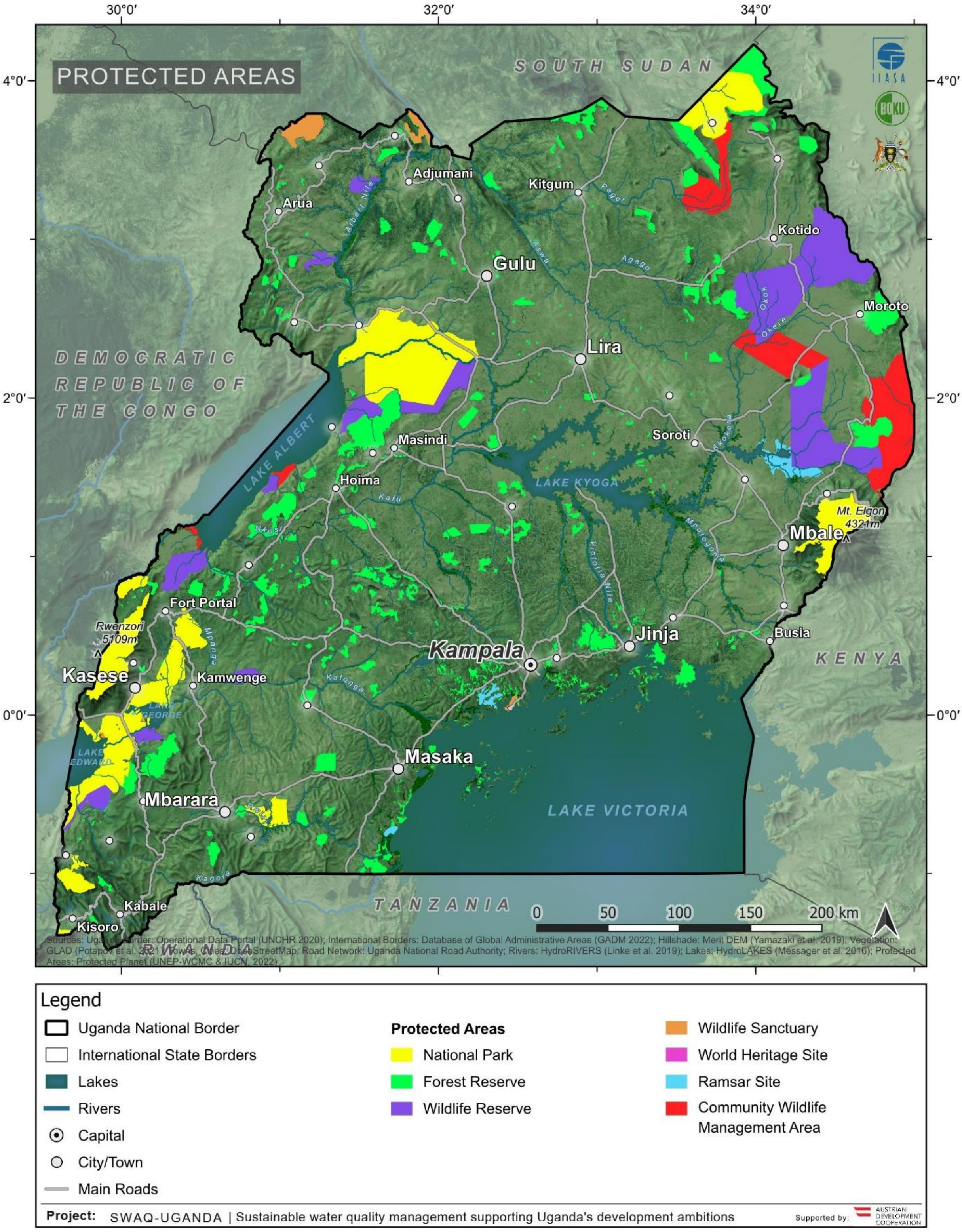

Figure 6: Protected areas in Uganda

Figure 6 presents various **protected areas** in Uganda. This dataset, provided by UNEP-WCMC & IUCN (2022) (available at www.protectedplanet.net), shows the types of protected areas distributed throughout Uganda. Aside from Murchinson Falls National Park, which is located east of Lake Albert, the majority of protected land is found in the eastern and southwestern regions of the country. It is estimated that the displayed protected areas experience limited anthropogenic pollution. It is important to note that several areas are protected under multiple designations. Therefore, some polygons displayed here may represent more than one type of protected area, especially around Lake Edward and Lake George.

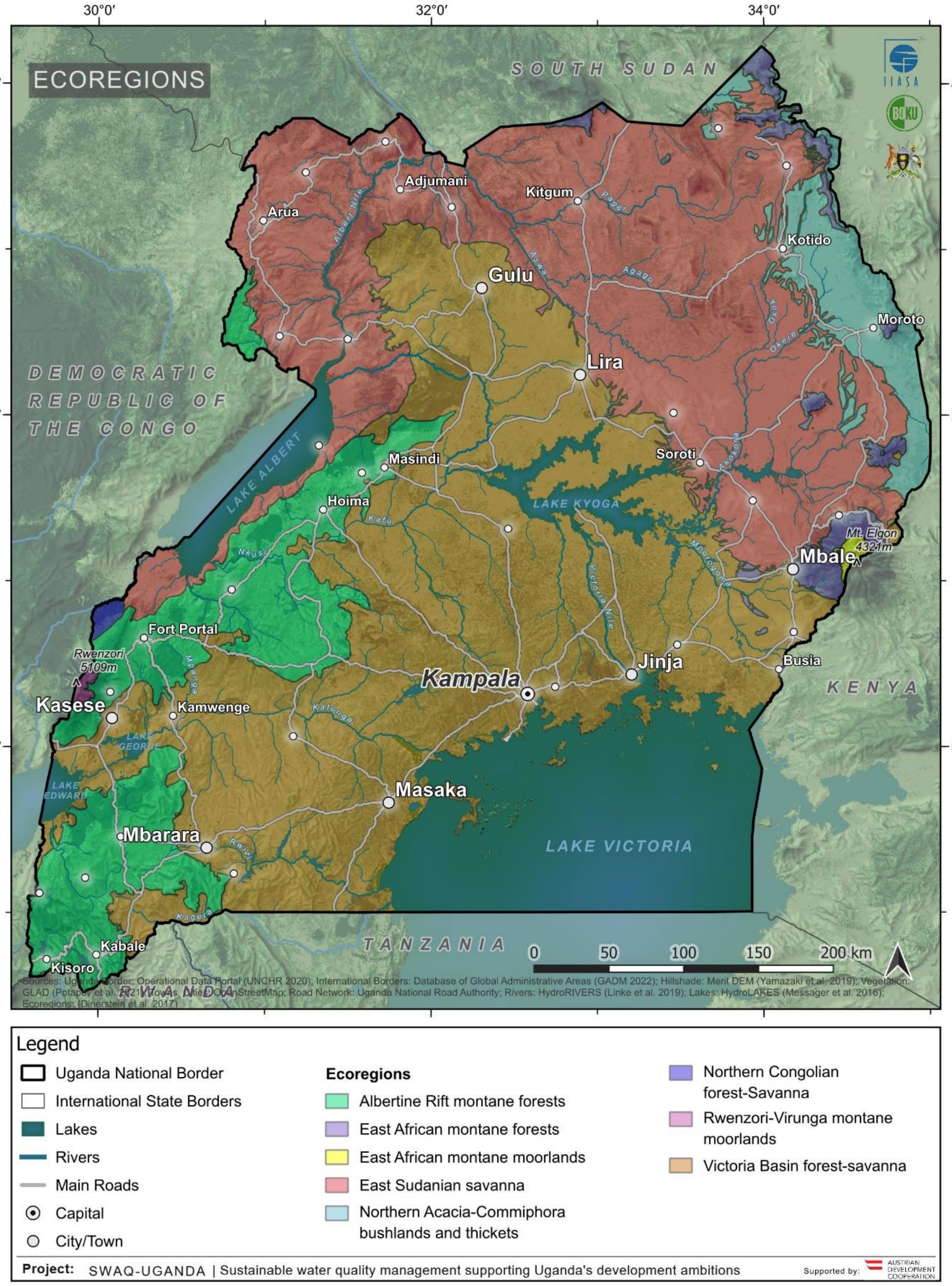

Figure 7: Ecoregions in Uganda

Figure 7 exhibits eight different **ecoregions** as defined by Dinerstein et al. (2017). The most prominent ecoregions in Uganda include Victoria Basin forest-savannah, East Sudanian savannah, and Albertine Rift montane forests. In aquatic bioassessment, ecoregions are frequently used as part of a classification framework for waterbodies (Gerritsen et al., 2000).

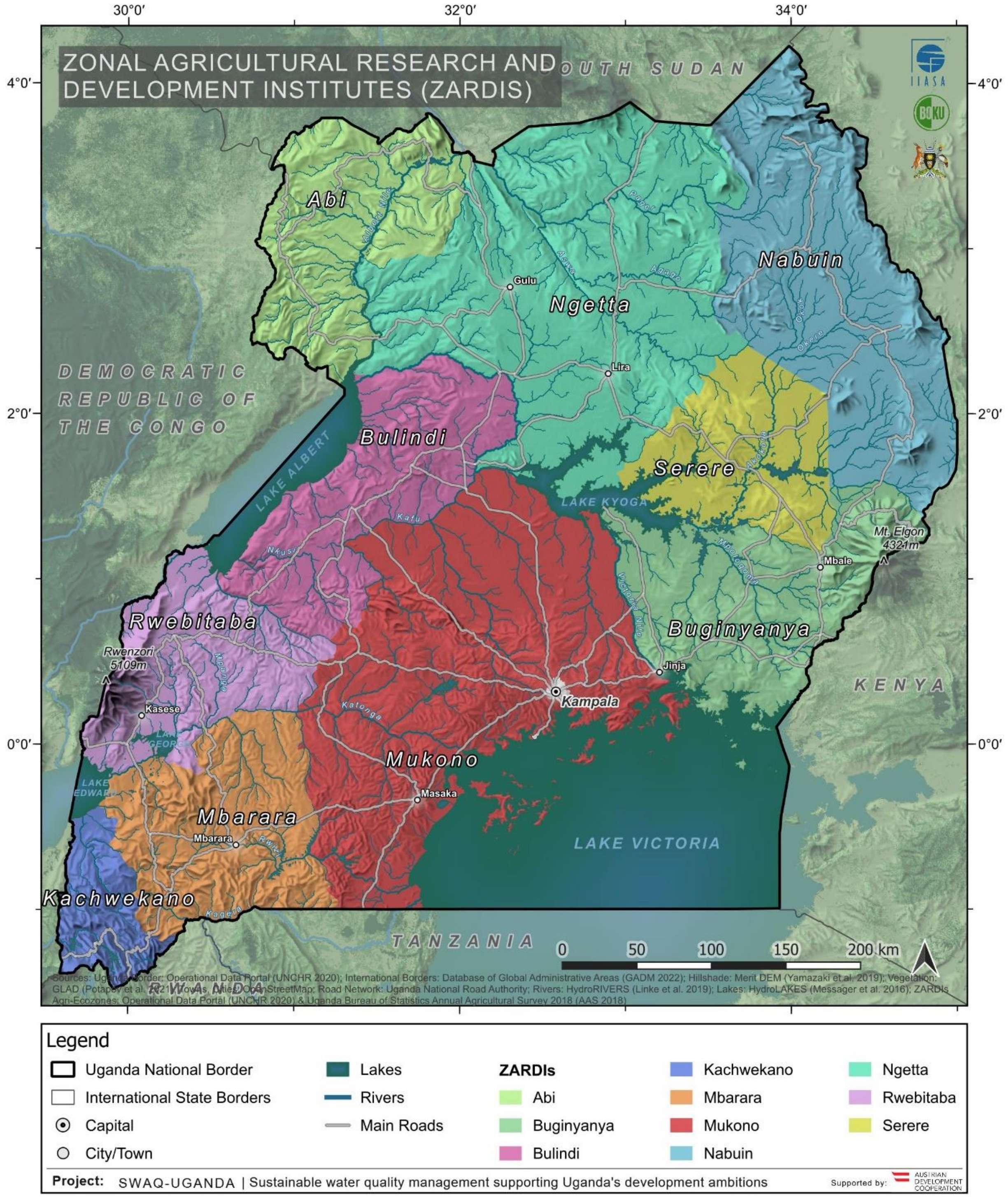

Figure 8: ZARDIS Agro-Ecological Zones of Uganda

Figure 8 displays the **agro-ecological zones** of Uganda represented by the Uganda's Zonal Agricultural Research and Development Institutes (ZARDIS). ZARDIS were derived from the Uganda district shapefile from UNCHR's Operational Data Portal and from information provided by *Figure 1.1: Map of the Zardis in Uganda* in Uganda Bureau of Statistics (UBOS) Annual Agricultural Survey 2018 (UBOS AAS, 2020; UNHCR, 2020). ZARDIS conduct research and development activities pertaining to agricultural activities within their regions.

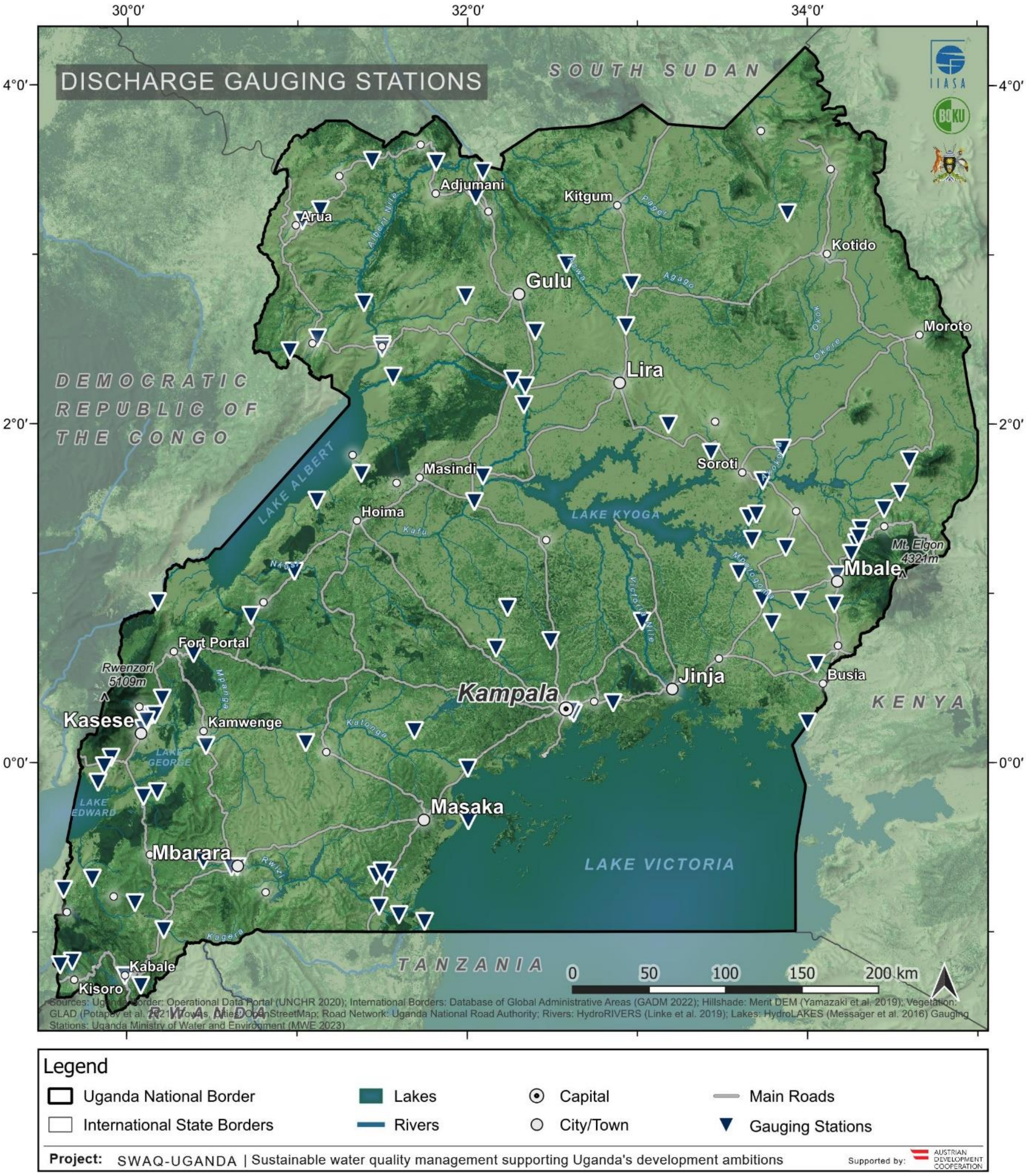

Figure 9: Discharge gauging stations in Uganda

Figure 9 exhibits 100 **discharge gauging stations** in Uganda. This dataset was obtained in 2023 from the Ministry of Water and Environment in Uganda and includes gauging stations that are both operational, non-operational and under construction. Gauging stations listed include locations in wetlands (n=25), rivers (n=52), and unspecified (n=23). Note that this dataset does not cover all discharge measurement stations in Uganda and does not provide information on actual data availability

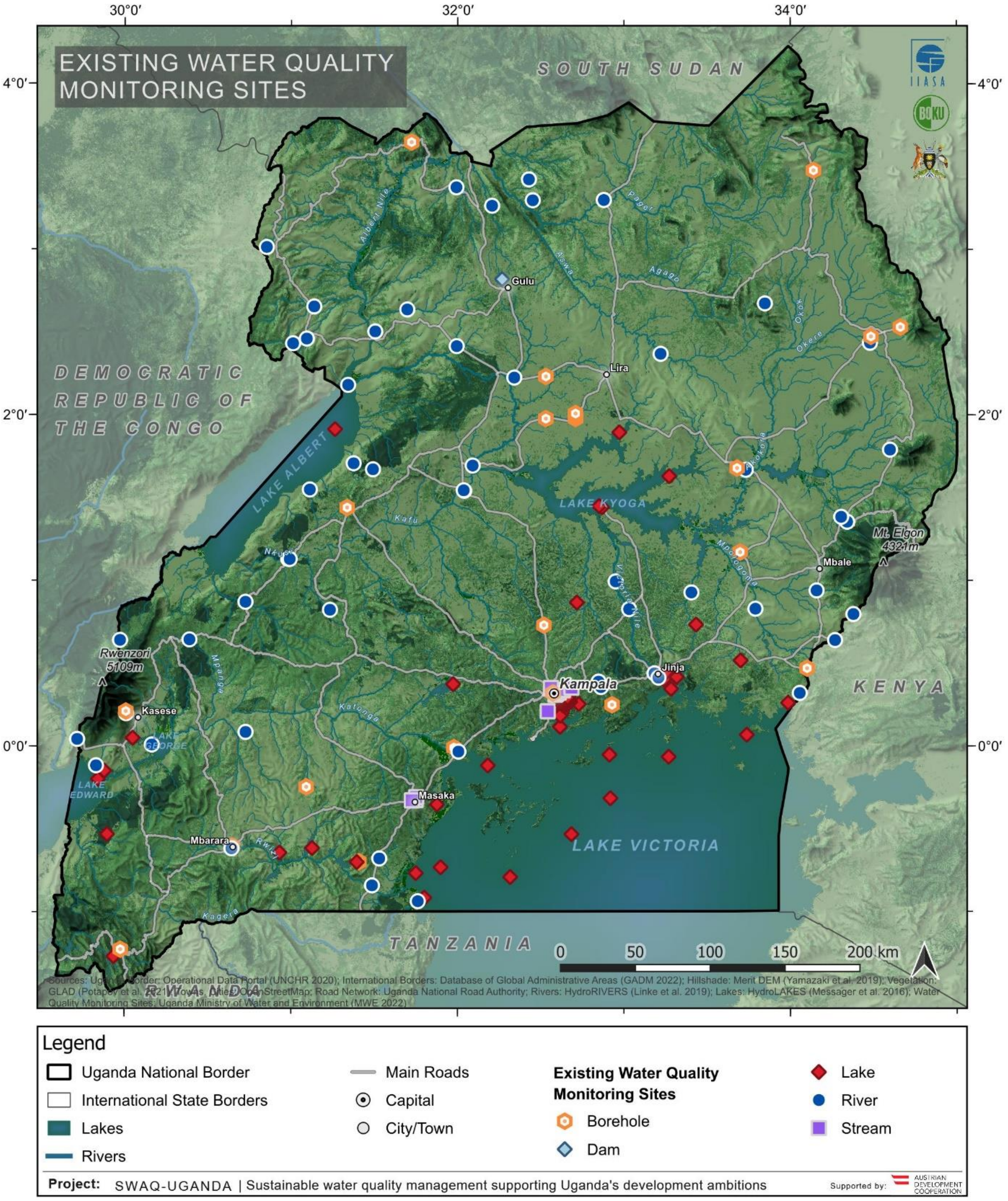

Figure 10: Existing water quality monitoring sites in Uganda

Figure 10 shows 152 existing **water quality monitoring sites** in Uganda. Sites include boreholes, dams, lakes, rivers and streams. This dataset was provided by Uganda's Ministry of Water and Environment in March 2022 (MWE, 2022b). Note that this dataset may not reflect a complete record of all monitoring sites.

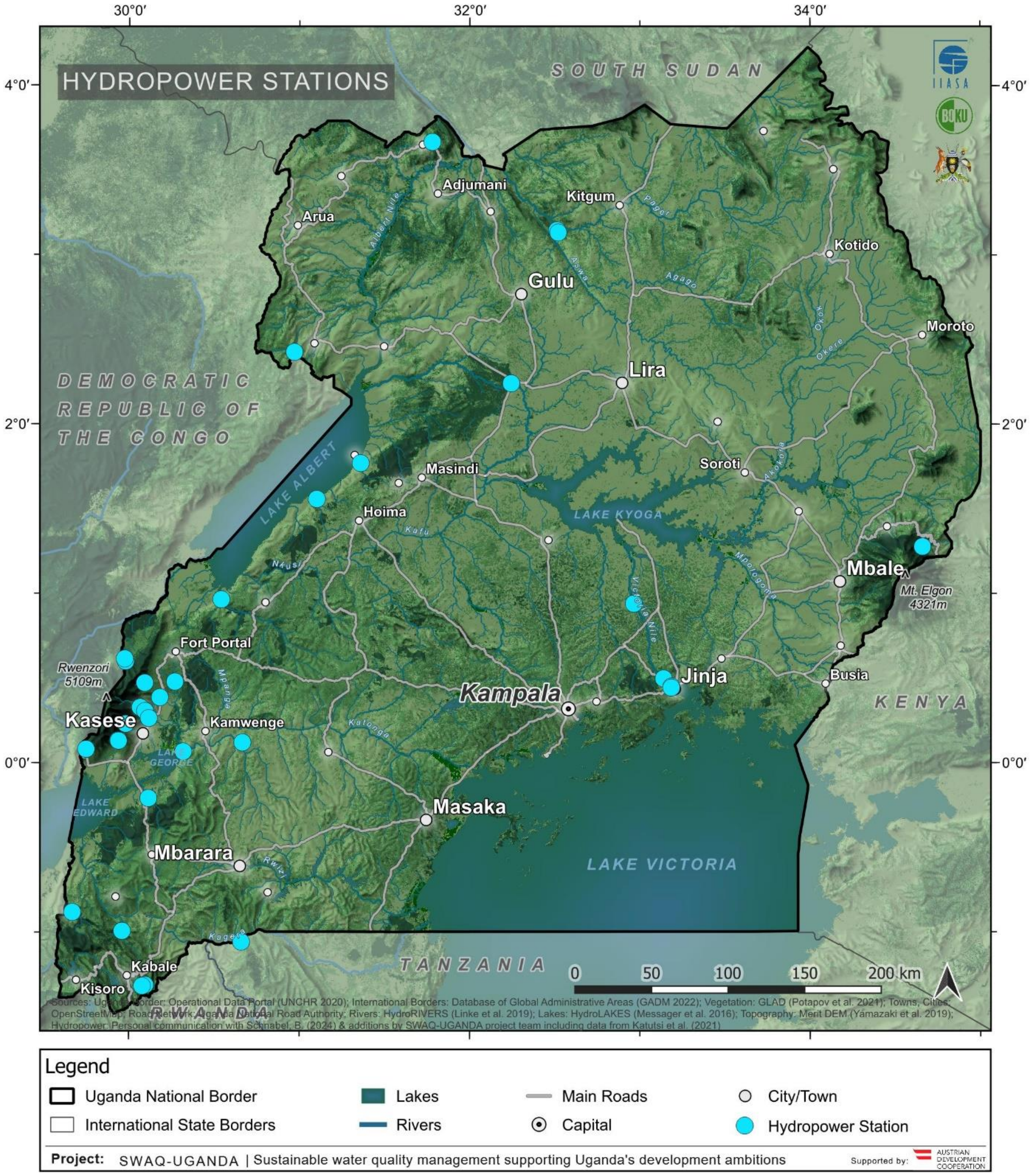

Figure 11: Hydropower in Uganda

Figure 11 presents **hydropower stations** in Uganda. Note that this is not necessarily a complete record. This dataset was obtained through personal communication with Schnabel (2024) with additions made by the SWAQ-UGANDA project team. Additional information was added to the dataset based upon (Katutsi et al., 2021). According to the Uganda Electricity Generation Company Ltd (UEGCL), major power stations include the Kiira Power Station, Nalubaale Power Station, Karuma Hydropower Station, Isimba Hydro Power Station, and the Muzizi Hydro Power Station (Uganda Electricity Generation Company Ltd, 2024). Additional information regarding hydropower in Uganda can be found at: https://www.era.go.ug/

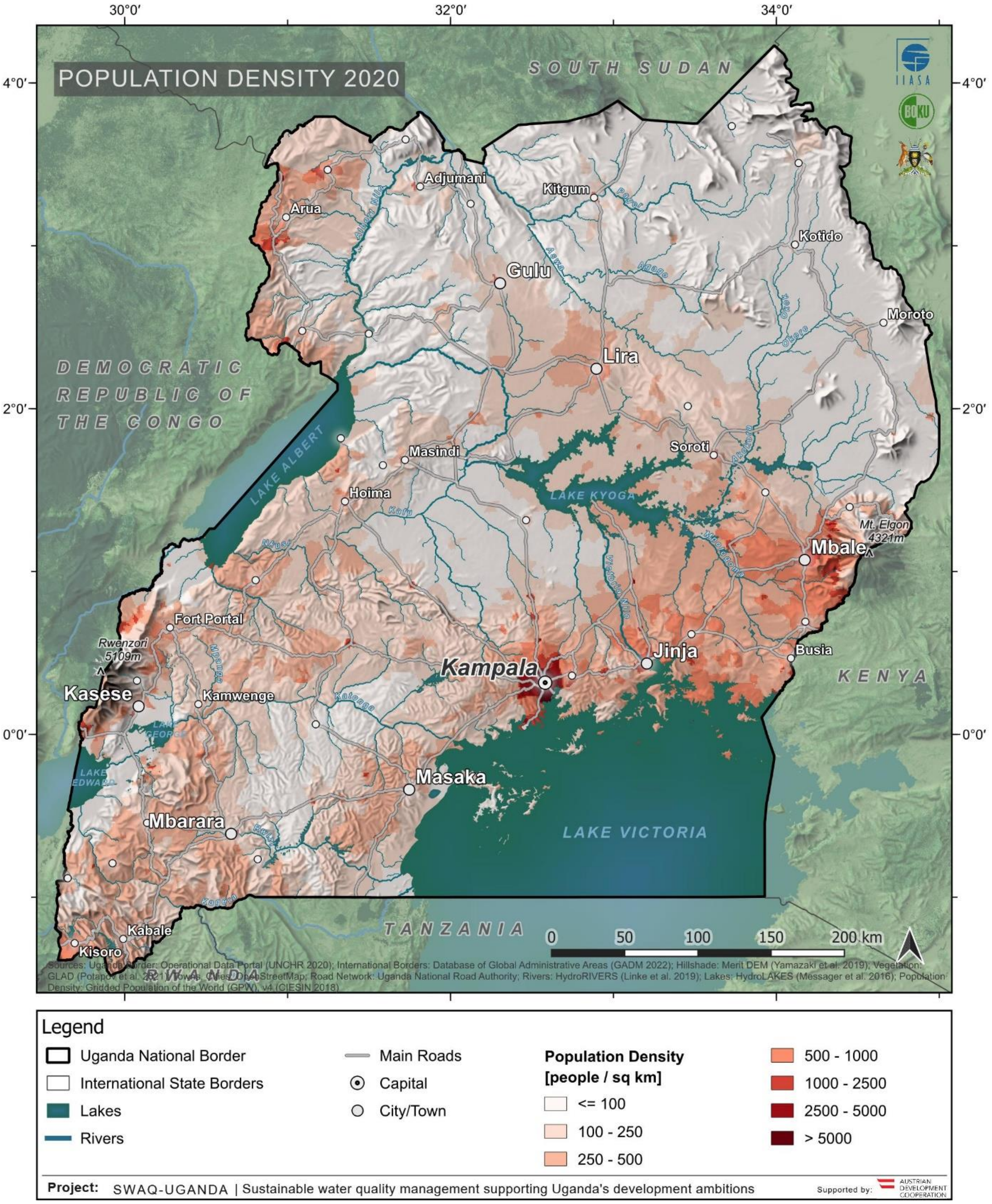

Figure 12: Uganda population density

Figure 12 shows the **population density** (people per km²) of Uganda for the year 2020. The Gridded Population of the World Version 4 (GPWv4) dataset was obtained from the Socioeconomic Data and Application Center (SEDAC) and has a resolution of 30 arcseconds (~ 1 km at equator) (Center for International Earth Science Information Network (CIESIN), 2018). Densely populated areas are found in the southeast along the border with Kenya, as well as around Kampala and Mbale. The northeast is less densely populated.

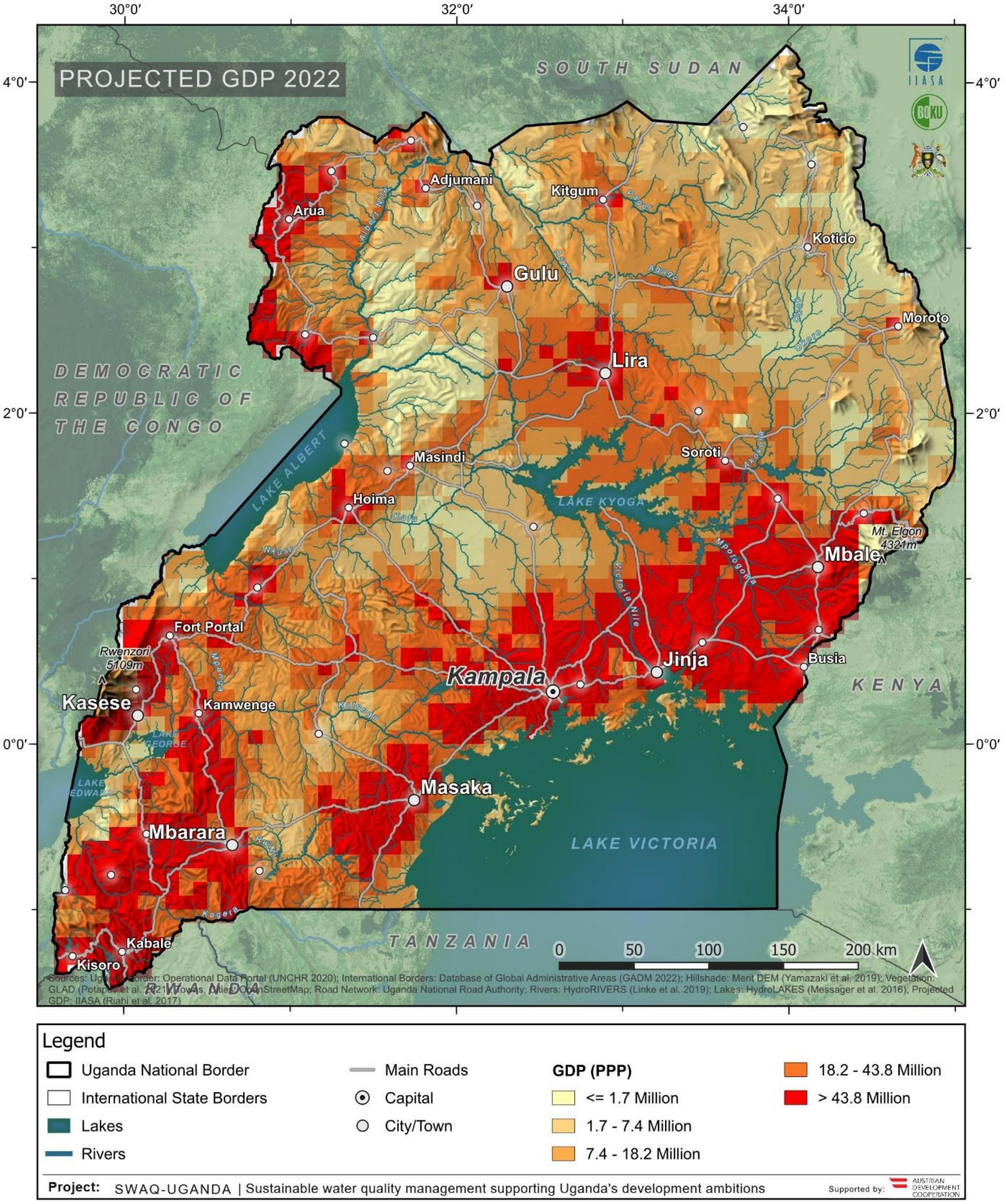

Figure 13: Gridded gross domestic product (GDP)

Figure 13 presents the **gridded gross domestic product (GDP)** projected using purchasing power parity (PPP) and the international dollar. The projected GDP dataset was based on the 2022 Shared Socioeconomic Pathway 1 (SSP1) projection by (Riahi et al. (2017) which assumes that the world will move towards a more sustainable future. This dataset has a resolution of 5 arcminutes (~ 9.3km at equator) and considers 2005 USD value. High economic activity can be found in the areas surrounding Lake Victoria, in southwestern Uganda, and in the northwest along the border with Democratic Republic of Congo.

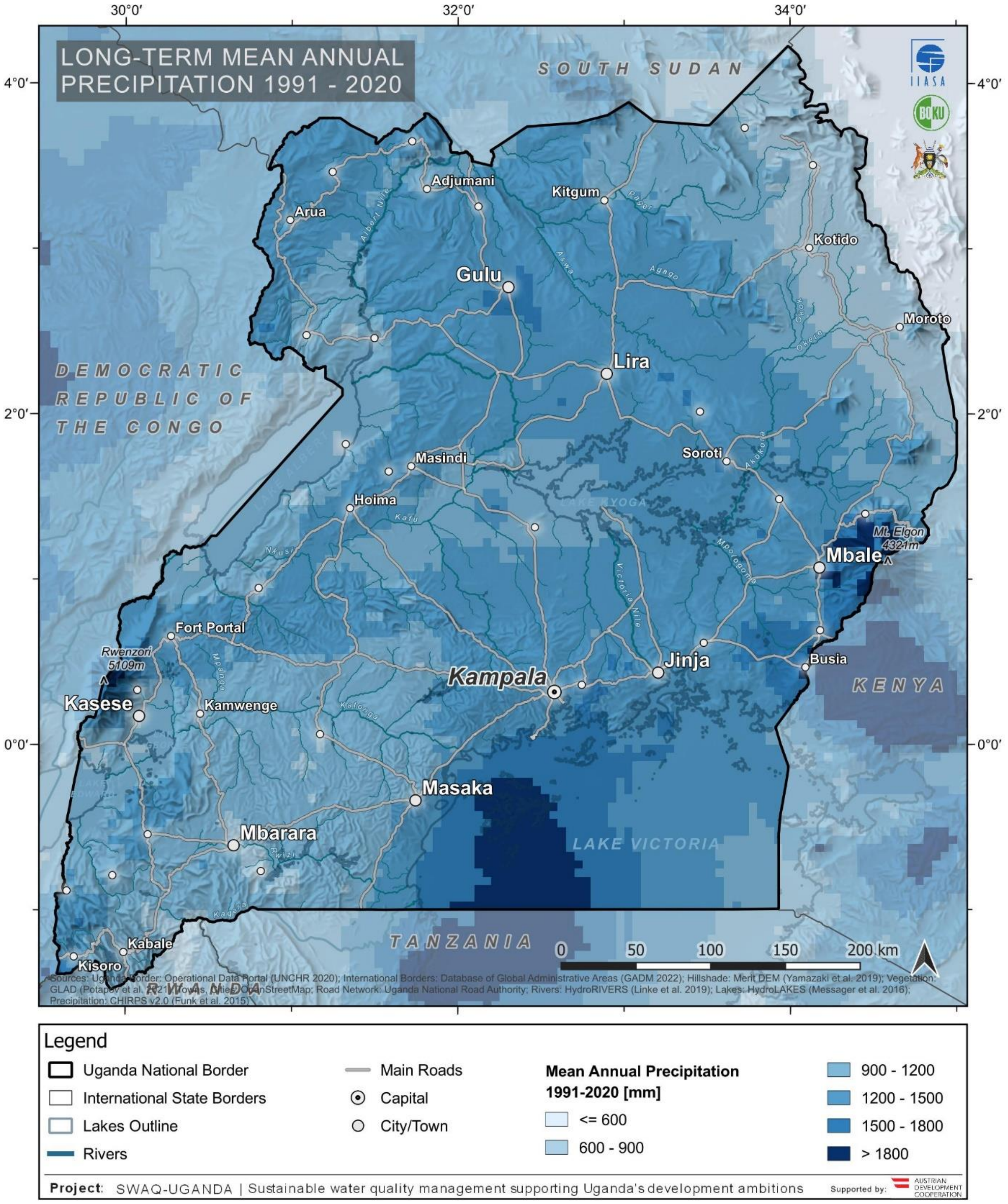

Figure 14: Long-term mean annual precipitation (1991-2020)

Figure 14 displays the **long-term mean annual precipitation sums considering data from 1991-2020**. The precipitation dataset used was the Climate Hazards Group InfraRed Precipitation with Station data (CHIRPS) Version 2, with a resolution of 0.05° (~ 5.5 km at the equator) (Funk et al., 2015). The highest average yearly precipitation values (> 1800mm) are observed over the western side of Lake Victoria, around Mount Elgon and in the Rwenzori Mountains.

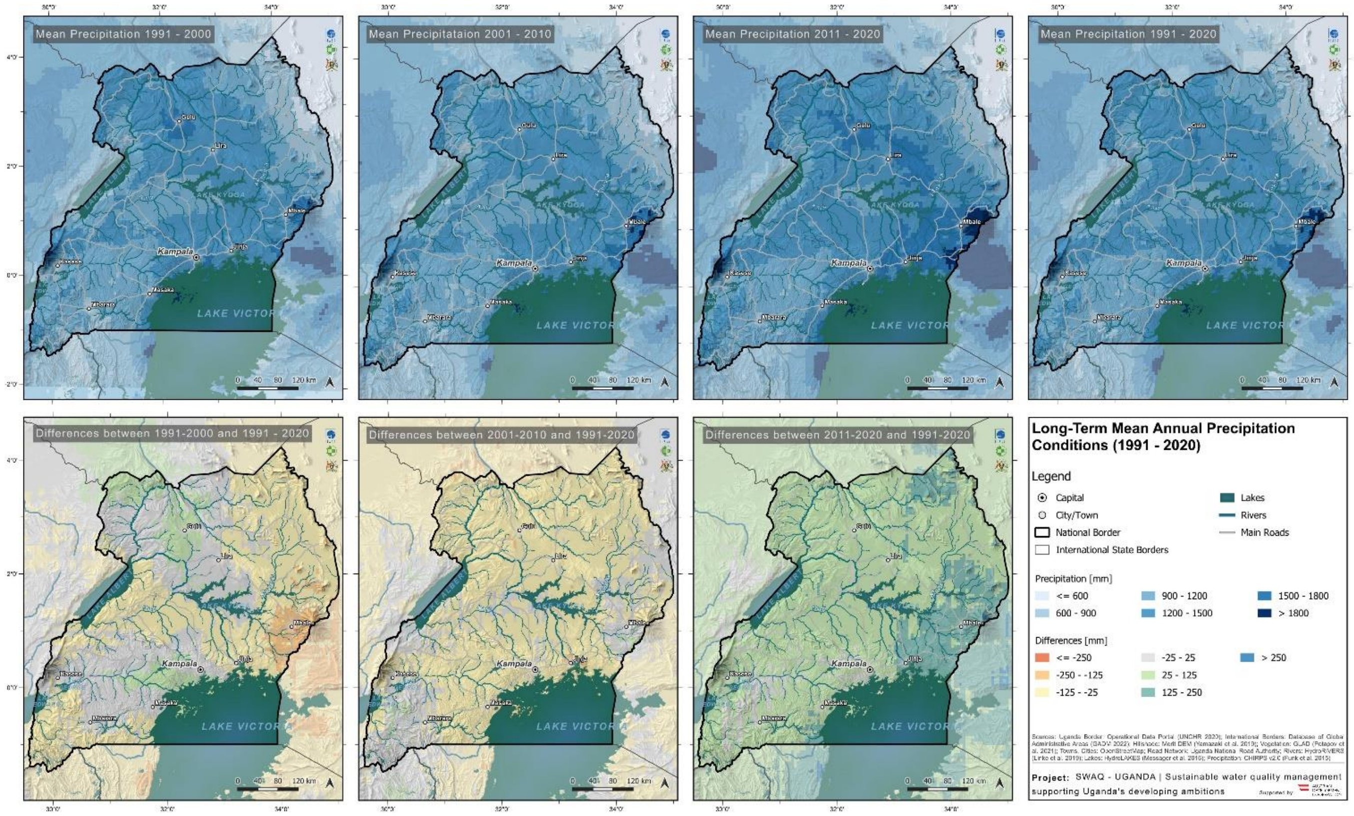

Figure 15: Decadal precipitation conditions

Figure 15 shows **mean annual precipitation sums and deviations for the decades between 1991 to 2020**. The decadal precipitation sums and trends are displayed in the top and lower panels. The long-term mean annual precipitation from 1991 to 2020 is presented in the top right panel for comparison. All mean annual precipitation maps exhibit a consistent spatial pattern regardless of the decade. Highest mean annual precipitation values (> 1800 mm/year) are observed over the western side of Lake Victoria, around Mount Elgon and in the Rwenzori Mountains. The southwest and northeast experience low mean annual precipitation (< 750 mm/year). In the bottom panels, the decadal precipitation deviations from the long-term mean are shown. The period from 2011 to 2020 was the wettest, showing higher annual mean precipitation compared to the long-term average for almost the entire country. Negative deviations (drier conditions) compared to the long-term average were observed for the two other decades. The greatest deviations were revealed when comparing the earliest decade (1991 to 2000) to the long-term average. For this comparison, high negative deviations (> 250 mm/year) are present in eastern Uganda. Conversely, precipitation over Lake Victoria and in the northwest were higher from 1991 – 2020 compared to the long-term mean. In the period from 2001 to 2010, lower annual mean precipitation can be noted for almost the entire country. The precipitation dataset used was the Climate Hazards Group InfraRed Precipitation with Station data (CHIRPS) Version 2 (Funk et al., 2015) with a resolution of 0.05° (~ 5.5 km at the equator).

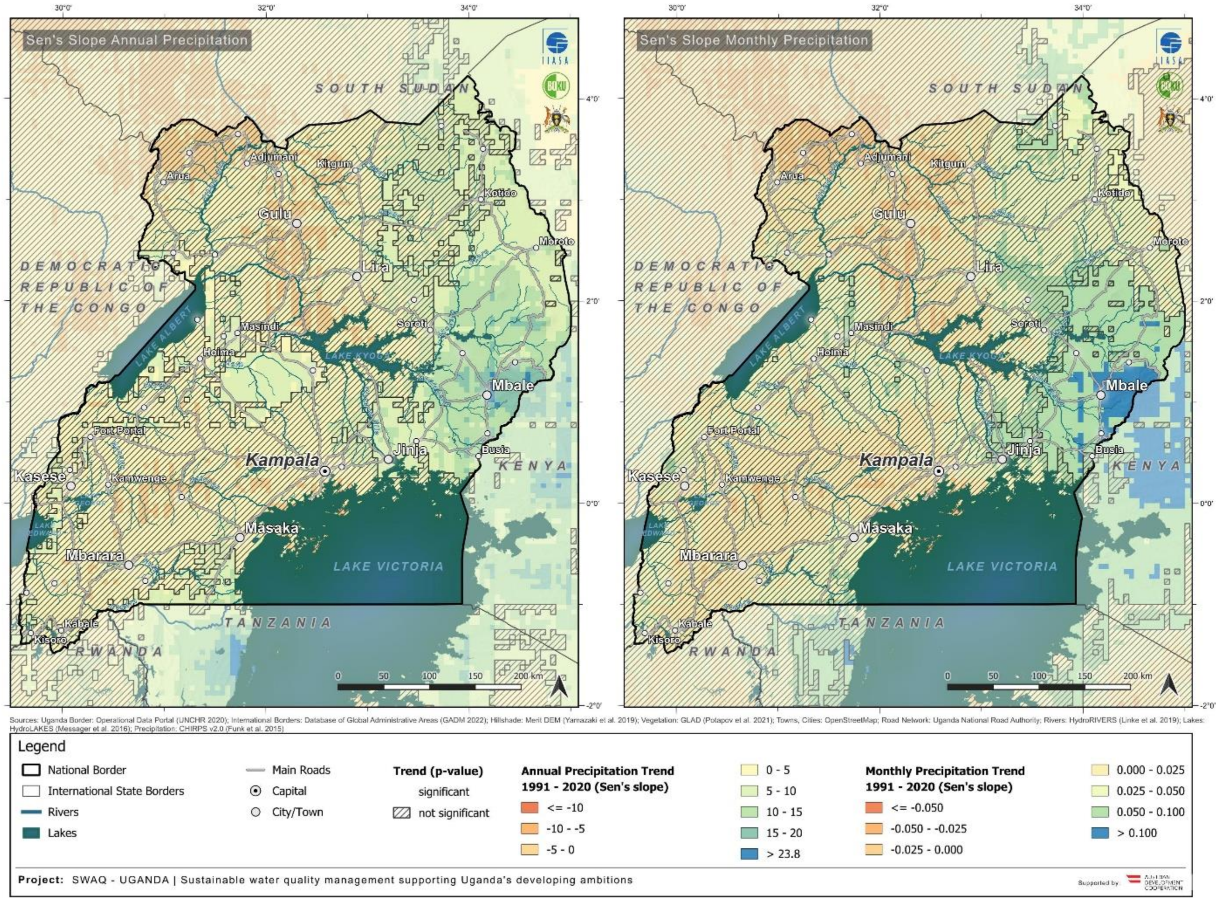

Figure 16: Precipitation trends (1991-2020)

Figure 16 shows the **Sen's slope of annual precipitation (left panel) and monthly precipitation (right panel)** from 1991 to 2020. Sen's slope is a robust, non-parametric estimation of slope that indicates the long-term monotonic trend of change in a time series. A significant positive trend indicates an increase in long-term precipitation. Significant trends occurred largely in the eastern part of Uganda. Non-significant trends were masked by grey lines. Large areas of Uganda thus did not show a significant precipitation trend in the analyzed time period. Again, the precipitation dataset used to derive this analysis was the Climate Hazards Group InfraRed Precipitation with Station data (CHIRPS) Version 2 (Funk et al., 2015) with a resolution of 0.05° (~ 5.5 km at the equator).

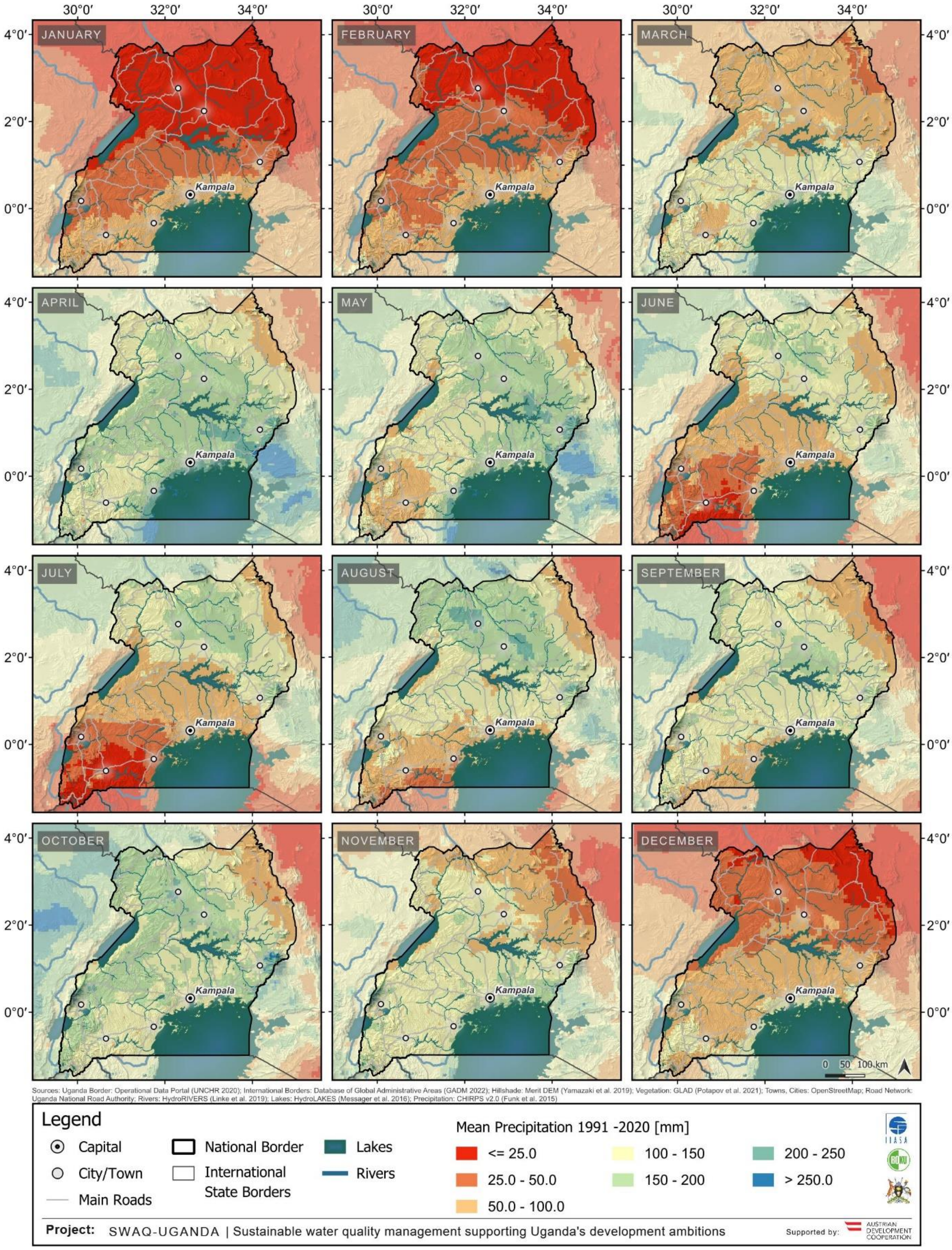

Figure 17: Long-term mean monthly precipitation (1991-2020)

Figure 17 shows the **long-term mean monthly precipitation (in mm) from 1991 to 2020**. The average monthly precipitation exhibits a strong seasonal pattern. The intensity of this seasonal pattern varies regionally. Lower average precipitation values are observed during the dry season in December, January, and February. Precipitation increases from March to May, especially centrally and over Lake Victoria. Lower precipitation is observed in June and July, especially in the southwest. In August, precipitation increases in the northern areas of Uganda. Almost the whole country is exposed to higher precipitation in October. This reflects the bimodal precipitation pattern. The precipitation dataset used here was the Climate Hazards Group InfraRed Precipitation with Station data Version 2 (Funk et al., 2015) with a resolution of 0.05 arcminutes (~ 5km at the equator).

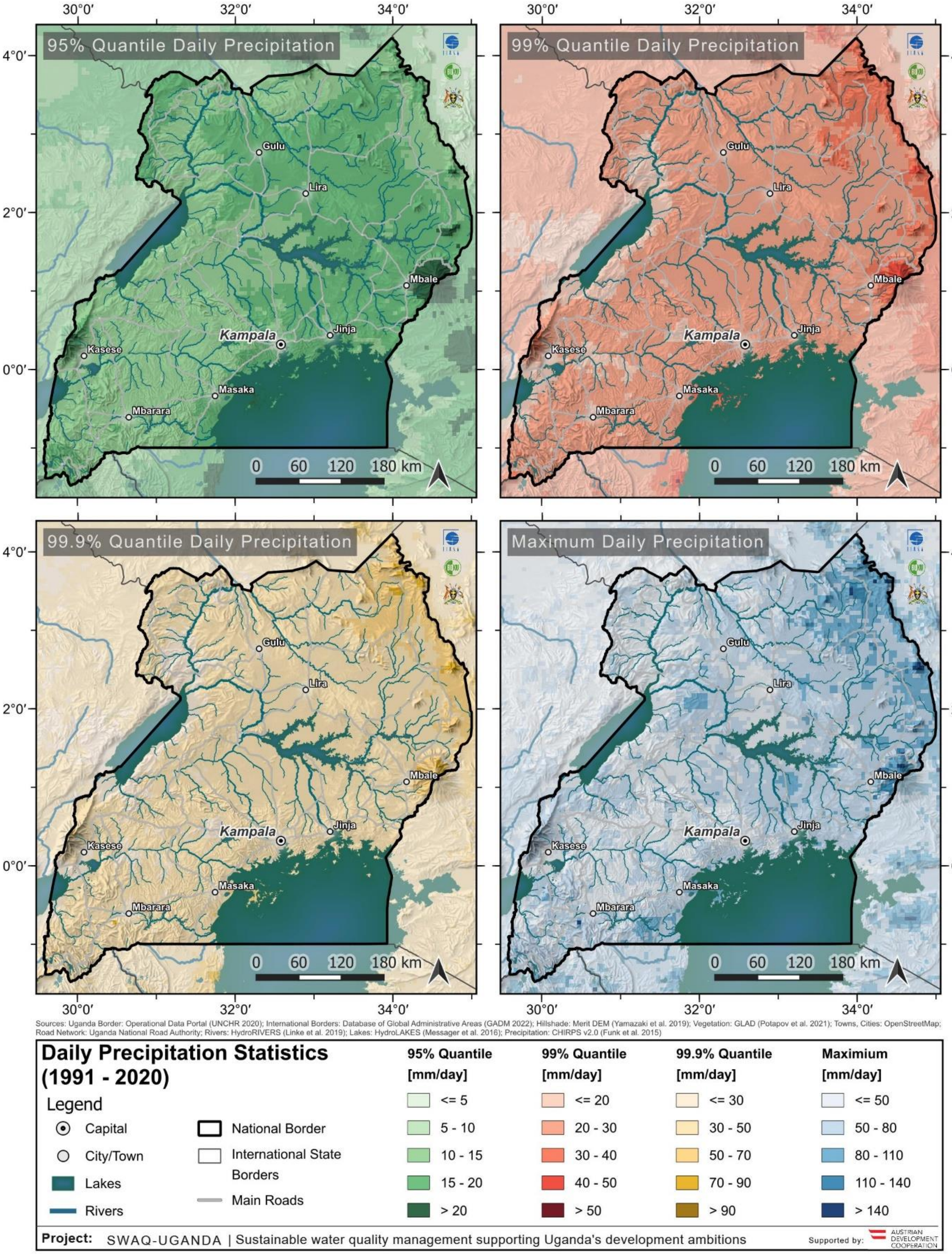

Figure 18: Daily precipitation extremes

Figure 18 displays different **daily precipitation extremes for the time period 1991 to 2020**. The Climate Hazards Group InfraRed Precipitation with Station data (CHIRPS) Version 2 dataset was used (Funk et al., 2015). This data has a resolution of 0.05° (~ 5.5 km).The four maps feature the 95 %, 99 %, and 99.9 % quantiles, as well as the maximum daily precipitation sum over the entire 30-year time span. A similar spatial pattern is observed in all figures. The strongest precipitation events occurred along the eastern border and in the Lake Victoria region. Extreme precipitation is also noted along the Rwenzori mountains at the southwestern border.

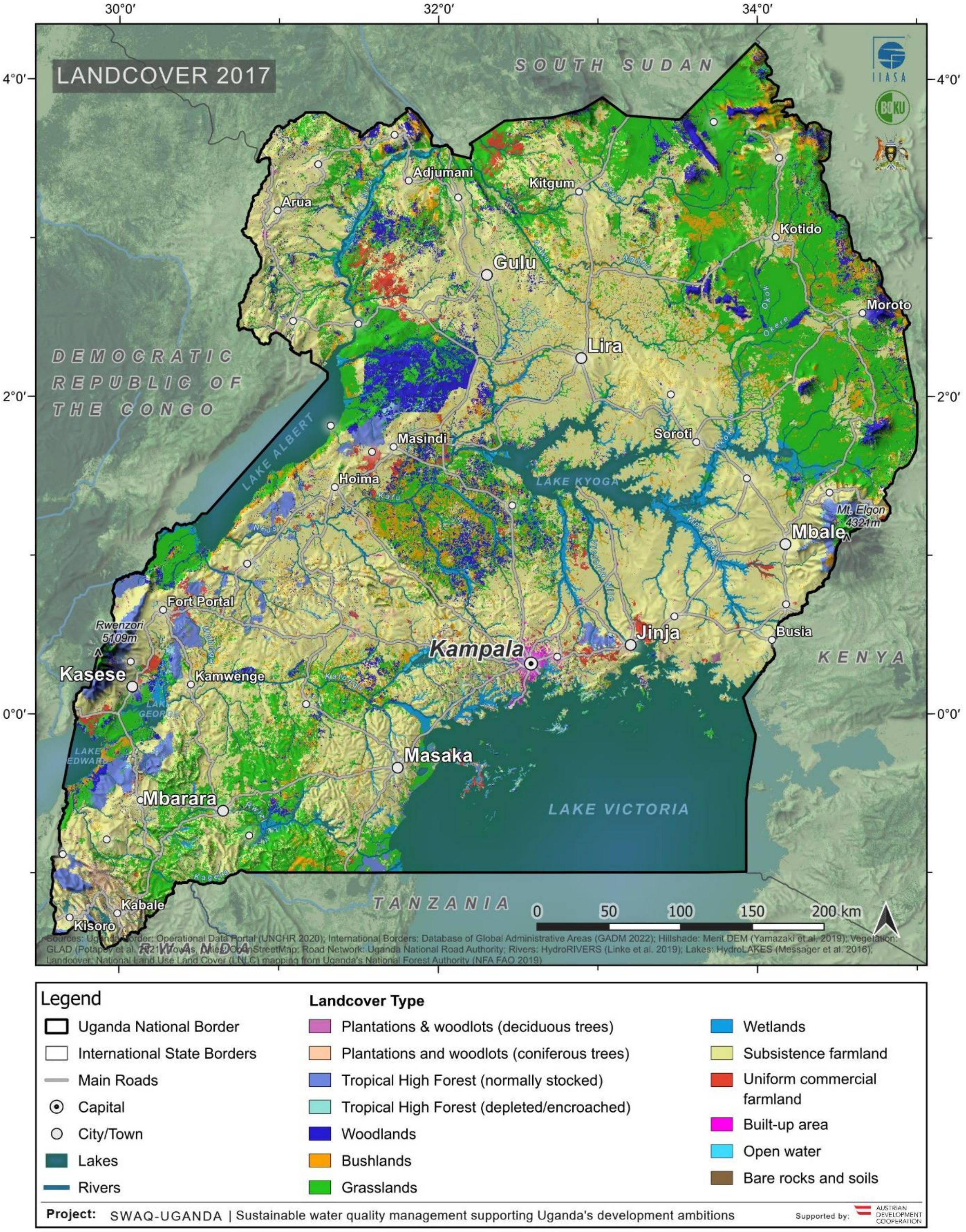

Figure 19: Uganda Landcover

Figure 19 presents **landcover** in Uganda in 2017. This landcover dataset was produced by Uganda's National Forest Authority (NFA) in cooperation with FAO and was obtained from the FAO Map Catalog (NFA & FAO, 2019). The National Biomass Study (NBS) classification system includes 13 LULC classes: Plantations & woodlots (deciduous trees/broadleaves), Plantations & woodlots (coniferous trees), Tropical High Forest (THF) normally stocked, Tropical High Forest (THF) depleted/encroached, Woodland (trees & shrubs average height > 4m), Bushland (bush, thickets, scrubs average height < 4m), Grassland (rangelands, pastureland, open Savannah), Wetlands (wetland vegetation; swamp areas, papyrus and other sedges), Subsistence farmland (mixed farmland, small holdings), Uniform commercial farmland (mono-cropped, non-seasonal farmland), Built-up areas (urban or rural), Open water (Lakes, rivers, and ponds), and Impediments (bare rocks and soils). Dominant landcover types in Uganda include subsistence farmland and grasslands.

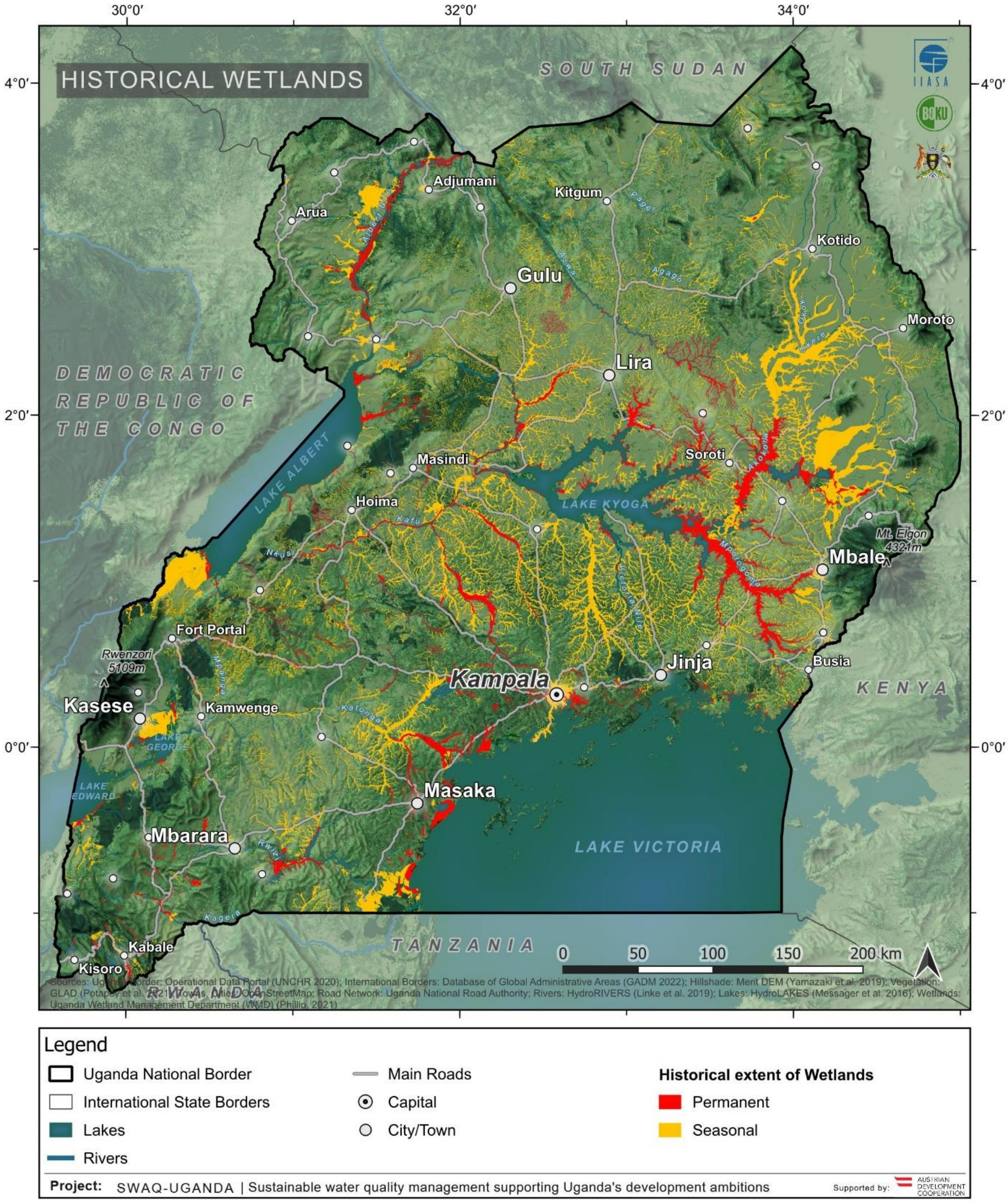

Figure 20: Historical wetlands in Uganda

Figure 20 exhibits the **historical wetland distribution** of Uganda. Historical wetland data was derived from a 2008 dataset obtained from the Wetland Management Department (WMD) and published online by the National Environment Management Authority (Phillip, 2021b). The original dataset classes included currently built up areas, floating vegetation, grassland, palms and thickets, papyrus, sedges subsistence farmland, and swamp forest. These classes were reclassified to display seasonal and permanent wetlands. All classes were included to present the historical wetland extent.

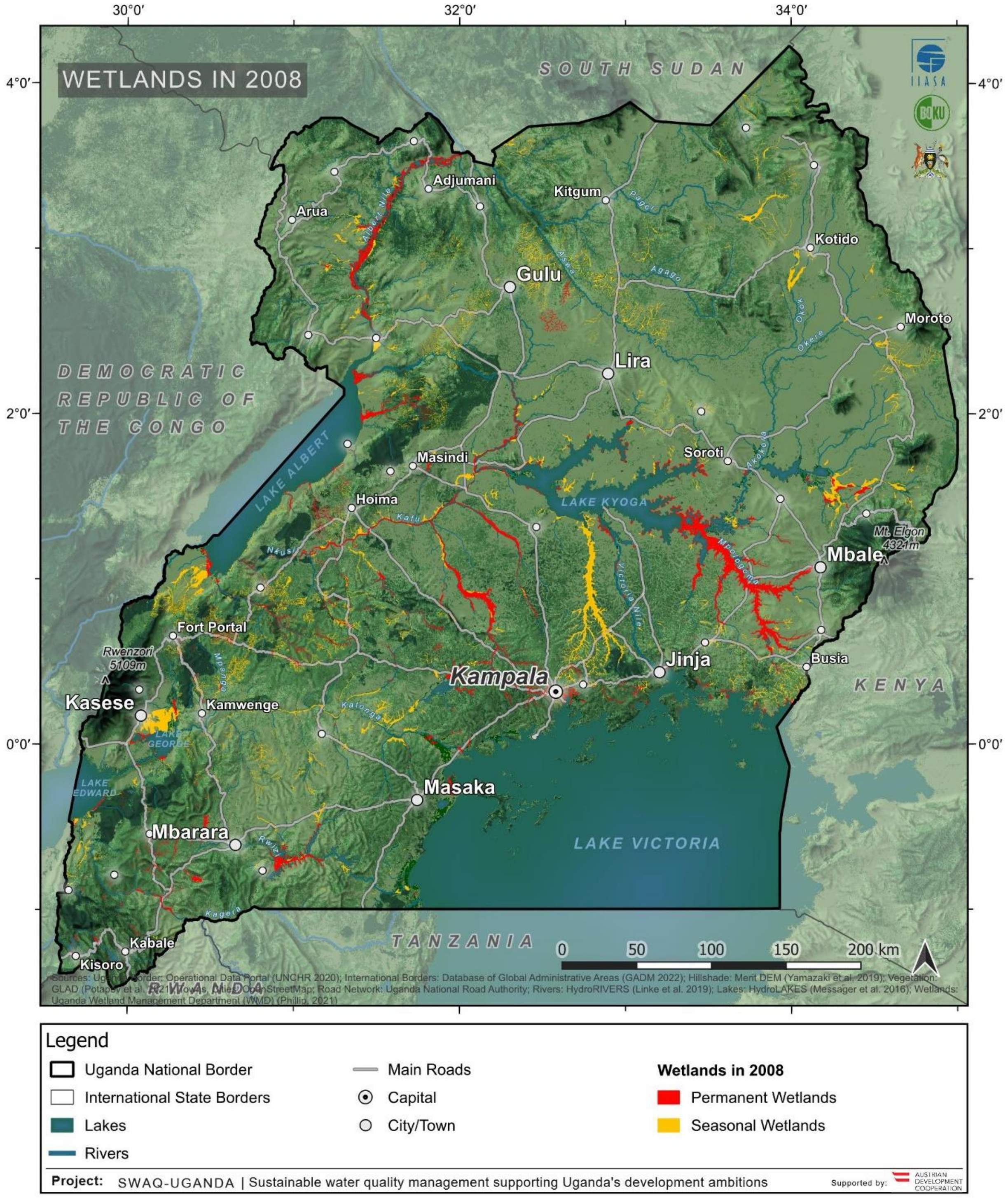

Figure 21: Wetlands in Uganda in 2008

Figure 21 shows **wetland distribution in Uganda in 2008**. This dataset, obtained from the Wetland Management Department (WMD), was published by the National Environment Management Authority (Phillip, 2021b). The original dataset classes included built up areas, floating vegetation, grassland, palms and thickets, papyrus, sedges subsistence farmland, and swamp forest. However, for presentation of the 2008 wetland distribution, several classes were excluded. Farmlands, grasslands, and built-up wetlands were excluded due to degradation of wetlands associated with those landcover types. The remaining categories were reclassified to show seasonal and permanent wetlands. Significantly less wetlands are observed in this iteration when compared to the historical wetland extent in Figure 20.

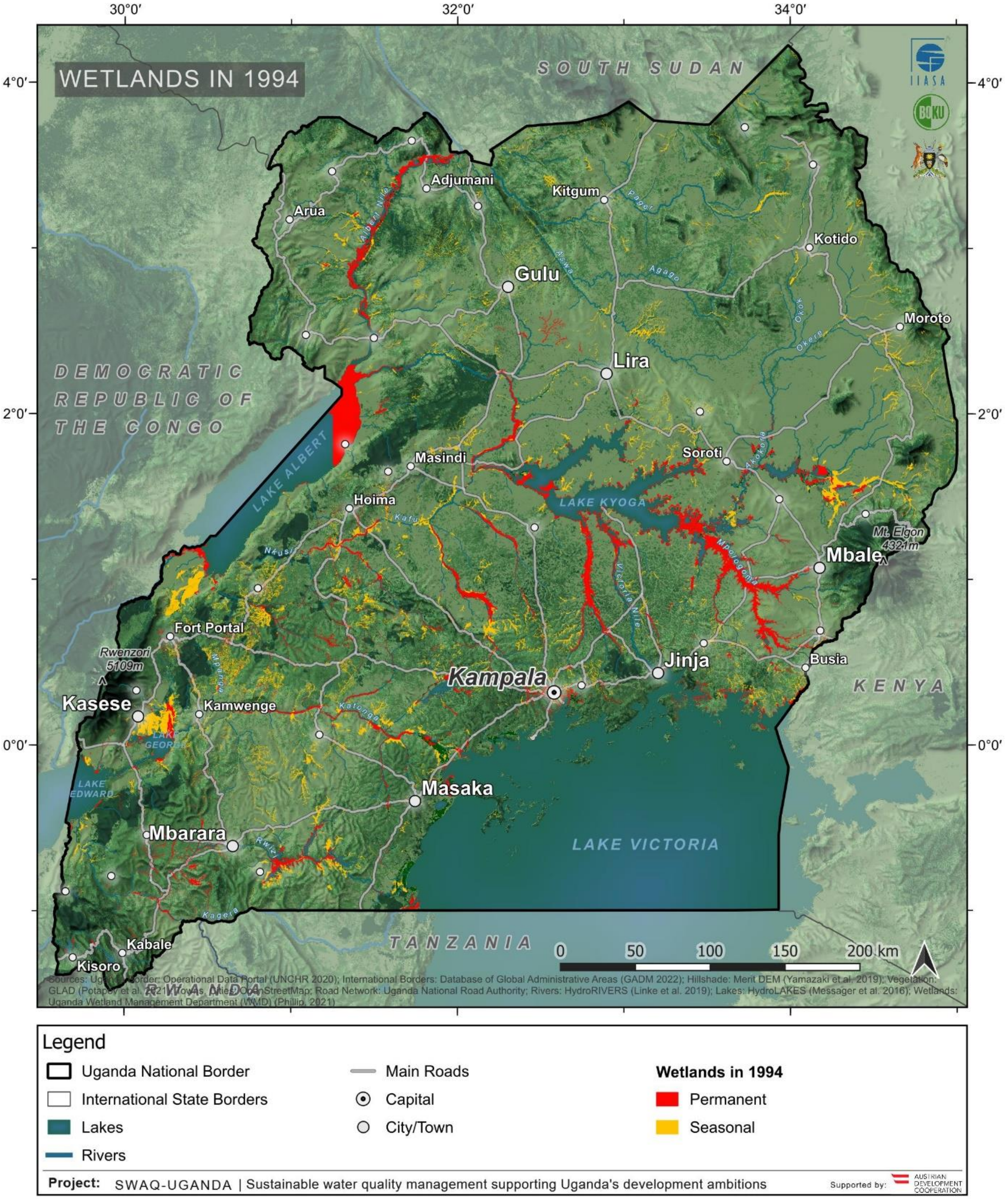

Figure 22: Wetlands in Uganda in 1994

Figure 22 displays the **wetland distribution in Uganda from 1994**. This dataset, obtained from the Wetland Management Department (WMD), was published by the National Environment Management Authority (Phillip, 2021a). Similarly to Figure 21, farmlands, grasslands and built-up wetlands were excluded due to degradation of wetlands associated with those landcover types. Data were reclassified to display seasonal and permanent wetlands. Documented wetland distribution in 1994 shows some differences compared to wetlands in 2008. Specifically, there is a larger area of wetlands North of Lake Albert in the 1994 dataset. Discrepancies in these two datasets are likely due to changes in data collection methods.

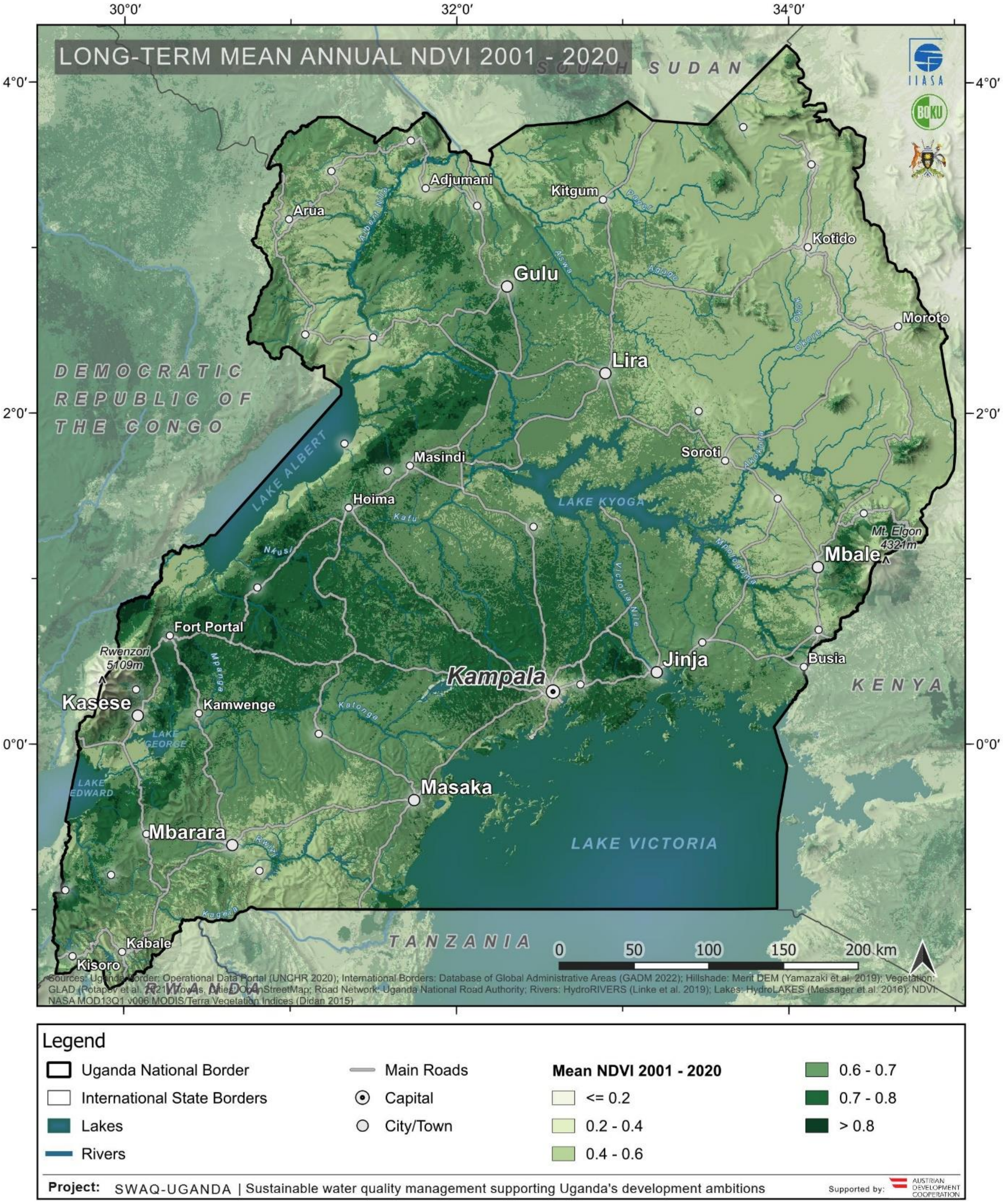

Figure 23: Long-term mean Normalized Difference Vegetation Index (NDVI; 2001-2020)

Figure 23 presents the **long-term mean annual vegetation conditions** based on the Normalized Difference Vegetation Index (NDVI) from 2001-2020. The NDVI value serves as a proxy for vegetation cover and is often used for assessing vegetation health and density. NDVI values range from -1 to 1. Lower NDVI values (<0.2) generally indicate areas with little to no vegetation, such as water, snow, or bare ground. Values between 0.2 and 0.4 represent sparse vegetation like grasslands or shrubs. Moderate vegetation cover, as observed in agricultural areas or transitional forests, fall within the range of 0.4 to 0.6. NDVI values between 0.6 and 0.7 often signify healthy, lush vegetation, while values above 0.7 indicate dense, green vegetation like rainforests. This dataset was obtained from NASA's MOD13Q1 MODIS/Terra Vegetation Indices 16-Day L3 Global 250m dataset and has a resolution of 250m (Didan, 2015). The dataset is available at https://doi.org/10.5067/MODIS/MOD13Q1.006.

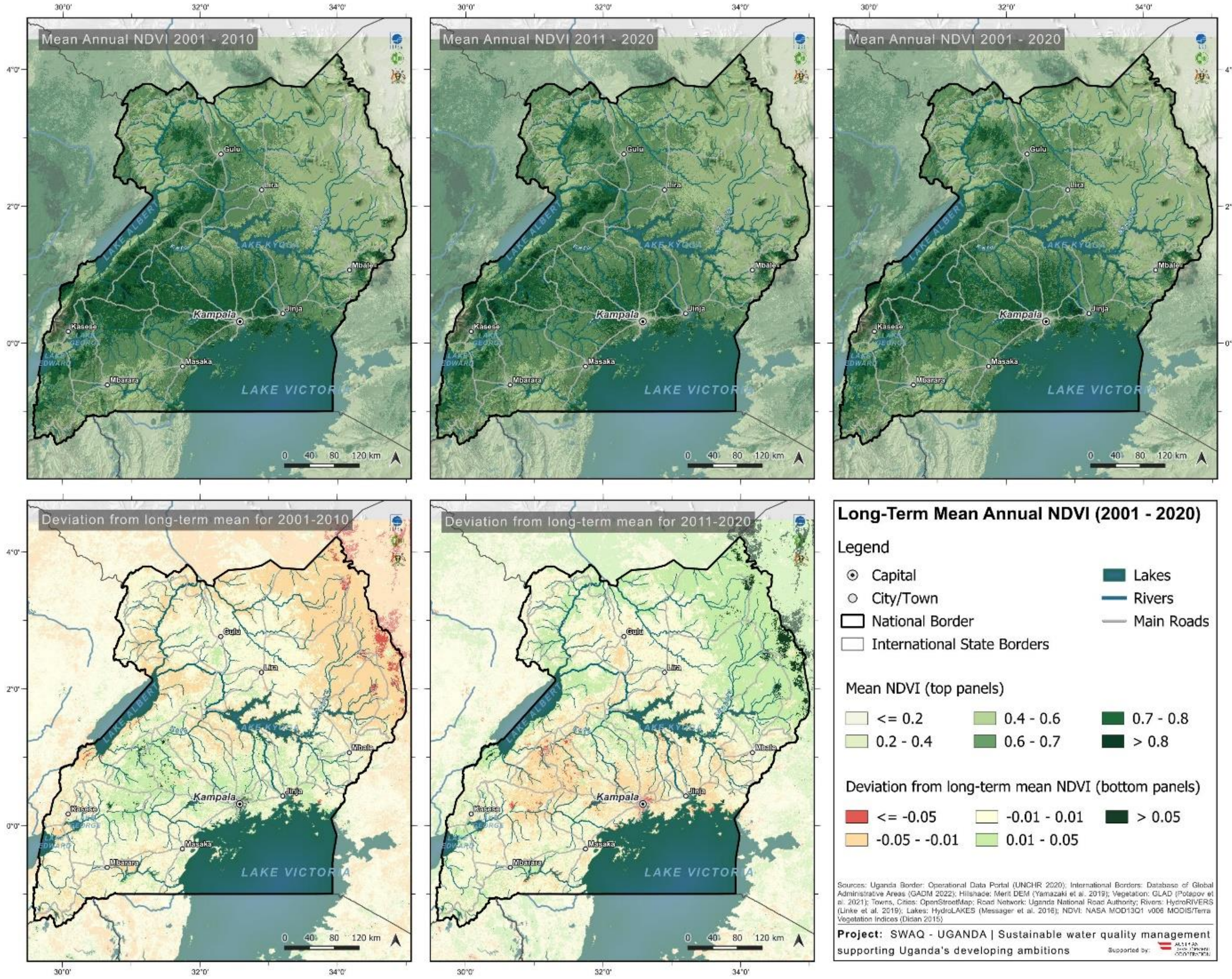

Figure 24: Vegetation Dynamics – NDVI

Figure 24 shows the **decadal mean annual Normalized Difference Vegetation Index** (NDVI) and deviations for the decades between 2001 and 2020. The decadal NDVI spatial trends are displayed in the top left two panels representing the annual average NDVI for 2001-2010 and 2011-2020 respectively. The long-term mean annual NDVI from 2001 to 2020 is presented in the top right panel for comparison. The spatial distribution of vegetation is similar in both decades with lower NDVI values more prevalent in the northeast. The period from 2001 to 2020 shows lower values in northwest Uganda, central Uganda and in the west of Kamapala, compared to the period from 2011 to 2020. In the bottom panels, the decadal NDVI deviations from the long-term mean are shown. Opposite spatial patterns are observed in the deviation figures for these two decades. For the period from 2001 to 2010, NDVI values were higher than the long-term average in central Uganda, and lower in the northeastern and western regions. The opposite trend was observed when examining deviations for the following decade. Positive deviations (higher NDVI values than the long-term mean) may indicate more vegetation during that decade compared to the long-term average. Positive deviations (>= 0.05) were observed in the northeast along the border to Kenya for the 2011 – 2020 decade. Negative deviations (decreased NDVI compared to the long-term average) were observed at the same scale in the same region for the 2001 – 2010 decade. These data were derived from NASA's MOD13Q1 MODIS/Terra Vegetation Indices 16-Day L3 Global 250m dataset (Didan, 2015) and have a resolution of 250 m.

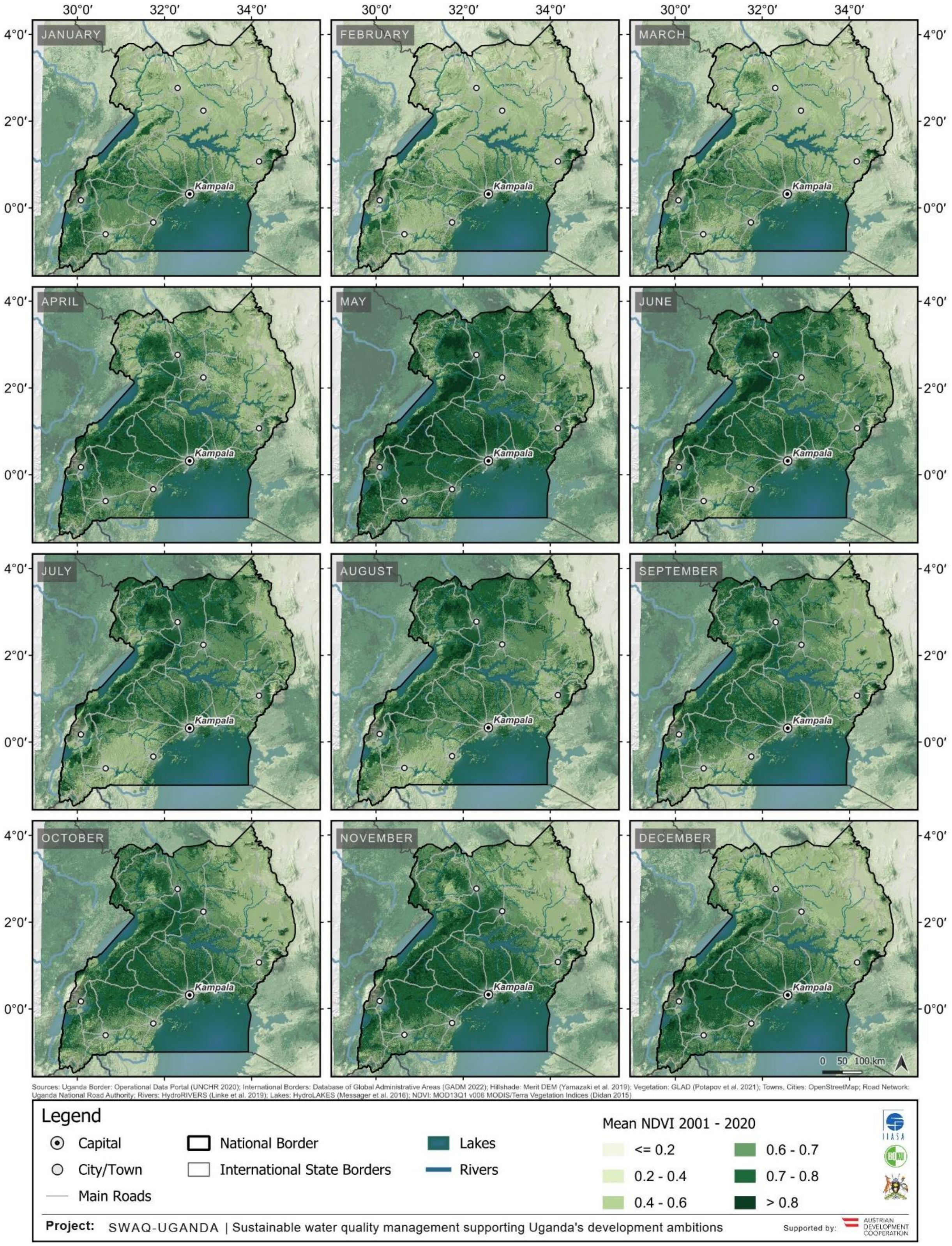

Figure 25: Long-term mean monthly NDVI (2001-2020)

Figure 25 displays the **long-term mean monthly Normalized Difference Vegetation Index (NDVI)** characteristics for the time period 2001 to 2020. Similar to monthly precipitation trends, the mean monthly NDVI follows a seasonal pattern with regional differences. The lowest NDVI values are generally found in the north and northeast regions, with the north experiencing the lowest vegetation cover in January. Low vegetation cover is also noted in February and March. The highest average monthly NDVI throughout the country appears in May. Vegetation cover slightly decreases after May. In September, NDVI values slightly increase again. The vegetation index is given in a resolution of 250 m and derived from MOD13Q1 MODIS/Terra Vegetation Indices 16-Day L3 Global 250m dataset (Didan, 2015).

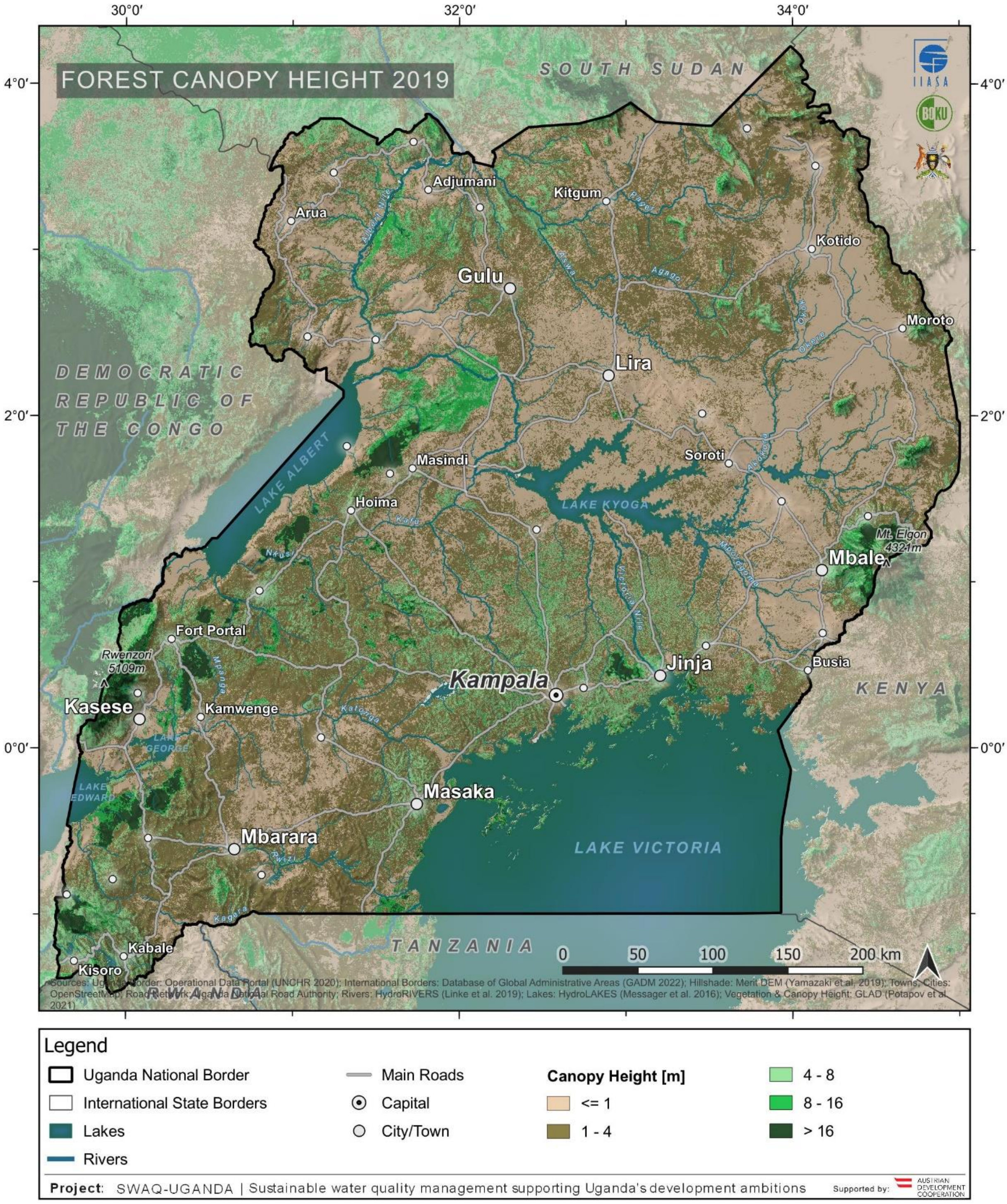

Figure 26: Forest canopy height (2019)

Figure 26 represents the **forest canopy height in 2019**. This dataset was obtained from the Global Land Analysis and Discovery (GLAD) laboratory at the University of Maryland (Potapov et al., 2021). Canopy height measurements were extrapolated by (Potapov et al. (2021) using Landsat data. The spatial resolution of this dataset is 30 m. Generally, the highest canopy heights (16-60 m) were observed in protected areas. For instance, high canopy heights are visualized in the Rwenzori Mountains National Park, Mount Elgon National Park, Queen Elizabeth National Park, Murchison Falls National Park, Kibale National Park and Mabira Central Forest Reserve. Lower canopy heights were observed north of Lake Kyoga, and in the northeast and eastern regions.

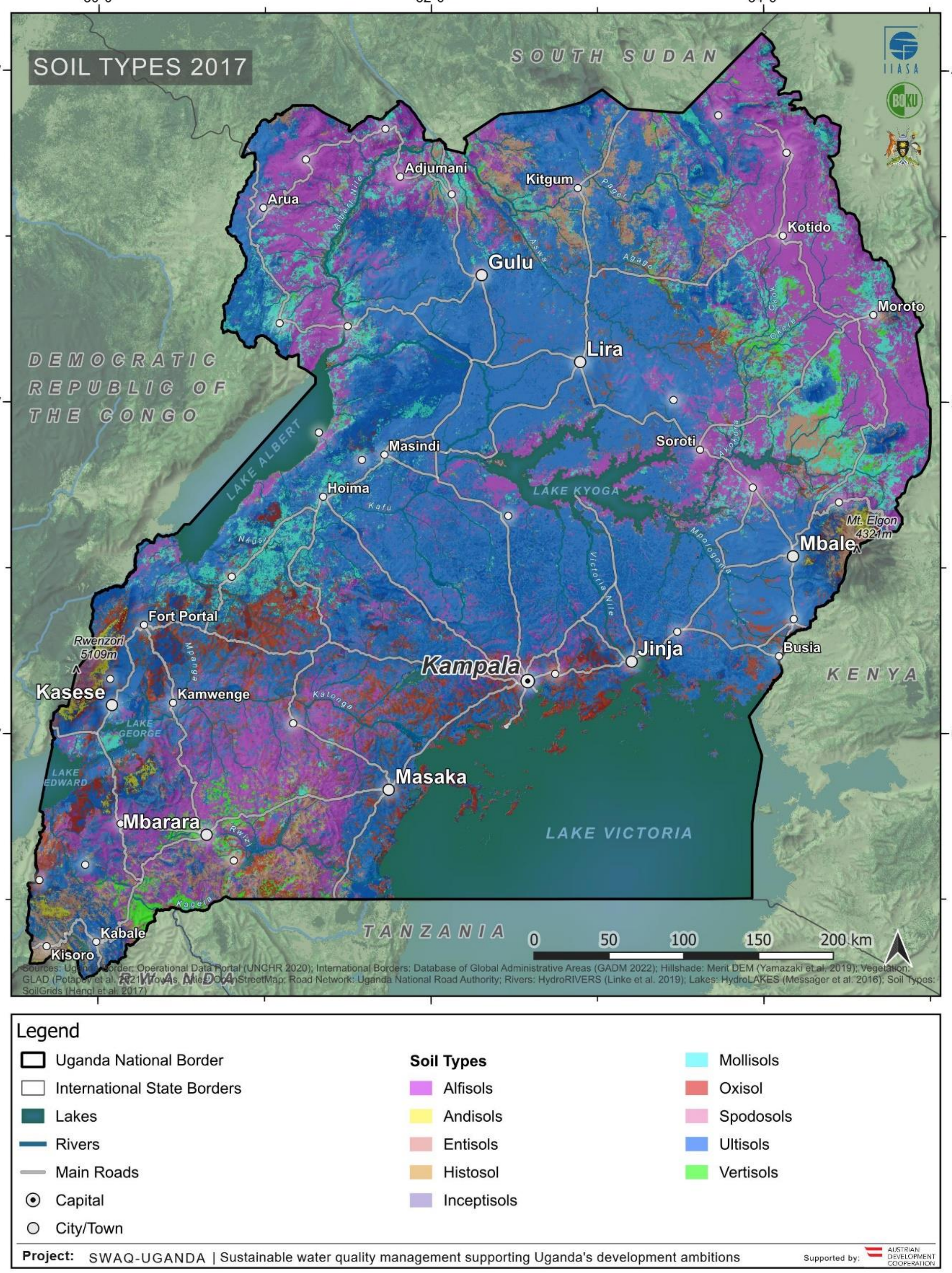

Figure 27: Soil types in Uganda

Figure 27 shows the distribution of **soil types** in Uganda based on taxonomy from the United States Department of Agriculture (USDA). The soil data presented is part of the SoilGrids 250m dataset which was produced using machine learning by (Hengl et al., 2017). This dataset was obtained from World Soil Information (ISRIC) at https://www.isric.org/explore/soilgrids/faq-soilgrids-2017. Soil types in central Uganda are relatively homogenously dominated by ultisols. Ultisols are the most prevalent type of soil type in Uganda followed by alfisols.

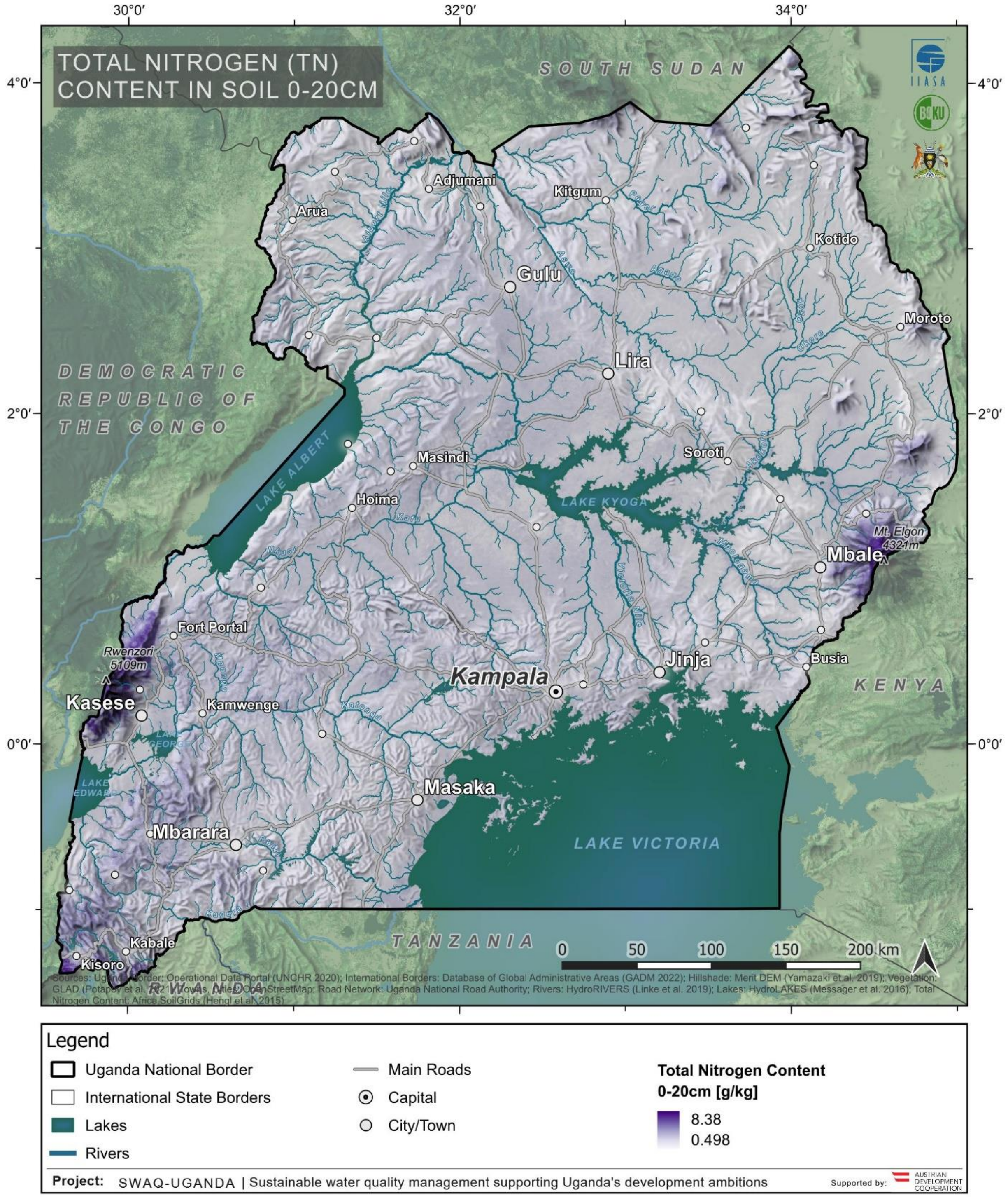

Figure 28: Total Nitrogen content at soil depth of 0-20cm

Figure 28 depicts **total nitrogen** content of the fine earth fraction in the **topsoil** at 0-20 cm of depth. The concentration of total nitrogen in this soil layer ranges from 0.5 to 8.4 g/kg. Nitrogen in the topsoil can reach surface waters via leaching and soil erosion. In the upper soil layer, total nitrogen concentrations are highest in the Mount Elgon region, eastern Uganda, and the Mount Rwenzori region in southwestern Uganda. This dataset was obtained from (Hengl et al. (2015) and has a resolution of 250m. It was produced using remote sensing imagery, sample datasets from the Africa Soil Information Service (AfSIS) project, and a machine learning algorithm (Hengl et al., 2015).

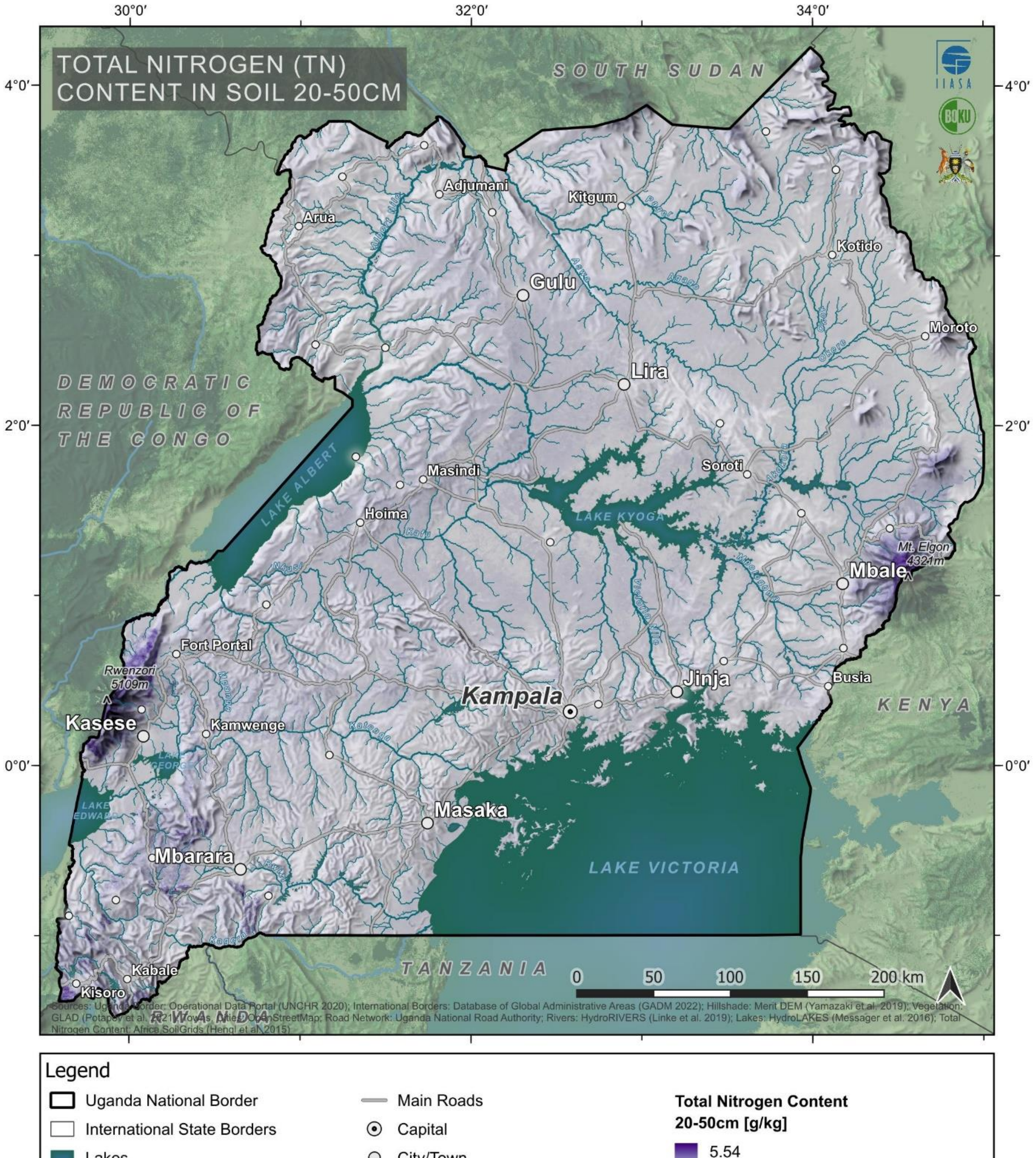

Figure 29: Total Nitrogen content at soil depth of 20-50cm

Figure 29 presents **total nitrogen** content of the fine earth fraction in the **subsoil** at depths of 20 to 50 cm. The concentration ranges from 0.3-5.5 g/kg in this soil layer. Spatial trends of total nitrogen in the subsoil are very similar to those of the upper soil layer. Total nitrogen concentrations in the subsoils are highest in the Mount Elgon region, eastern Uganda, and the Mount Rwenzori region in southwestern Uganda. This dataset was obtained from (Hengl et al. (2015) and has a resolution of 250 m. It was produced using remote sensing imagery, sample datasets from the Africa Soil Information Service (AfSIS) project, and a machine learning algorithm (Hengl et al., 2015).

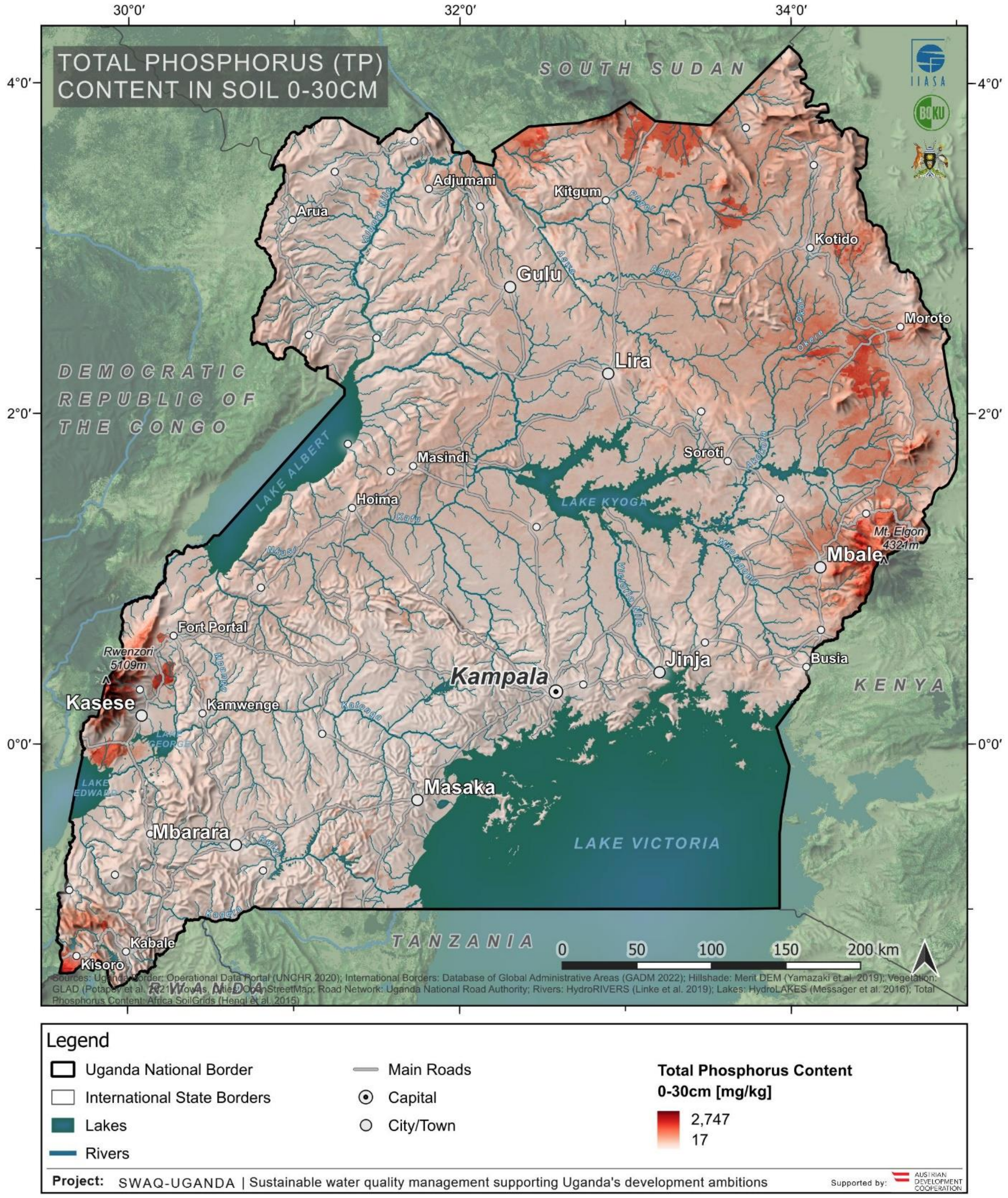

Figure 30: Total Phosphorus content at soil depth 0-30cm

Figure 30 shows **total phosphorus concentrations in the soil layer at a depth of 0-30cm**. Total phosphorus concentration ranges from 17 to 2747 mg/kg. Total phosphorus concentrations are high in the northcentral, northeastern, and southwestern regions of Uganda. This dataset was obtained from Hengl et al. (2015) and has a resolution of 250m. It was produced using remote sensing imagery, sample datasets from the Africa Soil Information Service (AfSIS) project, and a machine learning algorithm (Hengl et al., 2015).

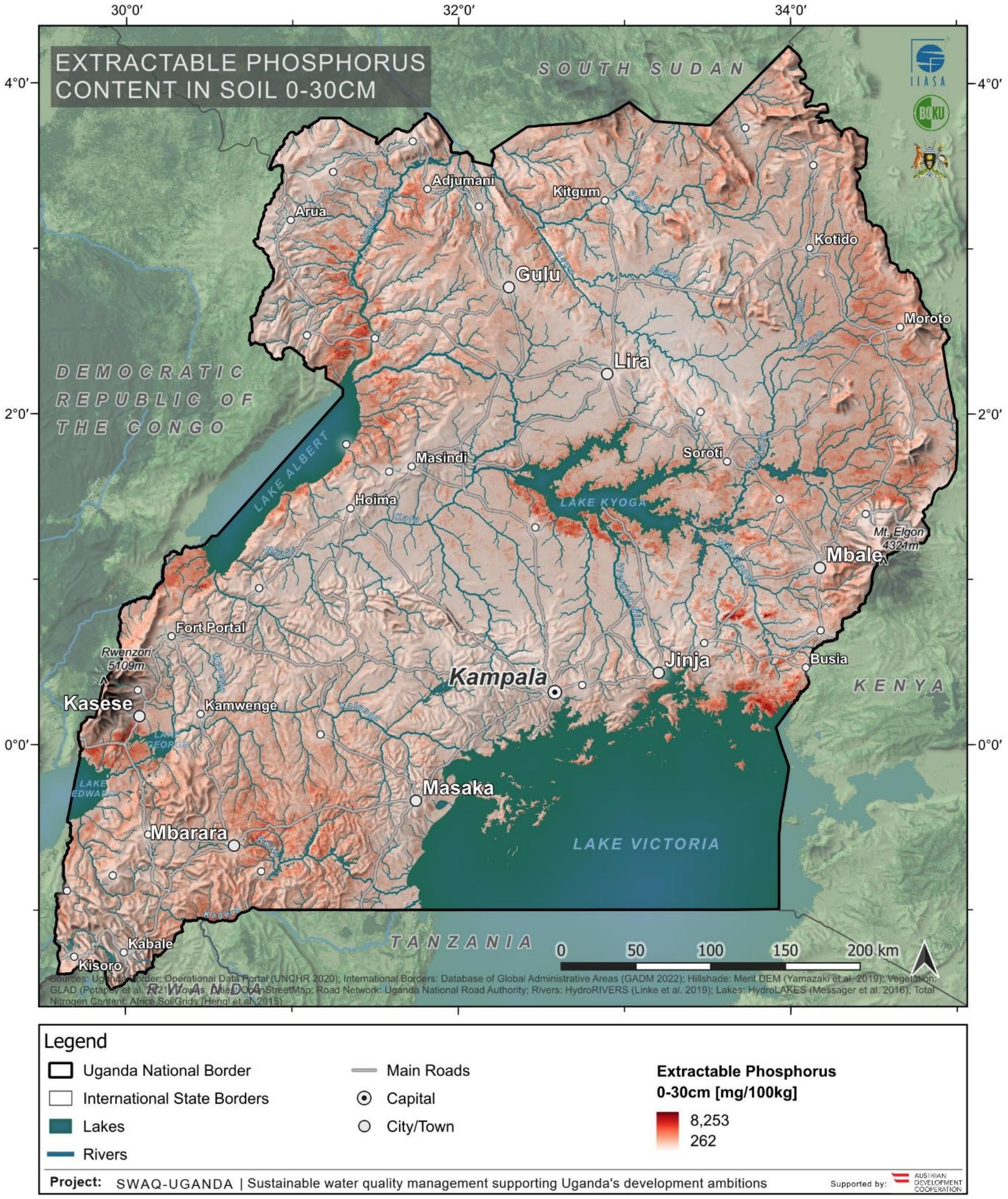

Figure 31: Extractable Phosphorus content at soil depth 0-30cm

Figure 31 presents **extractable phosphorus concentrations at soil depths of 0 to 30 cm**. The concentration of extractable phosphorus ranges from 262 to 8253 mg/100kg. Extractable phosphorus concentration is highest around lakes and rivers. This dataset was obtained from (Hengl et al. (2015) and has a resolution of 250m. It was produced using remote sensing imagery, sample datasets from the Africa Soil Information Service (AfSIS) project, and a machine learning algorithm (Hengl et al., 2015).

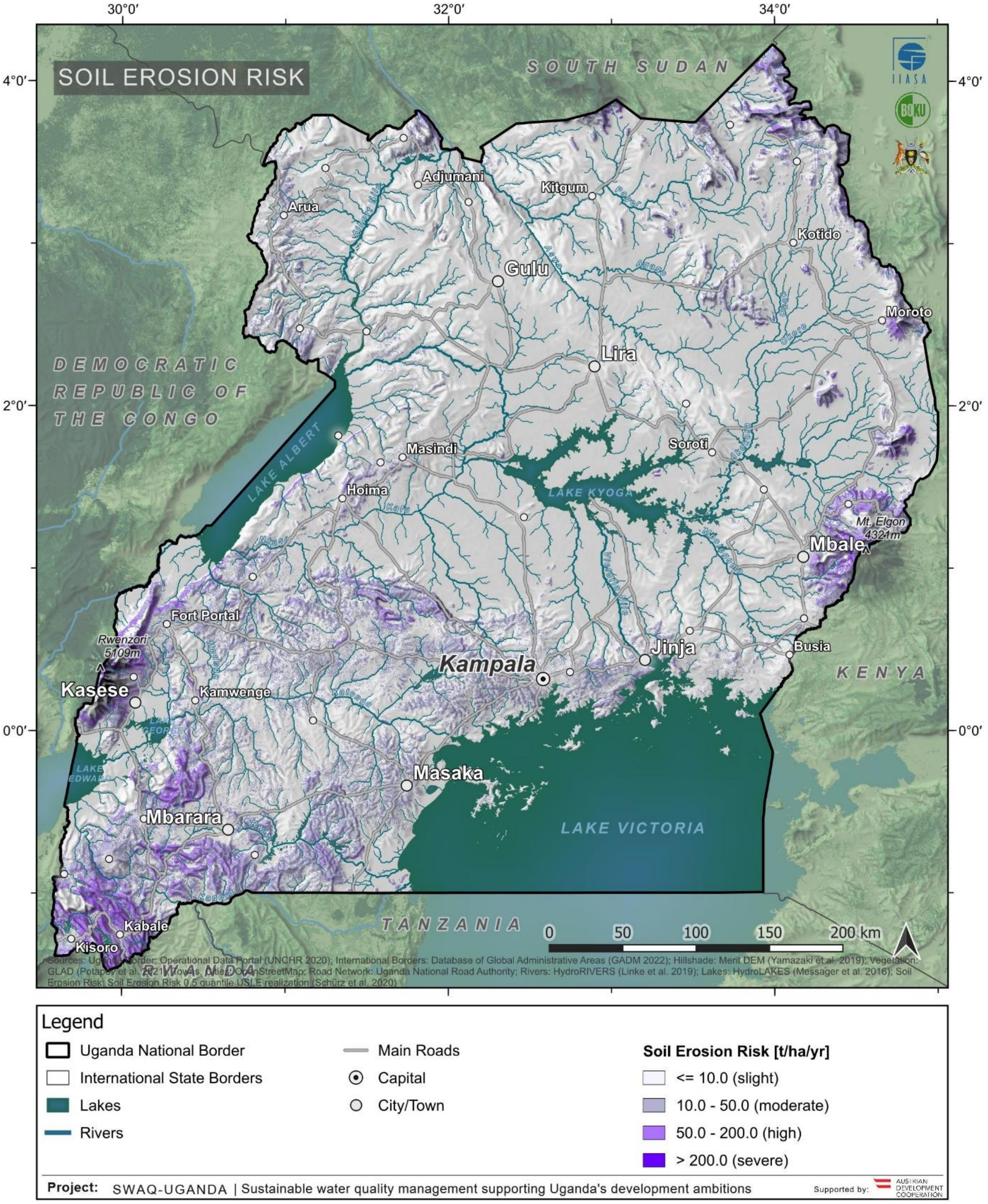

Figure 32: Soil erosion risk

Figure 32 displays the **annual average soil erosion risk** in tons of soil loss per hectare. This dataset shows the potential soil loss risk without considering soil water conservation practices. Higher risk of erosion is observed in areas with larger topographic gradients and steeper slopes. For example, high soil loss is observed in the Rwenzori mountains, around Mount Elgon, and in the southwest. Lower values occur in central and northeast Uganda. The data set was derived from (Schürz et al. (2020) and represents the median soil loss risk from 972 different model realizations. This dataset has 90m resolution.

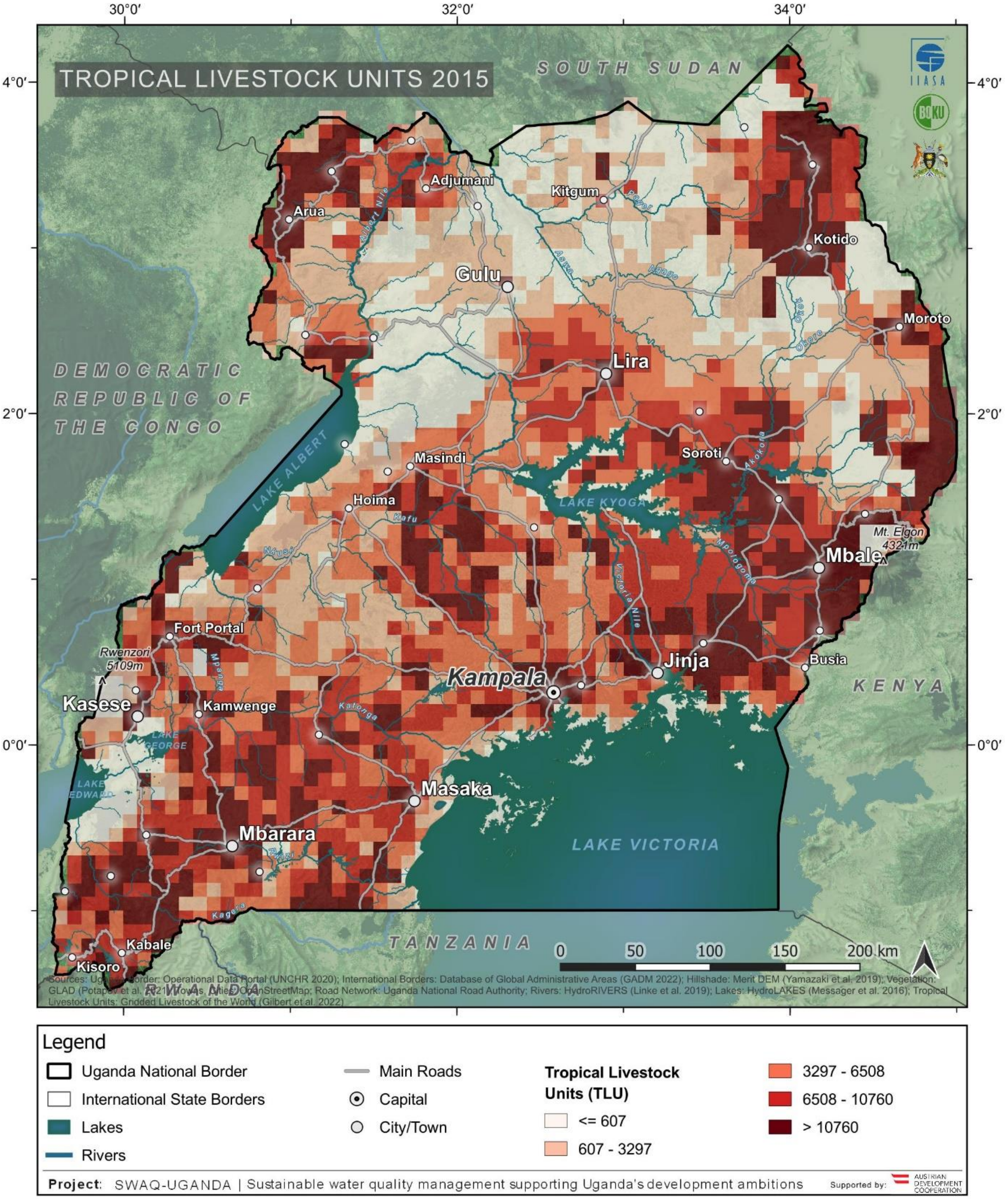

Figure 33: Tropical Livestock Units (TLUs)

Figure 33 shows the distribution of **Tropical Livestock Units (TLUs)** at a resolution of 5 arcminutes (approximately 9.3km at the equator). This data is based on the Gridded Livestock of the World v.4 database (GLW4) (Gilbert et al., 2022). GLW4 provides a global distribution of animals with a reference year of 2015. The values are expressed as the total number of animals per grid cell for sheep, pigs, horses, goats, ducks, cattle, chickens, and buffalo. Tropical Livestock Units were calculated according to Njuki et al. (2011) and aggregated for all animal types to show total TLUs per pixel. The maximum TLU value of 100,292 is located directly northeast of Kampala. Additional high values are found in the Kampala City area and northeastern Uganda.

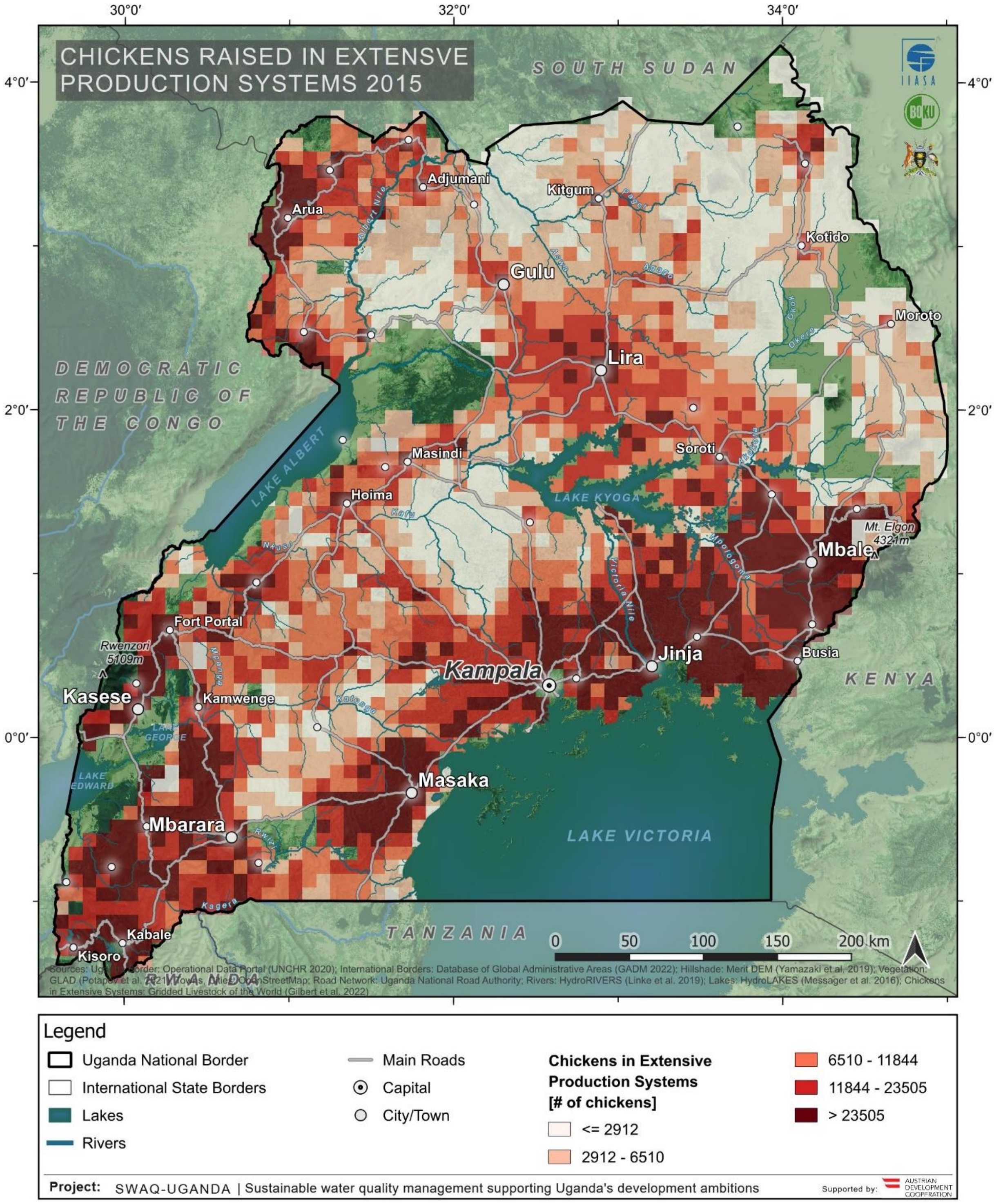

Figure 34: Chickens in extensive production systems

Figure 34 displays the number of **chickens raised in extensive production systems**. This data was obtained from the Gridded Livestock of the World v.4 database (GLW4) and has a resolution of 5 arcminutes (approximately 9.3km at the equator) (Gilbert et al., 2022). Higher densities of extensive chicken production are observed in the southwestern, southeastern, and northwestern regions.

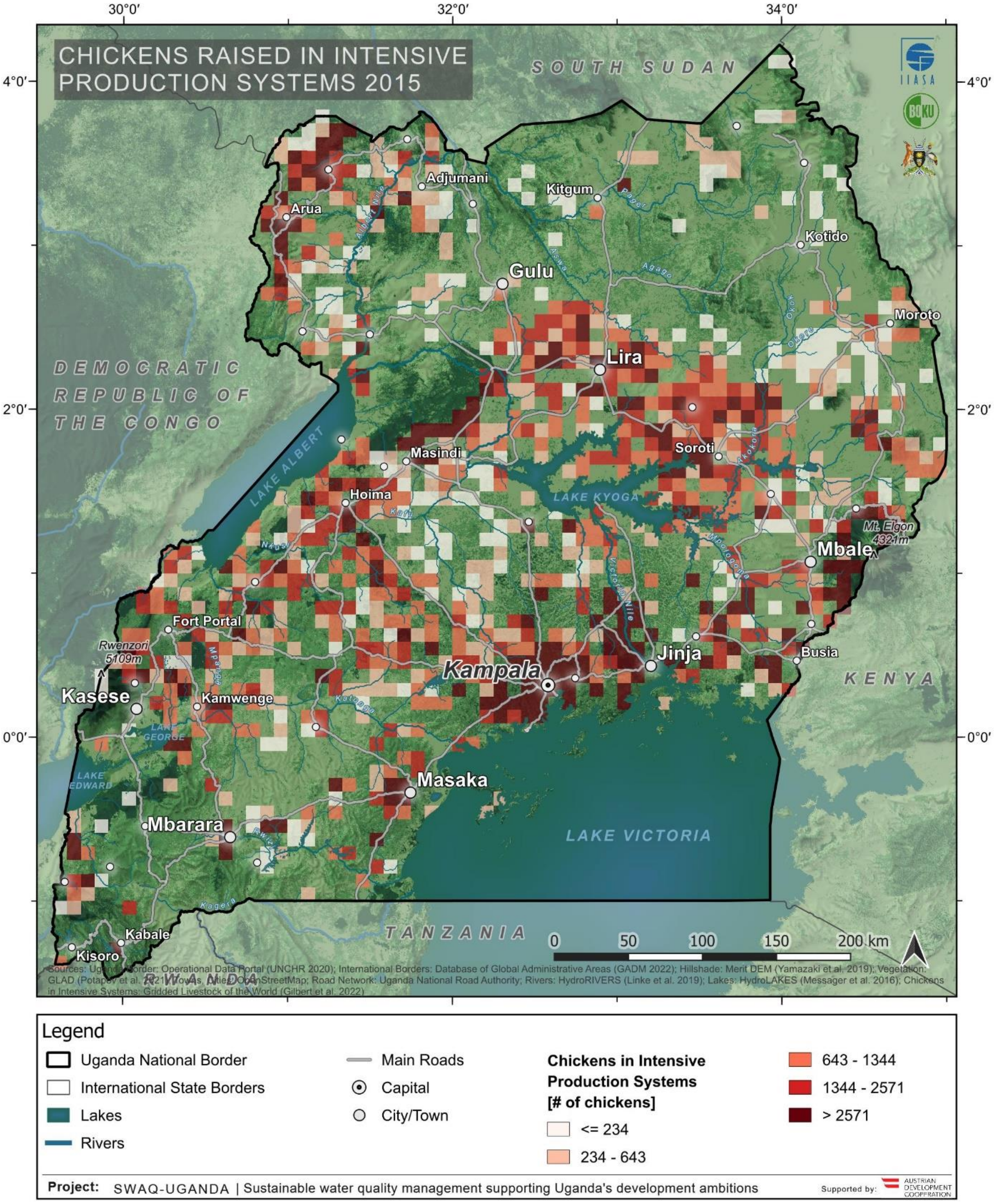

Figure 35: Chickens in intensive production systems

Figure 35 displays the number of **chickens raised in intensive production systems**. This data was obtained from the Gridded Livestock of the World v.4 database (GLW4) and has a resolution of 5 arcminutes (approximately 9.3km at the equator) (Gilbert et al., 2022). Higher densities of intensive chicken production are found around the Kampala area, east of Mbale, and west of Jinja.

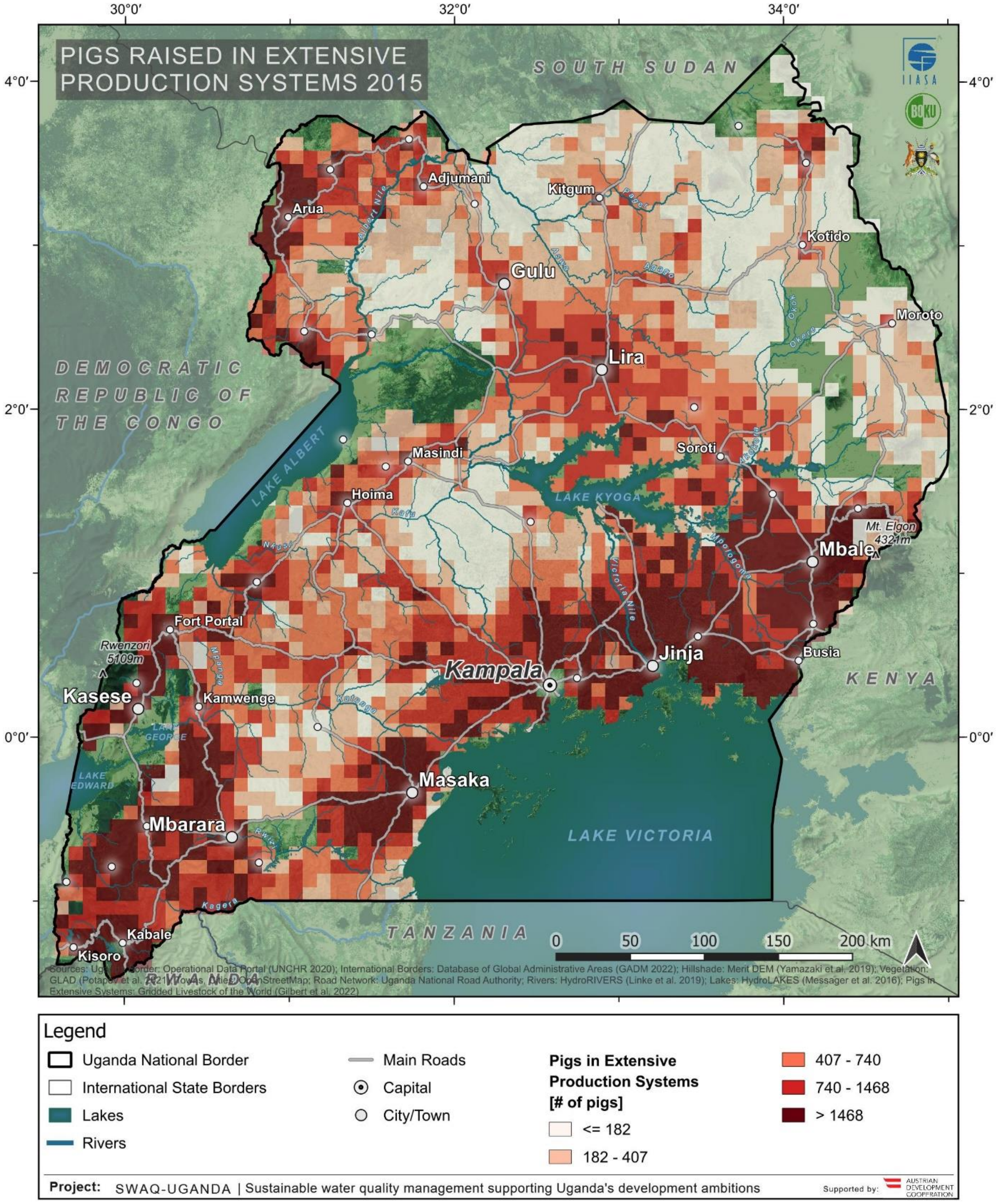

Figure 36: Pigs in extensive production systems

Figure 36 shows the number of **pigs raised in extensive production systems**. This data was obtained from the Gridded Livestock of the World v.4 database (GLW4) and has a resolution of 5 arcminutes (approximately 9.3km at the equator) (Gilbert et al., 2022). Extensive pig production follows a similar spatial pattern to extensive chicken production. Higher densities of extensive pig production are found in the southwestern, southeastern, and northwestern regions.

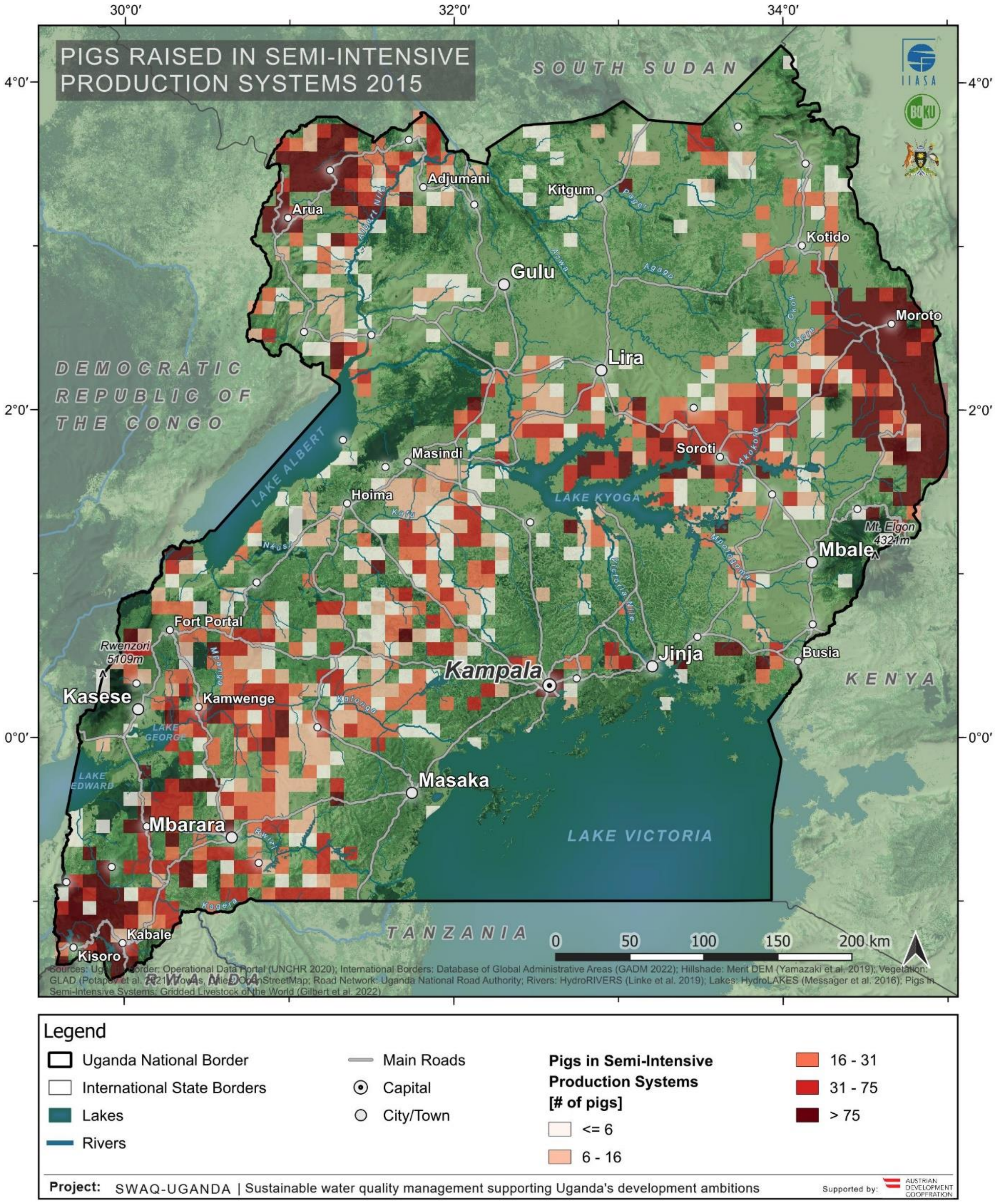

Figure 37: Pigs in semi-intensive production systems

Figure 37 presents the number of **pigs raised in semi-intensive production systems**. This data was obtained from the Gridded Livestock of the World v.4 database (GLW4) and has a resolution of 5 arcminutes (approximately 9.3km at the equator) (Gilbert et al., 2022). Higher densities of semi-intensive pig production are found in the northwest, southwest, and in the east along the border to Kenya between Mount Elgon and Moroto.

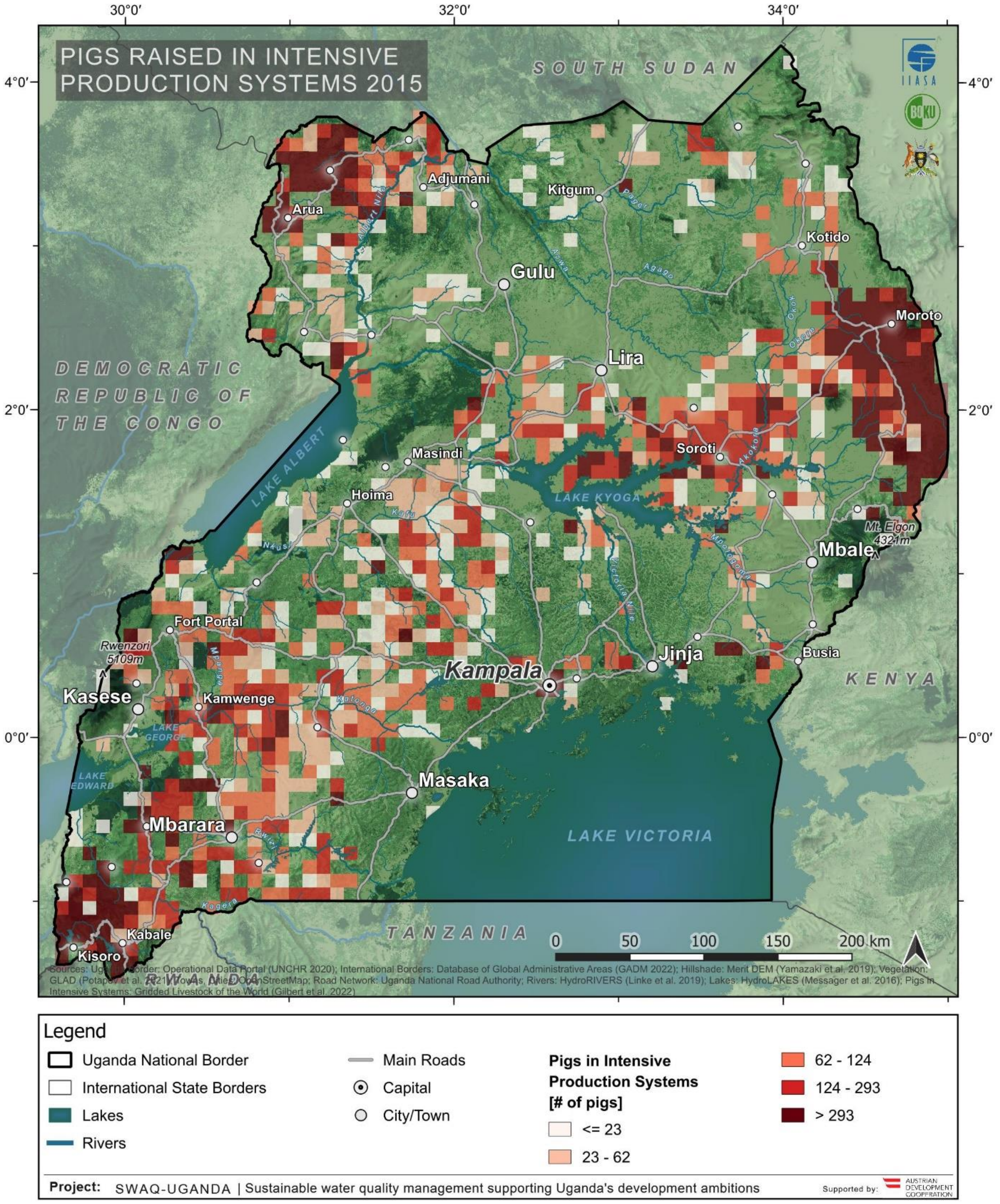

Figure 38: Pigs in intensive production systems

Figure 38 displays the number of **pigs raised in intensive production systems**. This data was obtained from the Gridded Livestock of the World v.4 database (GLW4) and has a resolution of 5 arcminutes (approximately 9.3km at the equator) (Gilbert et al., 2022). The spatial distribution of intensive pig production follows that of semi-intensive pig production. Higher densities of intensive pig production are found in the northwest, southwest and eastern regions.

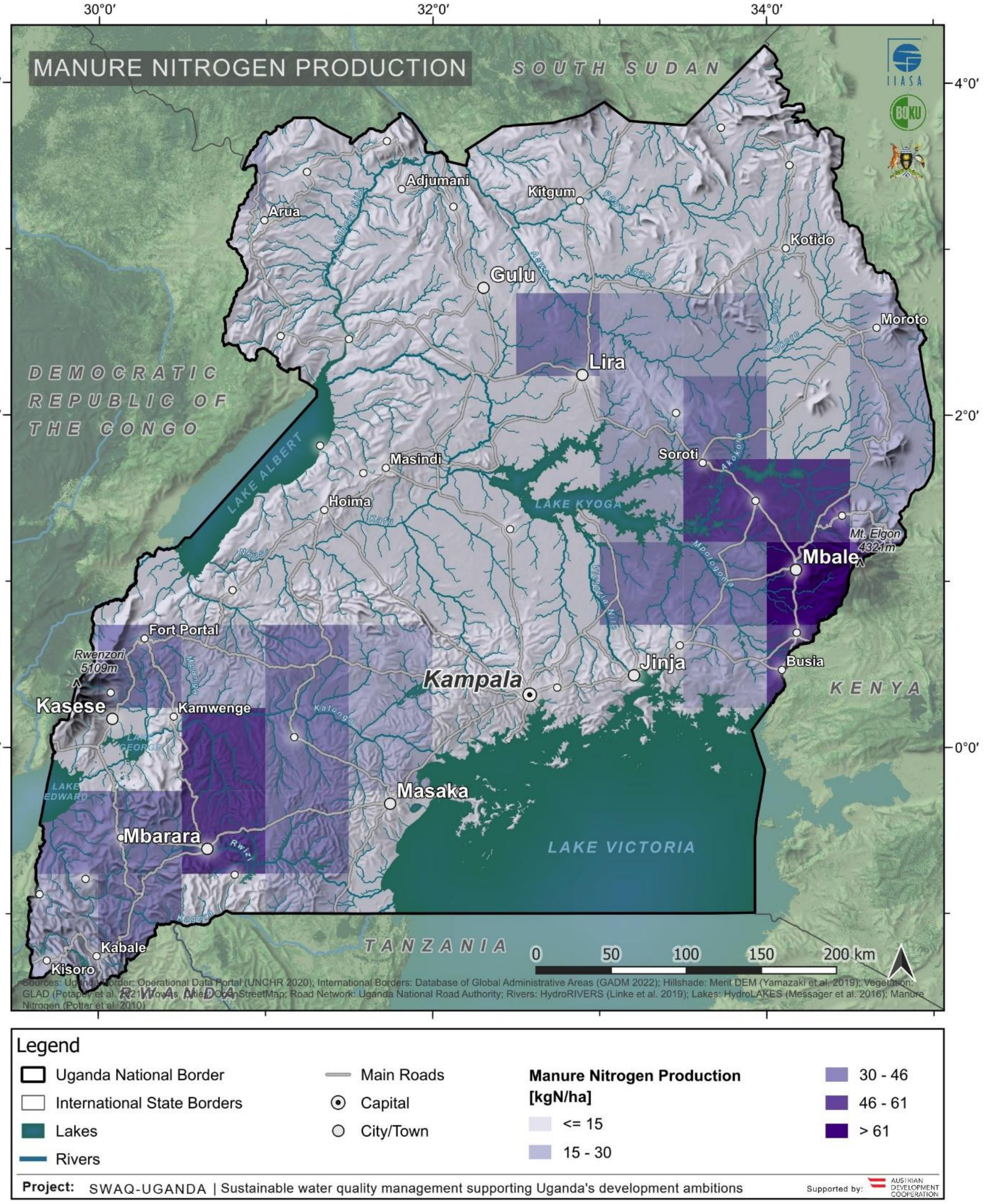

Figure 39: Nitrogen production from manure

Figure 39 shows **nitrogen production from all livestock manure**. This data obtained from Potter et al. (2010) considers livestock counts from the early 2000s. Manure estimates were based on livestock distribution from FAO Gridded Livestock of the World v1, and on the national average nutrient excretion rates from 2008 provided by the Organization for Economic Co-operation and Development (OECD) (Potter et al., 2010). The spatial resolution for this dataset is 0.5° (~ 55km). The maximum annual manure nitrogen production was estimated to be 75.93 kg/ha.

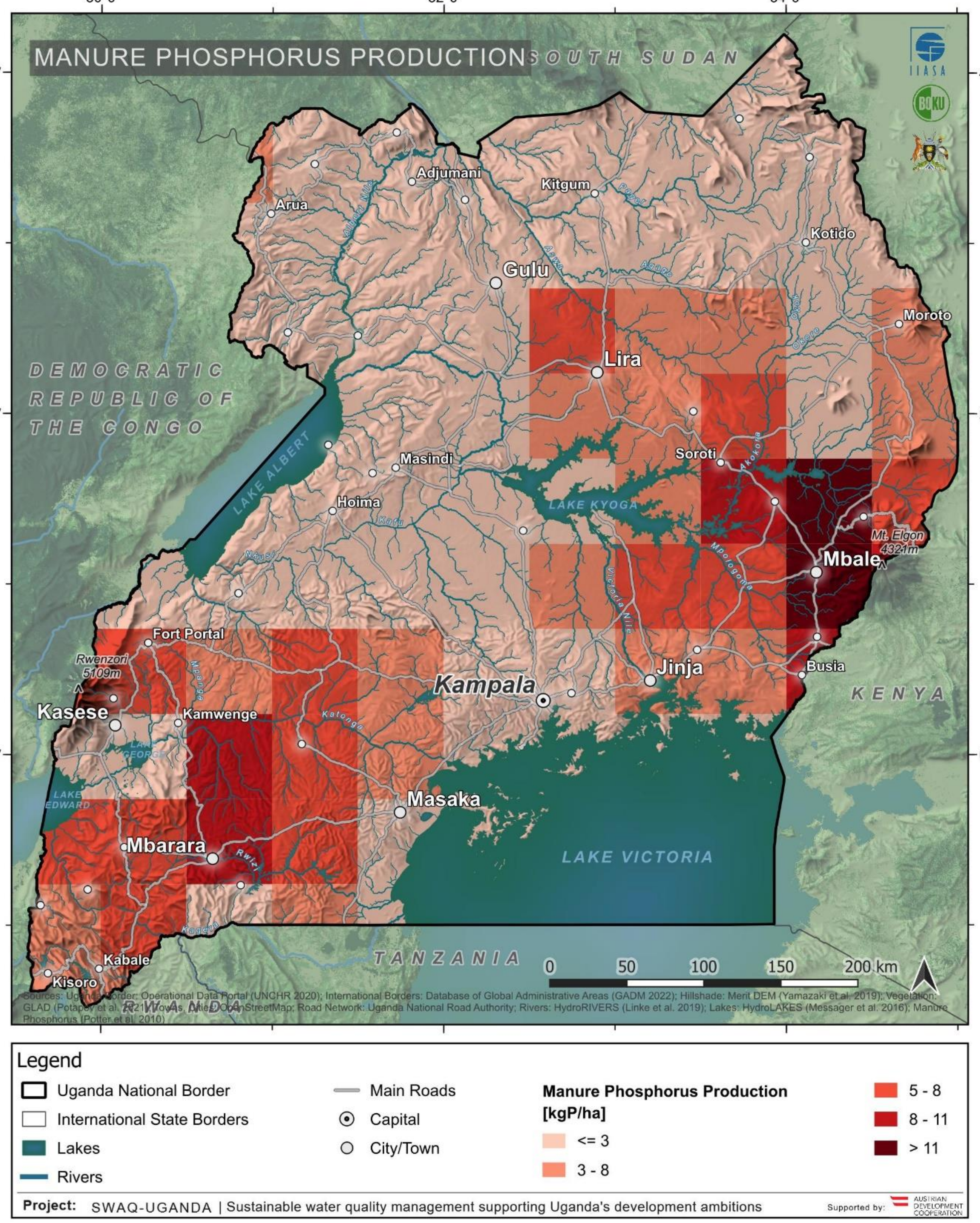

Figure 40: Phosphorus production from manure

Figure 40 displays **phosphorus production from all livestock manure**. This data obtained from Potter et al. (2010) considers livestock counts from the early 2000s. Manure estimates were based on livestock distribution from FAO Gridded Livestock of the World v1, and on the national average nutrient excretion rates from 2008 provided by the Organization for Economic Co-operation and Development (OECD) (Potter et al., 2010). The spatial resolution for this dataset is 0.5° (~ 55 km). The maximum annual manure phosphorus production was estimated to be 13.38 kg/ha.

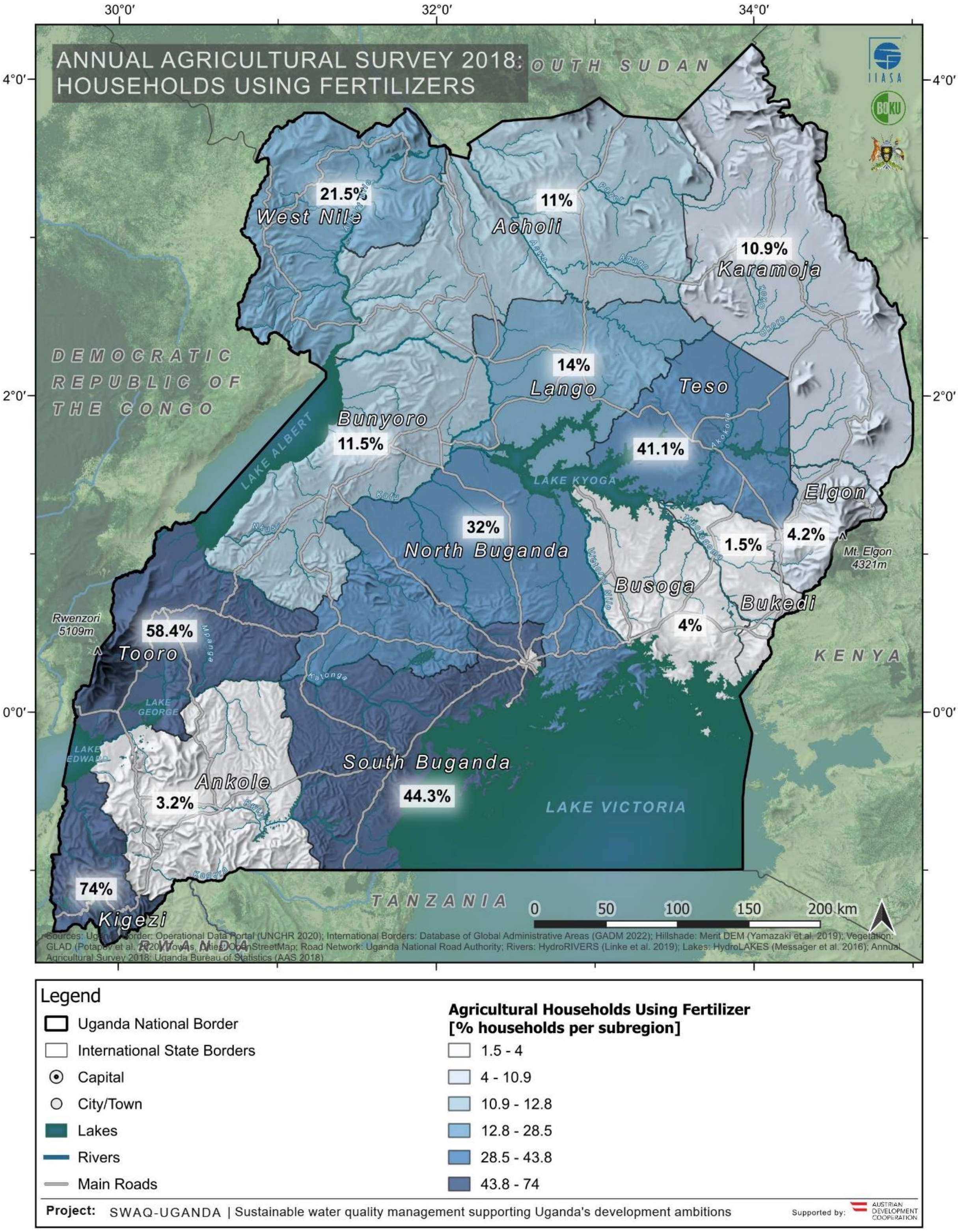

Figure 41: Annual Agricultural Survey 2018: Households using any fertilizer

Figure 41 displays the **percentage of agricultural households per subregion using any type of fertilizer.** This data was obtained from the Uganda Data Portal. The statistics were based on the 2018 Uganda Annual Agricultural Survey conducted by the Uganda Bureau of Statistics (UBOS AAS, 2020). The numbers that overlay the subregions in this figure represent the specific percentage reported in the 2018 AAS. On average, 23.7% of agricultural households in Uganda reported using fertilizers. The highest percentage of households using fertilizers was in the Kigezi subregion with 74% reporting fertilizer use. The subregion with the lowest proportion of fertilizer use was Bukedi with 1.5%.

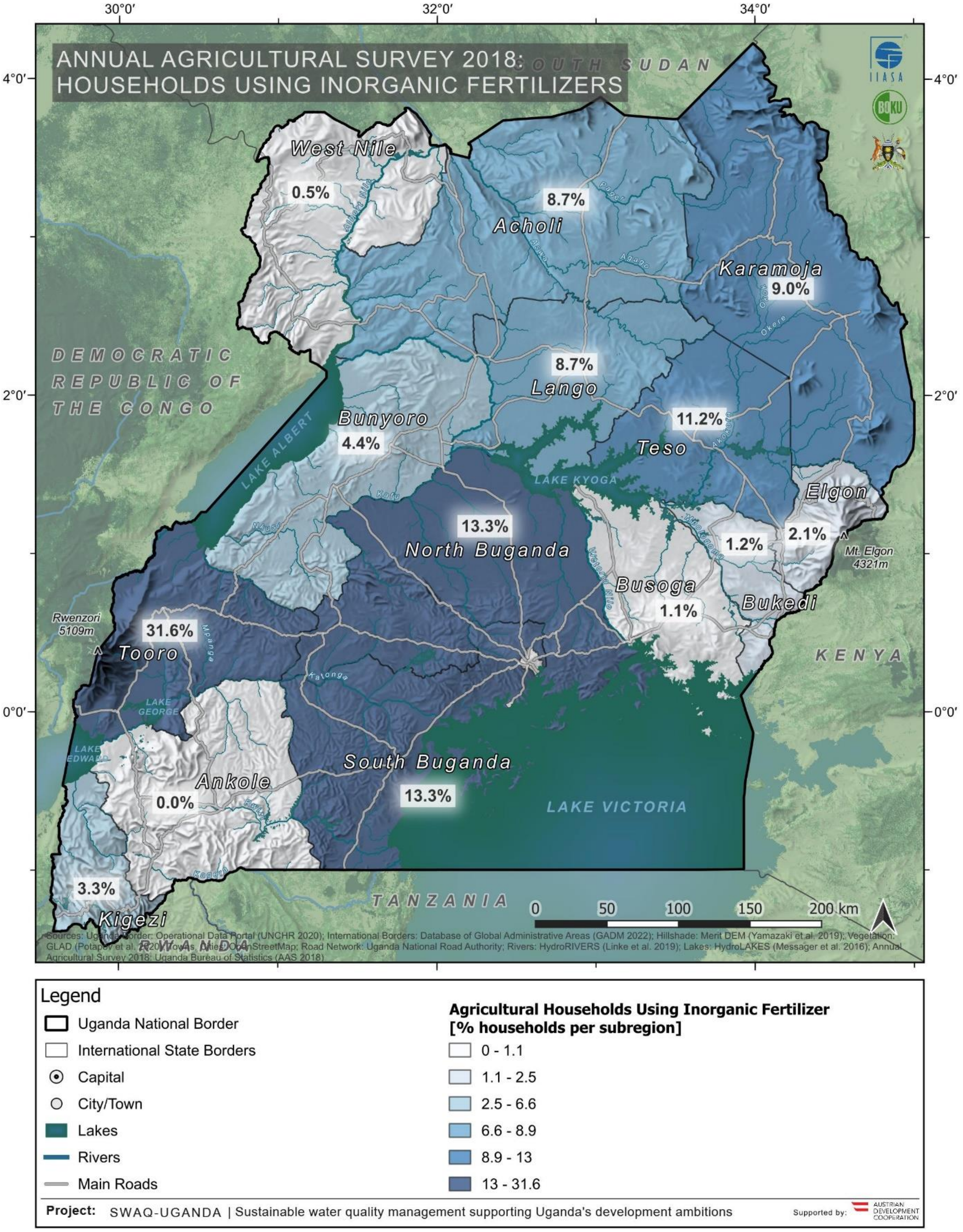

Figure 42: Annual Agricultural Survey 2018: Households using inorganic fertilizer

Figure 42 displays the **percentage of agricultural households per subregion using inorganic fertilizer** per subregion. This data was obtained from the Uganda Data Portal. The statistics were based on the 2018 Uganda Annual Agricultural Survey conducted by the Uganda Bureau of Statistics (UBOS AAS, 2020). The numbers that overlay the subregions in this figure represent the specific percentage reported in the 2018 AAS. Subregions with the highest proportions of inorganic fertilizer use are located in the south. These include Tooro, North Buganda and South Buganda. The Tooro subregion reported the greatest proportion (31.6%) of agricultural households using inorganic fertilizers. North Buganda and South Buganda both reported 13.3%. However, many subregions nationally had less than 5% of households report use of inorganic fertilizers. The lowest proportions were observed in the West Nile and Ankole subregions with 0.5% and 0.0% of households reporting use of inorganic fertilizers respectively.

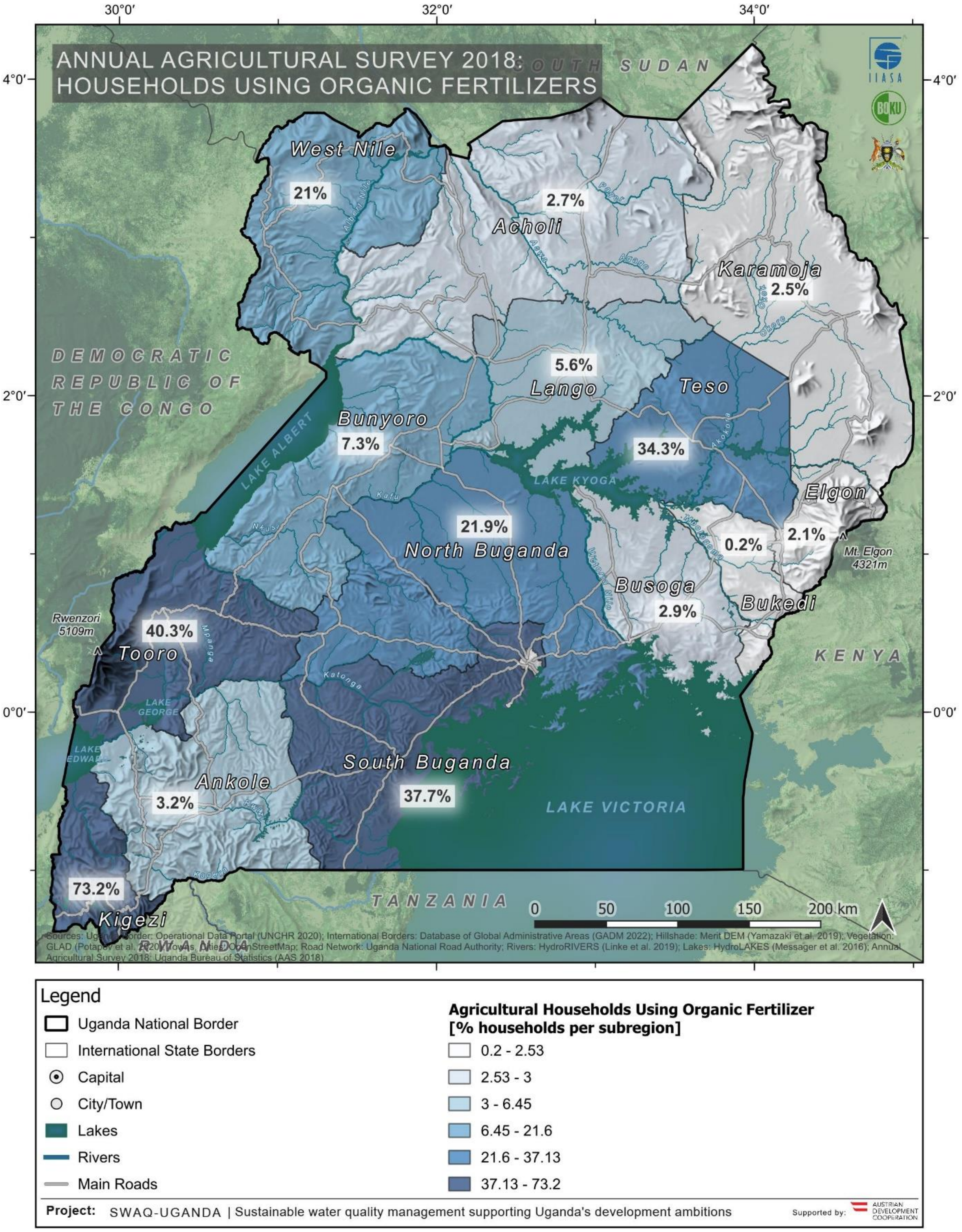

Figure 43: Annual Agricultural Survey 2018: Households using organic fertilizer

Figure 43 presents the **percentage of household heads using organic fertilizer** per subregion. This data was obtained from the Uganda Data Portal. The statistics were based on the 2018 Uganda Annual Agricultural Survey conducted by the Uganda Bureau of Statistics (UBOS AAS, 2020). The numbers that overlay the subregions in this figure represent the specific percentage reported in the 2018 AAS. Similarly to the trend observed with inorganic fertilizer use, subregions with the highest proportions of organic fertilizer use are located in the south. These include Kigezi, Tooro, and South Buganda. The Kigezi subregion reported the greatest proportion (73.2%) of agricultural households using organic fertilizers. The lowest percentage (0.2%) was observed in Bukedi.

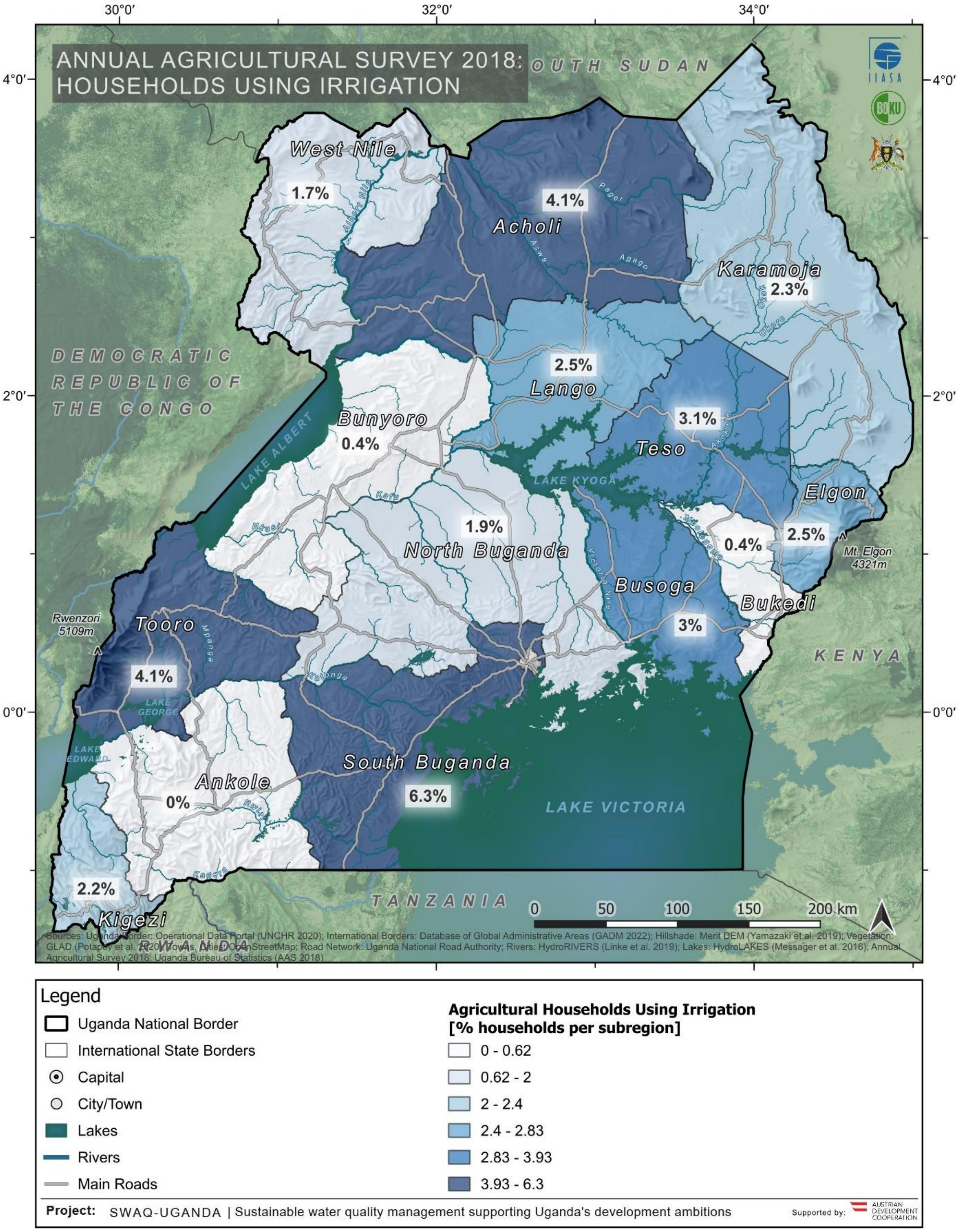

Figure 44: Annual Agricultural Survey 2018: Households using irrigation

Figure 44 shows the **percentage of household heads using irrigation** per subregion. This data was obtained from the Uganda Data Portal. The statistics were based on the 2018 Uganda Annual Agricultural Survey conducted by the Uganda Bureau of Statistics (UBOS AAS, 2020). The numbers that overlay the subregions in this figure represent the specific percentage reported in the 2018 AAS. The maximum percentage of households per subregion who reported irrigation use was 6.3% in South Buganda. Meanwhile, the subregions with the lowest irrigation use included Ankole, Bunyoro and Bukedi with 0%, 0.4% and 0.4% respectively.

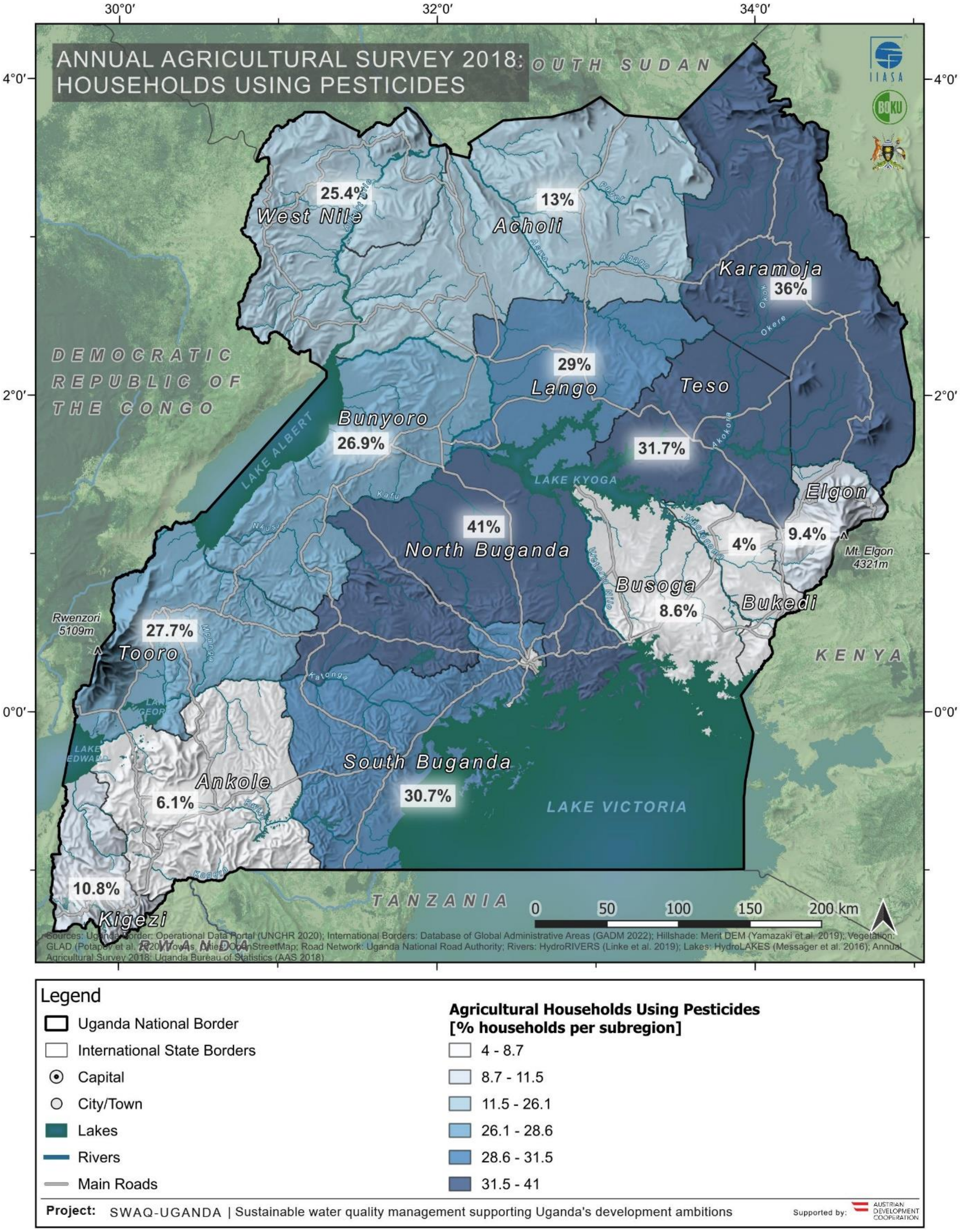

Figure 45: Annual Agricultural Survey 2018: Households using pesticides

Figure 45 shows the **percentage of household heads using pesticides** per subregion. This data was obtained from the Uganda Data Portal. The statistics were based on the 2018 Uganda Annual Agricultural Survey conducted by the Uganda Bureau of Statistics (UBOS AAS, 2020). The numbers that overlay the subregions in this figure represent the specific percentage reported in the 2018 AAS. The greatest percentage of households was located in North Buganda with 41% reporting pesticide use. The AAS reported just over a third of all agricultural households in the northeast subregions of Karamoja and Teso used pesticides. Pesticide use in Uganda was less prevalent in the southeast and southwest subregions.

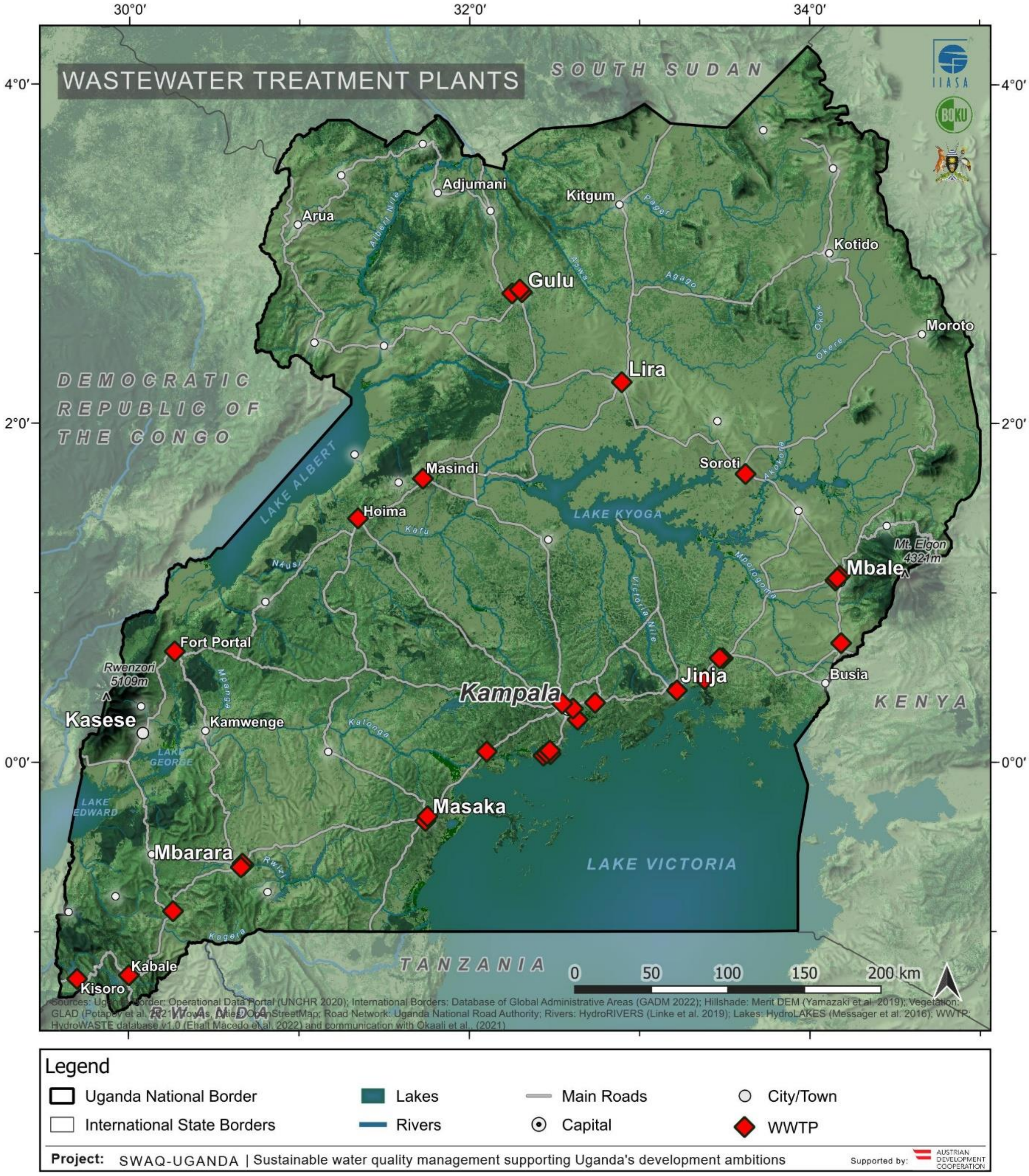

Figure 46: Wastewater treatment plants (WWTPs) in Uganda

Figure 46 displays **wastewater treatment plants (WWTPs)** in Uganda. Data was obtained from the HydroWASTE database v.1.0 (Ehalt Macedo et al., 2022) supplemented with data received from Okaali et al. (2021). Data was combined and duplicate WWTPs were removed. The resulting dataset contains a total of 33 treatment facilities, 17 of which were obtained from the HydroWASTE database. Further information (i.e. number of people served, total treated wastewater discharged, and level of treatment) is included for the WWTPs covered by the HydroWASTE database. Information on the designed capacity is not available in this dataset.

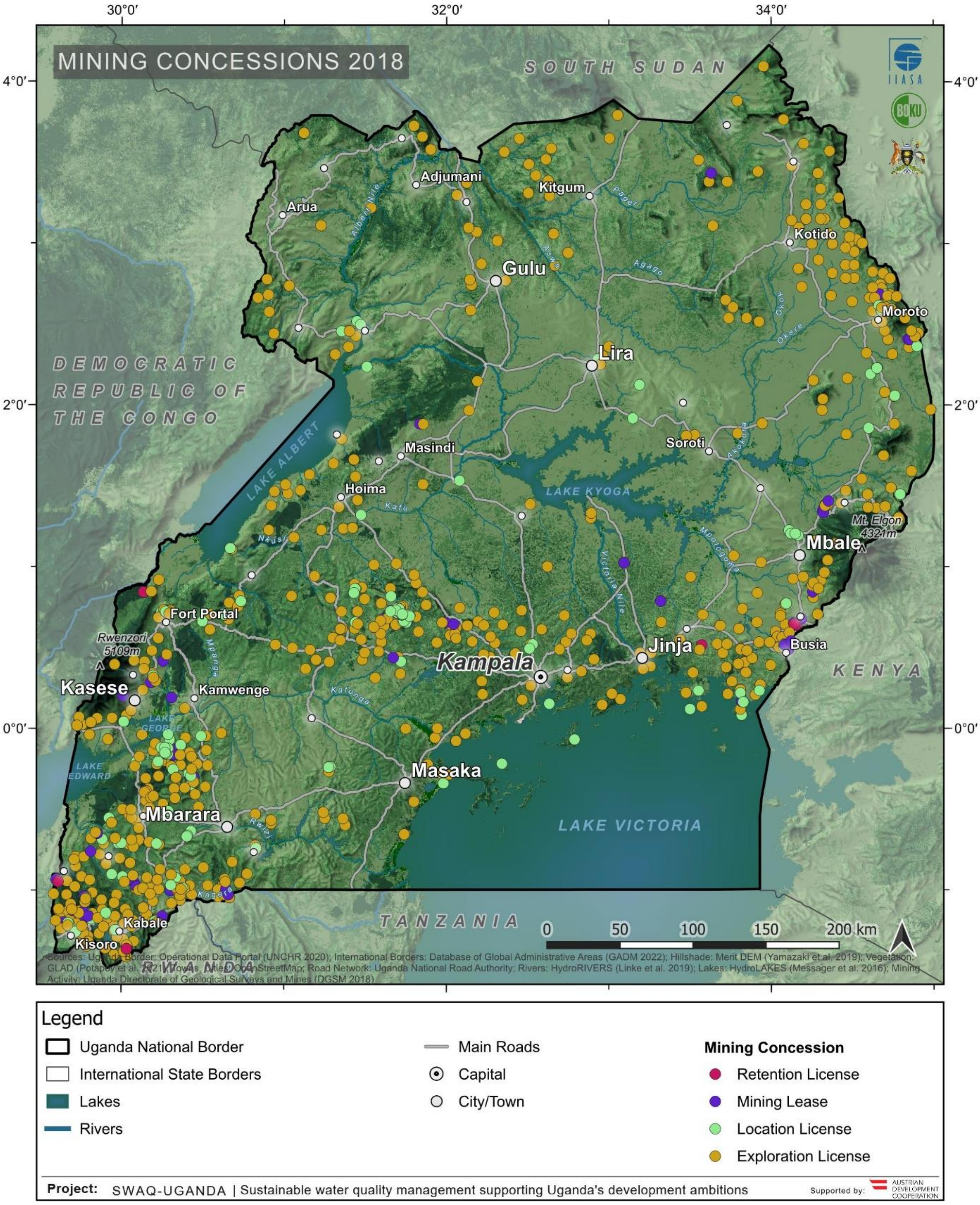

Figure 47: Mineral concessions in Uganda

Figure 47 displays the **mining concessions** in Uganda in 2018. Mining concessions are managed by the Directorate of Geological surveys and Mines (DGSM). This data was obtained online from data.ug, an open data portal run by the African Centre for Media Excellence (ACME). This dataset originated from the DGSM and provides information on the ownership, area, and commodity type (Ssenabulya, 2018). The following information on commissioning and license types originated from the DGSM and from (Katende, (2019): The exploration license (EL) is issued for up to three years, location specific with a maximum area of 250 km² and is renewable for two terms of two years. The retention license (RL) is granted to EL holders who have identified mineral deposits within the exploration area and want to retain mining rights for later. The RL has a maximum duration of three years and is renewable for two years. The mining lease (ML) gives the right to pursue mining operations in an area. It is granted for up to 20 years, or the estimated life of the ore body, whichever is shorter, and can be renewed for a maximum of 20 years. The location license (LL) is granted to citizens for small scale prospecting and mining. The total expenditure to set up operation must be under UGX 20,000,000 (USD 3,000).

Figure 48: Active Mining Leases and Licenses in Uganda

Figure 48 shows the location of **Mining Leases and Location Licenses** as of 2018. Both of these concession types give the holder the right to pursue mining activities. In 2018 there were a total of 41 active Mining Leases and 49 Location Licenses. The majority of leases and licenses are located in the southwest. This data was obtained online from data.ug and originated from Uganda's Directorate of Geological Surveys and Mines (Ssenabulya, 2018).

WATER QUALITY PRESSURE INDEX (WQPI)

Successful national water management is dependent upon an understanding of the spatial status of water quality. In the presence of reliable data, water quality can be defined by Water Quality Indices (WQIs). WQIs are composite indicators calculated using parameters such as temperature, dissolved oxygen, pH, turbidity, fecal coliforms, and other physiochemical parameters. However, in some countries such as Uganda there is often limited access to widespread water quality data for the parameters necessary to calculate a conventional WQI. With limited data on water quality in Uganda, proper allocation of resources to areas in need is challenging. Often researchers examining water quality in data-sparse regions select study areas based upon specific location properties such as population density, disease outbreak, or interest in the efficiency of wastewater treatment. There is a need for a method that can utilize more accessible data to provide an overview of water quality in these data-sparse regions.

Within the scope of the SWAQ-Uganda project, the Water Quality Pressure Index (WQPI) was developed to estimate water quality using available data on water quality drivers and pressures (Raskin, 2024; Stecher et al., 2024). Knowledge of regions experiencing higher pressures on water quality can be used to estimate water status. The WQPI utilizes a systemic approach rather than focusing on one or few factors affecting water quality. Therefore, the WQPI can more efficiently guide interested parties to areas of interest.

The methodology used for development of the WQPI is similar to other hydrological indices such as the WQI. Utilizing primarily QGIS and Microsoft Excel, the WQPI was calculated as a weighted average that incorporates geodata on multiple water quality pressures. Included geodata is listed in Table 3.

Table 3. Pillars of the Water Quality Pressure Index (WQPI)

Pillars of the Water Quality Pressure Index (WQPI)				
Environment	Water	Socioeconomic	Agriculture	Climate
Landcover Wetlands Protected Areas Soil Erosion Total Nitrogen (0-20cm) Total Nitrogen (20-50cm) Total Phosphorus (30cm)	Wastewater Treatment Plants	Population density Road network density Mining concessions	Tropical Livestock Units Phosphorous from manure Nitrogen from manure	Mean Annual Precipitation CHIRPS

The spatial unit used for the WQPI is based on HydroBASINS Africa Level 10 (Lehner & Grill, 2013). This resulting spatial unit had an average area of 134 km^2. Data on drivers and pressures was aggregated to this modified spatial unit and defined as "indicator data". Indicator data from each layer was ranked based upon the expected positive or negative influence on water quality. Rankings ranged from -3 to 3, where the higher the value, the greater the expected pressure. Negative values represent improvements or "negative pressures." Data layers were then weighted from 1 to 5 based upon their overall importance to water quality. A weighting of 1 suggested that a layer was less important, where a weighting of 5 represented layers that were considered extremely important to water quality. Several different weightings on indicators were tested to determine the robustness of the methodology. The raw WQPI was then calculated for each subbasin using the following equation:

$$raw\ WQPI = \frac{\sum(W_i * R_i)}{\sum W},$$

where W_i represents weights (assigned by layer) and R_i indicates ranked indicator data.

The WQPI was rescaled to ensure the resulting index was both easily interpretable and visually representative of both positive and negative pressures. When the raw WQPI was greater than 0, it was normalized to a value between 0 and 1, and simultaneously rescaled to a value between 0 and 3. When the raw WQPI was negative, it was first transformed to a value between -1 and 0, and then scaled to a value between *-max*(WQPI) and 0. The maximum value of the raw WQPI was considered because most subbasins experienced raw WQPI values greater than zero.

The WQPI, alongside other data, can be of critical importance to aid in assessing and managing water quality. It can also be applied to other regions with limited data collection capacity. Areas with higher WQPI values may benefit from improved monitoring and water treatment.

The final two figures of this report present the WQPI visualized using the modified HydroBASINS spatial unit (Figure 49), and visualized considering the river network (Figure 50). Thus, the final maps summarize the drivers and pressures outlined in this report.

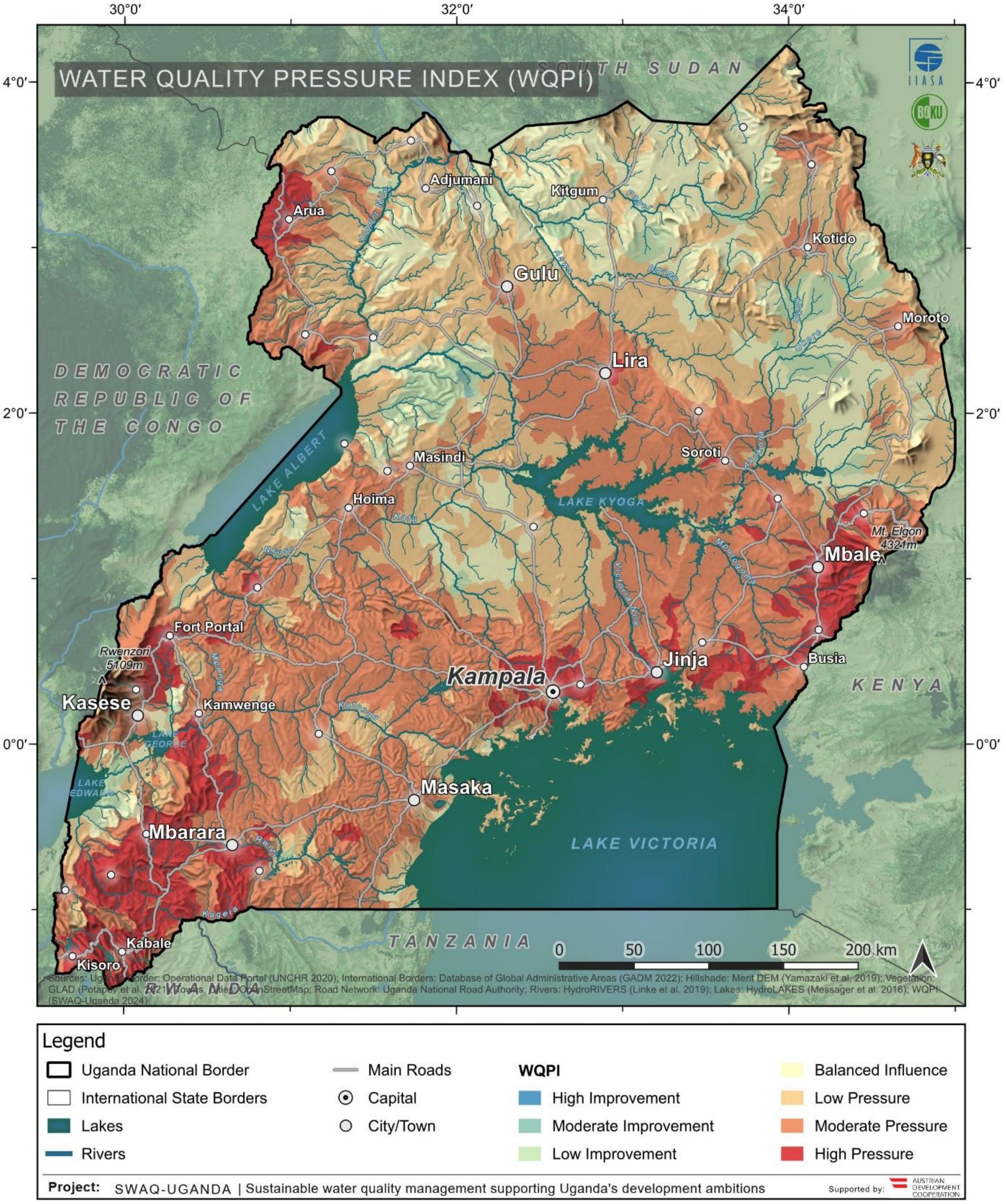

Figure 49: Water Quality Pressure Index

Figure 49 displays the **Water Quality Pressure Index (WQPI)** at the subbasin level. The WQPI is a novel composite indicator that was developed within the scope of the SWAQ-Uganda project in an effort to provide an integral estimate of water quality in Uganda. The WQPI was calculated as a weighted average based upon the influences of many of the drivers and pressures presented in this document. Greater pressures on water quality were estimated to occur in the southeast, southwest, and the northwest near Arua. Higher WQPI values were observed around cities such as Kampala, Jinja, Iganga, Busia, Mbale, Kaabong, Lira, Masindi, Hoima, Fort Portal, Mbarara, and Kabale.

Figure 50: Stream Network Water Quality Pressure Index: WQPI considering the stream network and hierarchy

Figure 50 displays the **WQPI considering the stream network and hierarchy**. This version of the WQPI integrates river flow to estimate water quality in Uganda's rivers. Lower pressures on water quality are noted in the northeast. Higher pressures on river water quality are estimated to occur in the southwest, as well as rivers around Mbale, Busia, Kampala and Arua.

SUMMARY

The goal of this activity was to establish a collection of geodata on factors that pertain to water quality in Uganda. Mapping of these data layers provides valuable insight into the spatial distribution of drivers, pressures, existing water management tools, and environmental conditions contributing to water quality.

Water quality drivers in this report included population density, gross domestic product (GDP), precipitation, landcover, wetlands, normalized difference vegetation index (NDVI), canopy height, soil types, soil nutrient content, and soil erosion risk. Included water quality pressures were tropical livestock units (TLU), chicken and pig production systems, manure nutrient content, fertilizer use, use of pesticides, irrigation use, wastewater treatment plants (WWTP), and mining activities. These drivers and pressures were combined to form the Water Quality Pressure Index (WQPI) in order to summarize water quality in Uganda. The culmination of these efforts aims to enhance data accessibility and expand knowledge about water stressors in Uganda.

Spatial trends among data were noted during the development of this report. For example, population density is correlated with the spatial distribution of several other drivers and pressures. As presented in Figure 12, the northeastern portion of Uganda is less densely populated compared to the southern, central and northwestern portions of the country. Several other maps follow this spatial trend. WWTPs are most commonly located in areas with a higher population. Additionally, a significant portion of mining concessions are in the southwest. The spatial distribution of these population related factors has implications for water management.

According to the WQPI, greater pressures were estimated in the southeast, southwest, and a small pocket in northwest Uganda bordering the Democratic Republic of the Congo. High WQPI values were observed around major cities such as Kampala, Jinja, Iganga, Busia, Mbale, Kaabong, Lira, Masindi, Hoima, Fort Portal, Mbarara, and Kabale. Rivers and lakes around these cities are predicted to experience significant pressures on water quality. Therefore, it is expected that water quality is degraded in these areas. Efforts should be made to improve water quality in regions experiencing higher WQPI values.

Although care was taken to provide a quality database, there are some noteworthy limitations affecting the reliability of this report. Due to scarcity of available data, temporal and spatial resolution of geodata is not consistent throughout this report and respective geodatabase. This variation in resolution means that the datasets within the report may be difficult to compare or interpret. Additionally, this report is not an exhaustive list of all drivers and pressures affecting Uganda’s water quality. Data for other factors influencing water quality should also be considered when making appropriate water management plans. For example, this report does not include data on manufacturing plants, oil drilling, laundromats, fisheries, and other drivers and pressures. Although they are not included, these factors also influence water quality. Finally, this geodatabase should be maintained and updated as new data becomes available. The data is also available as WebGIS under https://uganda.boku.ac.at/.

REFERENCES

Center for International Earth Science Information Network (CIESIN). (2018). *Gridded Population of the World, Version 4 (GPWv4) Revision 11*. NASA: Socioeconomic Data and Applications Center (SEDAC). https://sedac.ciesin.columbia.edu/data/collection/gpw-v4

Didan, K. (2015). MOD13Q1 MODIS/Terra Vegetation Indices 16-Day L3 Global 250m SIN Grid V006. In *NASA EOSDIS Land Processes Distributed Active Archive Center*. https://doi.org/10.5067/MODIS/MOD13Q1.006

Dinerstein, E., Olson, D., Joshi, A., Vynne, C., Burgess, N. D., Wikramanayake, E., Hahn, N., Palminteri, S., Hedao, P., Noss, R., Hansen, M., Locke, H., Ellis, E. C., Jones, B., Barber, C. V., Hayes, R., Kormos, C., Martin, V., Crist, E., … Saleem, M. (2017). An Ecoregion-Based Approach to Protecting Half the Terrestrial Realm. *BioScience*, *67*(6), 534–545. https://doi.org/10.1093/BIOSCI/BIX014

Directorate of Water Resources Management. (2019). *Republic of Uganda Ministry Of Water and Environment (MWE): Uganda Catchment Management Planning Guidelines*.

Ehalt Macedo, H., Lehner, B., Nicell, J., Grill, G., Li, J., Limtong, A., & Shakya, R. (2022). Distribution and characteristics of wastewater treatment plants within the global river network. *Earth System Science Data*, *14*(2), 559–577. https://doi.org/10.5194/ESSD-14-559-2022

Funk, C., Peterson, P., Landsfeld, M., Pedreros, D., Verdin, J., Shukla, S., Husak, G., Rowland, J., Harrison, L., Hoell, A., & Michaelsen, J. (2015). The climate hazards infrared precipitation with stations—a new environmental record for monitoring extremes. *Scientific Data 2015 2:1*, *2*(1), 1–21. https://doi.org/10.1038/sdata.2015.66

GADM. (2022). *Database of Global Administrative Areas (version 3.6)*. https://gadm.org/download_country_v3.html

Gerritsen, J., Barbour, M. T., & King, K. (2000). Apples, oranges, and ecoregions: on determining pattern in aquatic assemblages. *Https://Doi.Org/10.2307/1468109*, *19*(3), 487–496. https://doi.org/10.2307/1468109

Gilbert, M., Cinardi, G., Da Re, D., Wint, G. R. W., Wisser, D., & Robinson, T. P. (2022). Gridded Livestock of the World - 2015 (GLW 4). *Harvard Dataverse*, *1*.

Hengl, T., De Jesus, J. M., Heuvelink, G. B. M., Gonzalez, M. R., Kilibarda, M., Blagotić, A., Shangguan, W., Wright, M. N., Geng, X., Bauer-Marschallinger, B., Guevara, M. A., Vargas, R., MacMillan, R. A., Batjes, N. H., Leenaars, J. G. B., Ribeiro, E., Wheeler, I., Mantel, S., & Kempen, B. (2017). SoilGrids250m: Global gridded soil information based on machine learning. *PLOS ONE*, *12*(2), e0169748. https://doi.org/10.1371/JOURNAL.PONE.0169748

Hengl, T., Heuvelink, G. B. M., Kempen, B., Leenaars, J. G. B., Walsh, M. G., Shepherd, K. D., Sila, A., MacMillan, R. A., De Jesus, J. M., Tamene, L., & Tondoh, J. E. (2015). Mapping Soil Properties of Africa at 250 m Resolution: Random Forests Significantly Improve Current Predictions. *PLOS ONE*, *10*(6), e0125814. https://doi.org/10.1371/JOURNAL.PONE.0125814

Katende, S. (2019). LEX Africa - Guide to Mining in Uganda. In *Katende Ssempebwa & Company*. Katende Ssempebwa & Company.

Katutsi, V., Kaddu, M., Migisha, A. G., Rubanda, M. E., Adaramola, M. S., Katutsi, V., Kaddu, M., Migisha, A. G., Rubanda, M. E., & Adaramola, M. S. (2021). Overview of hydropower resources and development in Uganda. *AIMS Energy 2021 6:1299*, *9*(6), 1299–1320. https://doi.org/10.3934/ENERGY.2021060

Lehner, B., & Grill, G. (2013). Global river hydrography and network routing: baseline data and new approaches to study the world's large river systems. *Hydrological Processes*, *27*(15), 2171–2186. https://doi.org/10.1002/HYP.9740

Linke, S., Lehner, B., Ouellet Dallaire, C., Ariwi, J., Grill, G., Anand, M., Beames, P., Burchard-Levine, V., Maxwell, S., Moidu, H., Tan, F., & Thieme, M. (2019). Global hydro-environmental sub-basin and river reach characteristics at high spatial resolution. *Scientific Data 2019 6:1*, *6*(1), 1–15. https://doi.org/10.1038/s41597-019-0300-6

Messager, M. L., Lehner, B., Grill, G., Nedeva, I., & Schmitt, O. (2016). Estimating the volume and age of water stored in global lakes using a geo-statistical approach. *Nature Communications 2016 7:1*, *7*(1), 1–11. https://doi.org/10.1038/ncomms13603

MWE. (2020). *Water and Environment Sector Performance Report 2020*.

MWE. (2022a). *Natural Resources, Environment, Climate Change, Land and Water Management Programme Performance Report 2022*. https://www.mwe.go.ug/sites/default/files/library/NRECCLWM%20Programme%20Management%20%20Report%202022.pdf

MWE. (2022b). *Water Quality Stations of Uganda 2022*.

NFA & FAO. (2019). Uganda LULC for the year 2017. In *National Land Use Land Cover (LULC) Mapping by the National Forestry Authority*. https://data.apps.fao.org/map/catalog/static/api/records/1fb87d5b-225c-401a-b146-5ce37ae50146

Njuki, J., Poole, E. J., Johnson, J., Baltenweck, I., Pali, P. N., Lokman, Z., & Mburu, S. (2011). *Gender, livestock and livelihood indicators*. International Livestock Research Institute. https://hdl.handle.net/10568/3036

Phillip, K. (2021a). Uganda Wetlands 1994. In *National Environment Management Authority*. https://ug-geonode.geo4dev.org/layers/uganda_geonode_data:geonode:ugandawetlands1994/metadata_detail

Phillip, K. (2021b). *Uganda Wetlands 2008 (WMD)*. National Environment Management Authority, Wetland Management Department (WMD). https://ug-geonode.geo4dev.org/layers/geonode:ugandawetlands2008/metadata_detail

Potapov, P., Li, X., Hernandez-Serna, A., Tyukavina, A., Hansen, M. C., Kommareddy, A., Pickens, A., Turubanova, S., Tang, H., Silva, C. E., Armston, J., Dubayah, R., Blair, J. B., & Hofton, M. (2021). Mapping global forest canopy height through integration of GEDI and Landsat data. *Remote Sensing of Environment*, *253*, 112165. https://doi.org/10.1016/J.RSE.2020.112165

Potter, P., Ramankutty, N., Bennett, E. M., & Donner, S. D. (2010). Characterizing the Spatial Patterns of Global Fertilizer Application and Manure Production. *Earth Interactions*, *14*(2), 1–22. https://doi.org/10.1175/2009EI288.1

Raskin, J. (2024). *Development of a Water Quality Pressure Index (WQPI) under data-sparse conditions*. University of Natural Resources and Life Sciences, Vienna (BOKU).

Riahi, K., van Vuuren, D. P., Kriegler, E., Edmonds, J., O'Neill, B. C., Fujimori, S., Bauer, N., Calvin, K., Dellink, R., Fricko, O., Lutz, W., Popp, A., Cuaresma, J. C., KC, S., Leimbach, M., Jiang, L., Kram, T., Rao, S., Emmerling, J., … Tavoni, M. (2017). The Shared Socioeconomic Pathways and their energy, land use, and greenhouse gas emissions implications: An overview. *Global Environmental Change*, *42*, 153–168. https://doi.org/10.1016/J.GLOENVCHA.2016.05.009

Schnabel, B. (2024). *Personal Communication*.

Schürz, C., Mehdi, B., Kiesel, J., Schulz, K., & Herrnegger, M. (2020). A systematic assessment of uncertainties in large-scale soil loss estimation from different representations of USLE input factors-a case study for Kenya and Uganda. *Hydrology and Earth System Sciences*, *24*(9), 4463–4489. https://doi.org/10.5194/HESS-24-4463-2020

Ssenabulya, B. (2018). Mineral Concessions in Uganda as of 14 December 2018. In *Department of Geological Survey and Mines (DGSM)*. African Centre for Media Excellence (ACME). http://catalog.data.ug/dataset/mineral-concessions-in-uganda-as-of-14-december-2018

Stecher, G., Raskin, J., & Herrnegger, M. (2024). A novel approach to systematically assess large scale water quality degradation in Uganda – The Water Quality Pressure Index . *Uganda Water and Environment Week (UWEWK), Water Resource Institute*.

UBOS. (2012). *Towns: Uganda, 2009*. https://searchworks.stanford.edu/view/ry521vp2029

UBOS AAS. (2020). *Uganda Bureau of Statistics: Annual Agricultural Survey 2018*.

Uganda Electricity Generation Company Ltd. (2024). *Maps of Power Plants and Dams*. UEGCL Publications, Reports, Policies and Useful Resources. https://www.uegcl.com/publications/maps-of-power-plants-and-dams/

UNEP-WCMC & IUCN. (2022). *Protected Area Profile for Uganda from the World Database on Protected Areas*. https://www.protectedplanet.net/en

UNHCR. (2020). *Uganda Districts Shapefiles 2020*. UNCHR's Operational Data Portal. https://data.unhcr.org/en/documents/details/83043

VNR. (2020). *The Republic of Uganda: Voluntary National Review Report on the Implementation of the 2030 Agenda for Sustainable Development*. https://sustainabledevelopment.un.org/content/documents/26354VNR_2020_Uganda_Report.pdf

World Bank Group. (2007). *Uganda Roads compiled by Africon for AICD study (2009), with input from the Roads Agency Formation Unit (RAFU)*. https://datacatalog.worldbank.org/search/dataset/0041482

Yamazaki, D., Ikeshima, D., Sosa, J., Bates, P. D., Allen, G. H., & Pavelsky, T. M. (2019). MERIT Hydro: A High-Resolution Global Hydrography Map Based on Latest Topography Dataset. *Water Resources Research*, *55*(6), 5053–5073. https://doi.org/10.1029/2019WR024873